AD A057684

LEVEL

12

R866

TECHNICAL REPORT
CIVIL ENGINEERING LABORATORY

Naval Construction Battalion Center, Port Hueneme, California 93043

A VISCOELASTIC-PLASTIC CONSTITUTIVE MODEL WITH
A FINITE ELEMENT SOLUTION METHODOLOGY

By M. Katona, Ph D

D D C
RECEIVED
AUG 21 1978
A

June 1978

78 08 18 037

REPORT DOCUMENTATION PAGE		READ INSTRUCTIONS BEFORE COMPLETING FORM
1. REPORT NUMBER CEL-TR-866	2. GOVT ACCESSION NO. DN587001	3. RECIPIENT'S CATALOG NUMBER
4. TITLE (and Subtitle) A VISCOELASTIC-PLASTIC CONSTITUTIVE MODEL WITH A FINITE ELEMENT SOLUTION METHODOLOGY		5. TYPE OF REPORT & PERIOD COVERED Final; Aug 1974 – Aug 1977
		6. PERFORMING ORG. REPORT NUMBER
7. AUTHOR(s) M. Katona, PhD		8. CONTRACT OR GRANT NUMBER(s)
9. PERFORMING ORGANIZATION NAME AND ADDRESS CIVIL ENGINEERING LABORATORY Naval Construction Battalion Center Port Hueneme, California 93043		10. PROGRAM ELEMENT, PROJECT, TASK AREA & WORK UNIT NUMBERS 61152N; Z-R000-01-141
11. CONTROLLING OFFICE NAME AND ADDRESS Naval Material Command Washington, D.C. 20360		12. REPORT DATE June 1978
		13. NUMBER OF PAGES 159
14. MONITORING AGENCY NAME & ADDRESS(if different from Controlling Office) ZK00001		15. SECURITY CLASS. (of this report) Unclassified
		15a. DECLASSIFICATION DOWNGRADING SCHEDULE

16. DISTRIBUTION STATEMENT (of this Report)

Distribution unlimited; approved for public release.

17. DISTRIBUTION STATEMENT (of the abstract entered in Block 20, if different from Report)

ZK00001141

18. SUPPLEMENTARY NOTES

19. KEY WORDS (Continue on reverse side if necessary and identify by block number)

Finite element models, constitutive models, structural mechanics, material modeling, viscoelasticity, viscoplasticity, creep, virtual work

20. ABSTRACT (Continue on reverse side if necessary and identify by block number)

A textbook style development of viscoplasticity is presented. For completeness, the report also includes a detailed review of plasticity and viscoelasticity. The combination of plasticity and viscoelasticity is the basis for the so-called "viscoelastic-plastic" model developed herein. Other combo-viscoplastic models are also introduced. Each constitutive model is introduced with conceptual one-dimensional stress-strain models and then generalized for

(continued)

DD FORM 1473 EDITION OF 1 NOV 65 IS OBSOLETE
1 JAN 73

78 08 18

20. Continued

-multidimensional stress space. Furthermore, each model is cast in an incremental form appropriate for numerical solution techniques. Finite element algorithms are outlined for incorporating these nonlinear constitutive models into boundary value problems. In particular, tangent stiffness and initial strain methods are discussed. The viscoelastic-plastic model is compared to experimental data for plexiglas and sea-ice to illustrate the versatility of the model in replicating nonlinear creep and flow of these materials. Moreover, the identification of the model parameters are shown to be no more difficult than the identification of parameters for the classical theories of plasticity and viscoelasticity.

Library Card

Civil Engineering Laboratory
A VISCOELASTIC-PLASTIC CONSTITUTIVE MODEL
WITH A FINITE ELEMENT SOLUTION METHO-
DOLOGY (Final), by M. Katona, PhD
TR-866   159 pp illus   June 1978   Unclassified

1. Constitutive modeling   2. Material modeling   I. Z-R000-01-141

A textbook style development of viscoplasticity is presented. For completeness, the report also includes a detailed review of plasticity and viscoelasticity. The combination of plasticity and viscoelasticity is the basis for the so-called "viscoelastic-plastic" model developed herein. Other combo-viscoplastic models are also introduced. Each constitutive model is introduced with conceptual one-dimensional stress-strain models and then generalized for multidimensional stress space. Furthermore, each model is cast in an incremental form appropriate for numerical solution techniques. Finite element algorithms are outlined for incorporating these nonlinear constitutive models into boundary value problems. In particular, tangent stiffness and initial strain methods are discussed. The viscoelastic-plastic model is compared to experimental data for plexiglas and sea-ice to illustrate the versatility of the model in replicating nonlinear creep and flow of these materials. Moreover, the identification of the model parameters are shown to be no more difficult than the identification of parameters for the classical theories of plasticity and viscoelasticity.

CONTENTS

INTRODUCTION

At the forefront of modern research in structural mechanics is the problem of dealing with time-dependent, nonlinear material models. The stimulus for this interest is due to the increased use of new materials in structural systems, such as plastics, glues, resins, biological tissues, fuel propellants, soils, sea-ice, and high temperature metals.

Although constitutive theories for time-dependent, nonlinear models are still in their infancy, the ability to solve boundary value problems embracing these theories is well in hand. In particular, the well-known finite element method is capable of incorporating the most elegant constitutive models with relative ease and sufficient accuracy for engineering applications. This is a complete turn of events from classical mechanics, wherein constitutive theories were necessarily simplified to afford tractable solutions of boundary value problems.

Clearly, the time has come to re-focus attention on material modeling to develop constitutive theories that are representative of real material behavior and are on a par with modern analytical methods.

BACKGROUND

Time-dependent and nonlinear constitutive models can generally be identified as belonging to one of three classifications: creep, non-linear viscoelastic, or viscoplastic. The first two classifications are fairly well defined in the literature [1,2] and will not be pursued here. Suffice to say, these models have met with limited success in

1

some engineering applications, but they are not able to replicate many of the observed phenomena of real materials, such as the Bauschinger effect, anisotropic deformation, and cyclic phenomena [3].

As the name suggests, a viscoplastic model combines the features of viscous time-dependency with plasticity theory, and in its general form is capable of faithfully representing observed material behavior, such as a rate-dependent yield strength, Bauschinger effect, and loading and unloading phenomena. These concepts will be amplified throughout the text.

The general theory of viscoplasticity is well summarized by Perzyna [4], wherein he concludes further theoretical development is necessary. However, two important subsets of the general theory appear theoretically sound and tractable. The first will be called "elastic-viscoplastic" and the second, "viscoelastic-plastic." The former is characterized by an elastic region within the yield surface and a time-dependent yield function whose domain is not restricted to the yield surface. Zienkiewicz [5] has developed and demonstrated this model in several finite element applications.

The "viscoelastic-plastic" model is characterized by linear viscoelastic theory within the yield surface and the combined influence of viscoelasticity and plasticity on the yield surface. The yield function is restricted to the domain within and on the yield surface as in classical plasticity. This model is developed in detail in this report.

OBJECTIVE AND SCOPE

The objective of this study is to present an incremental constitutive development for the viscoelastic-plastic model, and furthermore, to incorporate the model into a finite element formulation. To achieve this objective, the classical theories of plasticity and linear viscoelasticity are individually developed in preparation for the combined

2

viscoelastic-plastic development. In themselves, the individual treatments contain many generalizations and unifications of plasticity and viscoelasticity heretofore scattered throughout the literature. Consequently, this work serves as a reference to plasticity and viscoelasticity in addition to viscoplasticity.

It is well recognized that any constitutive theory is useful only if it can be successfully incorporated into the field equations of boundary value problems. Accordingly, each of the models presented in this work is accompanied with a general finite element formulation and suggested solution algorithms. Since the finite element formulation is common to all material models, it will be presented at the outset of this study, thereby providing some insight into the desired form of the constitutive relationships.

Chapter 1

NONLINEAR FINITE ELEMENT FORMULATION OF EQUILIBRIUM EQUATIONS

The purpose of this section is to formulate a finite element methodology capable of handling all of the nonlinear constitutive models presented later in the text. At first thought, this may appear as putting the "cart before the horse." However, this ordering of the presentation provides the reader with an informative preview of the assumptions common to all constitutive theories, as well as demonstrating how the various constitutive laws are utilized to solve boundary value problems.

Perhaps the most powerful physical law in analytical mechanics is the principle of virtual work. By evoking this law under isothermal conditions, the resulting statement is completely general and valid for both geometric and material nonlinearities. To wit, virtual work may be stated as: Given a deformed body in equilibrium under a set of external loads, and subjected to any small virtual displacement compatible with the constraints of the deformed body; then, the virtual work of the internal forces is equal to the virtual work of the external loads. Furthermore, by d'Alembert's principle, inertia loads may be treated as equivalent external loads, thereby extending the virtual work concept to dynamic problems. In equation form this statement is:

$$\int_V \delta \underset{\sim}{\epsilon}^T \underset{\sim}{\sigma} \, dv = \int_S \delta \underset{\sim}{u}^T \underset{\sim}{t} \, ds + \int_V \delta \underset{\sim}{u}^T (\underset{\sim}{f} - \underset{\sim}{\ddot{u}}) \rho \, dv \qquad (1-1)$$

where $\underset{\sim}{\sigma}$ = stress vector with respect to deformed body (i.e., Cauchy stress)

$\underset{\sim}{\varepsilon}$ = infinitesimal strain vector with respect to deformed body

$\underset{\sim}{u}$ = displacement vector measured from some fixed inertial Cartesian reference system ($\underset{\sim}{\ddot{u}}$ denotes acceleration)

$\underset{\sim}{t}$ = surface traction vector on deformed body

ρ = current mass density per unit volume

$\underset{\sim}{f}$ = body force vector per unit mass

v = current volume of body

s = current surface of body

$\delta(\ )$ $\Rightarrow$ variational quantity

$(\underset{\sim}{\ })$ $\Rightarrow$ vector quantity

$(\underset{\sim}{\ })^T$ $\Rightarrow$ transpose of a vector

With regard to large deformations, Equation 1-1 poses a rather difficult nonlinear problem since all quantities are referenced to the unknown deformed configuration. The above formulation of the problem is often called the "Eulerian description," or "moving coordinate approach." Alternatively, it is possible to recast the formulation so that all quantities are measured with respect to the original or initial configuration; this is known as the "Lagrangian description." By this description, all derivatives and integrals are easily computed with respect to the initial fixed coordinate system. However, the stress and strain vectors take on new definitions consistent with their reference to the original configuration. Namely, they become the second Piola-Kirchoff stress vector and the Green-Lagrange strain vector [6], both of which are nonlinear with respect to the deformation gradient.

Eulerian and Lagrangian descriptions represent the end points on a spectrum of possible formulations for large deformation analysis. Many innovative combinations and approximations of these formulations have

been presented in the literature [7,8,9]. However, the most significant point to be kept in mind, with regard to both geometric and material nonlinearity, is that the constitutive law must be defined in a manner consistent with the formulation. For example, a Lagrangian formulation requires that the law relate second Piola-Kirchoff stress to Green-Lagrange strain.

For the remainder of this development, infinitesimal strain theory will be assumed and inertia loads will be neglected so that attention can be focused on material nonlinearity. Nonetheless, the constitutive models presented herein are equally valid for large deformations and dynamic loadings, provided they are used in a consistent fashion as noted above.

In accordance with infinitesimal strain theory, the deformed configuration is assumed to differ infinitesimally from the undeformed configuration; consequently, Equation 1-1 is assumed valid for all quantities measured with respect to the undeformed configuration. Accordingly, the stress and strain vectors have the classical definition.

In addition to Equation 1-1, the complete formulation of a boundary value problem requires the specification of (1) the strain-displacement relationship, (2) constitutive law (i.e., the stress-strain relationship), and (3) the boundary conditions. For the present, no restrictions on the form of the constitutive law will be assumed; however, the strain-displacement relationship will be assumed linear in accordance with infinitesimal strain theory, and the boundary conditions will be introduced via the finite element method.

Thus, the strain-displacement relationship takes the form:

$$\underset{\sim}{\varepsilon} = \underset{\approx}{\partial}\underset{\sim}{u} \tag{1-2}$$

6

where $\underset{\sim}{O}$ is a linear operator on $\underset{\sim}{u}$. For example, in a Cartesian coordinate system, $\underset{\sim}{O}$ has the form such that the normal strain components are given by $\varepsilon_{ii} = \partial u_i / \partial X_i$ (no sum on i), and the shear strain components are given by $2\varepsilon_{ij} = \gamma_{ij} = \partial u_i / \partial X_j + \partial u_j / \partial X_i$.

At this juncture, the fundamental finite element approximation is introduced. The body is subdivided into a discrete set of elements whereby the integrations in Equation 1-1 apply to each element. Within each element, the displacement vector is approximated by an assumed spatial interpolation function. Associated with the interpolation function are a set of unknown nodal displacements located on the surface of each element. Adjacent elements share common nodes, thereby providing nodal point compatibility between the elements. If the interpolation function is admissible [10], it can be shown that the finite element approximation will provide the "exact" solution to the boundary value problem with a sufficient number of elements. Symbolically, the finite element approximation is written as:

$$\underset{\sim}{u} = \underset{\sim}{h} \, \underset{\sim}{\hat{u}} \qquad (1-3)$$

where $\underset{\sim}{h}$ = matrix of admissible interpolation functions dependent only on space

$\underset{\sim}{\hat{u}}$ = vector of nodal displacements dependent only on time (or load step)

Inserting Equation 1-3 into Equation 1-2, the strain-displacement relationship within each element is given as:

$$\underset{\sim}{\varepsilon} = \underset{\approx}{B} \, \underset{\sim}{\hat{u}} \qquad (1-4)$$

7

where $\underset{\sim}{B}$ equals $\underset{\sim\sim}{\partial h}$, which is the strain-to-nodal displacement matrix dependent only on spatial coordinates. Returning to the statement of virtual work, and introducing the finite element approximations imbedded in Equations 1-3 and 1-4, Equation 1-1 can be written as (neglecting inertia):

$$\delta \hat{\underset{\sim}{u}}^T \left(\sum \int_V \underset{\sim}{B}^T \underset{\sim}{\sigma}\ dv \right) = \delta \underset{\sim}{u}^T \sum \left(\int_V \underset{\sim}{h}^T \underset{\sim}{f}\ \rho\ dv + \int_S \underset{\sim}{h}^T \underset{\sim}{t}\ ds \right) \quad (1\text{-}5)$$

Here the symbol $\sum$ denotes summation over the elements with the special understanding that the contributions of each element are properly assigned to the corresponding location of the nodal displacement vector.

Since each variation of $\hat{\underset{\sim}{u}}$ is independent, Equation 1-5 represents a set of simultaneous equations. In preparation for the incremental constitutive relationships to be introduced next, and without loss of generality, Equation 1-5 can be written in incremental form by replacing $\underset{\sim}{\sigma}$, $\underset{\sim}{t}$, and $\underset{\sim}{f}$ by $\Delta\underset{\sim}{\sigma}$, $\Delta\underset{\sim}{t}$ and $\Delta\underset{\sim}{f}$, respectively, to give the set of simultaneous equations:

$$\sum \int_V \underset{\sim}{B}^T \Delta\underset{\sim}{\sigma}\ dv = \Delta\underset{\sim}{P} \quad (1\text{-}6)$$

where

$$\Delta\underset{\sim}{P} = \sum \left(\int_V \underset{\sim}{h}^T \Delta\underset{\sim}{f}\ \rho\ dv + \int_S \underset{\sim}{h}^T \Delta\underset{\sim}{t}\ ds \right) \quad (1\text{-}7)$$

In a similar manner, the strain displacement relationship can be written in incremental form as:

8

$$\Delta \underset{\sim}{\varepsilon} \;=\; \underset{\bullet}{\mathbf{B}} \; \Delta \hat{\underset{\sim}{u}} \tag{1-8}$$

Thus far in the discussion no assumptions have been made with regard to the form of the constitutive relationship. Therefore, Equations 1-6, 1-7, and 1-8, which are completely general with regard to material laws, provide the proper starting point for incorporating material models into a finite element formulation. For present purposes, no special restrictions will be imposed on the form of the constitutive relationships. However, for the sake of clarity and ease of presentation, the constitutive relationship will be symbolically denoted as:

$$\Delta \underset{\sim}{\sigma} \;=\; \underset{\bullet n}{\mathbf{D}} \; \Delta \underset{\sim}{\varepsilon} \tag{1-9}$$

Here, $\underset{\bullet n}{\mathbf{D}}$ represents a stress-strain relationship that may depend on total stress, total strain, and history of loading. Accordingly, $\underset{\bullet n}{\mathbf{D}}$ may be construed as an operator matrix rather than a simple matrix.

The motivation for introducing the incremental quantities $\Delta \sigma$ and $\Delta \varepsilon$ into Equation 1-9 is to facilitate linearization of $\underset{\bullet n}{\mathbf{D}}$. For example, if sufficiently small time steps (or load steps) are prescribed, it may be sufficiently accurate to determine $\underset{\bullet n}{\mathbf{D}}$ based on the stress-strain state at the beginning of the load step (tangent modulus approach). On the other hand, if larger time steps are prescribed or the material character is highly nonlinear, it may be necessary to determine $\underset{\bullet n}{\mathbf{D}}$ based on the average stress-strain state over the interval, thereby requiring iteration within the time step (modified tangent or chord modulus approach).

In either approach, the nature and the treatment of $\underset{\bullet n}{\mathbf{D}}$ are discussed individually for each constitutive model presented in later sections of this report. For now, it is simply assumed that $\underset{\bullet n}{\mathbf{D}}$ exists and may or may not be dependent upon the current time step.

With the above understanding, two basic solution strategies for
incorporating the incremental constitutive law into the finite element
formulation are (1) the "tangent stiffness method," and (2) the "initial
strain method." The names of both methods are misleading; however, the
use of this terminology is widespread in engineering literature [11,12]
and will be retained here. Broadly speaking, the tangent stiffness
method implies the constitutive relationship is incorporated directly
into the global stiffness matrix, whereas the initial strain method
incorporates the linear portion of the constitutive relationship into
the global stiffness matrix, treating nonlinear terms as load vectors.
Both methods are described below.

TANGENT STIFFNESS METHOD

The tangent stiffness method is a straightforward, brute force
technique that requires no further assumptions than already presented.
Formally, Equations 1-8 and 1-9 are combined to give $\Delta \underset{\sim}{\sigma} = \underset{\sim}{D}_n \underset{\sim}{B} \Delta \hat{\underset{\sim}{u}}$, and
this result is inserted into the global equilibrium equations, Equation
1-6, to give:

$$\underset{\sim}{K}_T \Delta \hat{\underset{\sim}{u}} = \Delta \underset{\sim}{P} \qquad (1-10)$$

where
$$\underset{\sim}{K}_T = \sum \int_V \underset{\sim}{B}^T \underset{\sim}{D}_n \underset{\sim}{B} \, dv \qquad (1-11)$$

In the above $\underset{\sim}{K}_T$ is the global stiffness matrix relating displace-
ment increments to load increments. Since $\underset{\sim}{D}_n$ is dependent on the
stress-strain state, $\underset{\sim}{K}_T$ changes accordingly.

The solution algorithm embodies the following steps, wherein it is
assumed the system is in equilibrium at time step "i" with known responses

10

$\underset{\sim}{\sigma}_i$, $\underset{\sim}{\epsilon}_i$, and $\underset{\sim}{\hat{u}}_i$. The objective is to find the response increments $\Delta\underset{\sim}{\hat{u}}$, $\Delta\underset{\sim}{\epsilon}$, and $\Delta\underset{\sim}{\sigma}$ over the interval i to $i + 1$.

1. Calculate load increment $\Delta\underset{\sim}{P}$ (Equation 1-7).

2. Assemble global stiffness $\underset{\sim}{K}_T$ based on value of $\underset{\sim}{D}_n$ at beginning of step (Equation 1-11).

3. Solve $\underset{\sim}{K}_T \Delta\underset{\sim}{\hat{u}} = \Delta\underset{\sim}{P}$, for $\Delta\underset{\sim}{\hat{u}}$.

4. Determine $\Delta\underset{\sim}{\epsilon}$ and $\Delta\underset{\sim}{\sigma}$ from Equations 1-8 and 1-9.

5. If desired, re-evaluate $\underset{\sim}{D}_n$ based on average values of stress-strain over the interval, and return to Step 2 to iterate within time step.

6. Add incremental responses to total responses, advance the time step, and return to Step 1.

In the above algorithm the global matrix $\underset{\sim}{K}_T$ must be assembled and triangularized for each load step and any iteration within the load step. For large problems this method may be prohibitively costly.

INITIAL STRAIN METHOD

The initial strain method generally provides a much more efficient algorithm; however, two additional assumptions are required with regard to the material behavior. First, it is assumed the strain increment can be decomposed into linear and nonlinear contributions. That is, the total strain increment is given by:

$$\Delta\underset{\sim}{\epsilon} = \Delta\underset{\sim}{\epsilon}_L + \Delta\underset{\sim}{\epsilon}_n \qquad (1-12)$$

11

where $\Delta\varepsilon_{\sim L}$ is the linear strain, and $\Delta\varepsilon_{\sim n}$ represents a combined lumping of all nonlinear strains. Secondly, it is assumed the total stress increment is persistently related to the linear strain increment by:

$$\Delta\sigma_{\sim} = D_{\sim L}\, \Delta\varepsilon_{\sim L} \qquad . \qquad (1\text{-}13)$$

where $D_{\sim L}$ is a linear material matrix. Combining Equations 1-12 and 1-13 gives:

$$\Delta\sigma_{\sim} = D_{\sim L}(\Delta\varepsilon_{\sim} - \Delta\varepsilon_{\sim n}) \qquad (1\text{-}14)$$

Recalling the general constitutive assumption, $\Delta\sigma_{\sim} = D_{\sim n}\, \Delta\varepsilon_{\sim}$, and using Equation 1-14, a relationship between total and nonlinear strain increments is obtained as:

$$D_{\sim L}\, \Delta\varepsilon_{\sim n} = (D_{\sim n} - D_{\sim L})\Delta\varepsilon_{\sim} \qquad (1\text{-}15)$$

To make use of the above in the initial strain formulation, $\Delta\sigma$ of Equation 1-6 is replaced by $\Delta\sigma_{\sim} = D_{\sim L}(\Delta\varepsilon_{\sim} - \Delta\varepsilon_{\sim n})$, and the nonlinear terms are brought to the right-hand side to give:

$$K_{\sim L}\, \Delta\hat{u}_{\sim} = \Delta P_{\sim} + \Delta F_{\sim n} \qquad (1\text{-}16)$$

where
$$K_{\sim L} = \sum \int_v B_{\sim}^T\, D_{\sim L}\, B_{\sim}\, dv \qquad (1\text{-}17)$$

12

and

$$\Delta F_{\sim n} = \sum \int_V B^T_{\sim} D_{\sim L} \Delta \varepsilon_{\sim n} \, dv \qquad (1\text{-}18)$$

Equation 1-16 is the global equilibrium equation for the initial strain formulation. $K_{\sim L}$ is the constant elastic stiffness matrix, and $\Delta F_{\sim n}$ represents a nonlinear force vector composed of nonelastic strain increments.

Since $\Delta F_{\sim n}$ is an unknown vector, it is treated iteratively. To this end, it is convenient to use Equation 1-15 and the strain displacement relationship to replace $D_{\sim L} \Delta \varepsilon_{\sim n}$ by $(D_{\sim L} - D_{\sim n}) B_{\sim} \hat{u}_{\sim}$. That is, $\Delta F_{\sim n}$ may be written as:

$$\Delta F_{\sim n} = \left[\sum \int_V B^T_{\sim}(D_{\sim L} - D_{\sim n}) B_{\sim} \, dv \right] \Delta \hat{u}_{\sim} \qquad (1\text{-}19)$$

Thus, the basic idea is to solve Equation 1-16 for $\Delta \hat{u}_{\sim}$ and then redefine $\Delta F_{\sim n}$ accordingly until convergence is achieved.

More formally, the basic steps of the initial strain algorithm are given below. It is assumed the system is in equilibrium at time step i. The objective is to determine the response increments $\Delta \hat{u}_{\sim i}$, etc., for the next time step i + 1.

1. Calculate load increment $\Delta P_{\sim i}$.

2. Estimate $\Delta F_{\sim n_i} = \Delta F_{\sim n_{i-1}}$.

3. Solve (back substitute): $K_{\sim L} \Delta \hat{u}_{\sim i} = \Delta P_{\sim i} + \Delta F_{\sim n_i}$.

4. Recalculate $F_{\sim n_i} = \sum \left[\int_V B^T_{\sim}(D_{\sim L} - D_{\sim n}) B_{\sim} \, dv \right] \Delta \hat{u}_{\sim i}$.

13

5. Compare successive estimates of ΔF_{n_i} or $\Delta \hat{u}_i$. If converged, go to Step 6. Otherwise, repeat iteration loop 3-4-5.

6. Advance load step, and return to Step 1.

The most significant feature of the initial strain algorithm is that K_L need only be triangularized once at the outset of the calculations, thereby allowing rapid solutions by back substitution. Furthermore, within the iteration loop, the matrix D_n need not be assumed constant but can be simultaneously modified in accordance with $\Delta \hat{u}$.

The initial strain algorithm will vary slightly for different constitutive theories (e.g., plasticity, viscoelasticity, and visco-plasticity). Nonetheless, the basic features remain the same.

SUMMARY

The intent of this section was to provide the reader with the framework for implementing the constitutive theories to be discussed. Moreover, it is hoped that an appreciation for some common assumptions inherent in nonlinear constitutive models was achieved. To wit, an incremental constitutive equation of the form $\Delta \sigma = D_n \Delta \varepsilon$ is the desired objective.

Chapter 2

PLASTICITY THEORY

INTRODUCTION

The original intention of this section was to provide a review of classical plasticity theory for the purpose of establishing notation and concepts to be used later in the presentation of viscoplasticity. However, upon reviewing plasticity literature, no single presentation was found that could be termed 'classical' in the sense that it was both complete and conceptually instructive. For example, introductory texts [13,14] deal almost exclusively with a particular form of plasticity, e.g., Prandtl-Reuss equations with isotropic hardening. Thus, their treatment is incomplete. On the other end of the scale, the presentation offered by Nayak and Zienkiewicz [15] is a unified, complete plasticity theory formulation; however, it offers lit. , in the way of conceptual insights. Furthermore, nowhere in the literature is there a general treatment of the "universal hardening law" which combines kinematic and isotropic hardening into a unified theory. This concept was originally introduced by Hodge [16], and further discussed by Goel and Malvern [17], but it has not yet been treated in a unified manner.

This presentation is an attempt at a unified plasticity theory with universal hardening. Moreover, an original one-dimensional model is presented that offers an insight into the nature of isotropic, kinematic, and universal hardening. Accordingly, it is hoped the developments herein will offer more than a simple review.

The final objective of this plasticity presentation is to obtain a constitutive relationship compatible with the finite element formulations previously developed. In particular, the following relationship is desired:

$$\Delta \underset{\sim}{\sigma} = \underset{\sim}{D}_{ep} \, \Delta \underset{\sim}{\varepsilon} \tag{2-1}$$

where $\Delta \underset{\sim}{\sigma}$ = stress increment vector

$\Delta \underset{\sim}{\varepsilon}$ = strain increment vector

$\underset{\sim}{D}_{ep}$ = incremental elasti -plastic constitutive matrix

To achieve this objective, a rather detailed development of plasticity theory is offered which ultimately produces the desired matrix $\underset{\sim}{D}_{ep}$. Lastly, the initial strain finite element formulation for plasticity is presented.

PLASTICITY ASSUMPTIONS AND CONDITIONS

Common to all plasticity developments is the assumption that total strain increment can be decomposed into elastic and plastic components, and further, it is assumed the stress increment is persistently related to the elastic strain increment through generalized Hook's law. That is:

$$\Delta \underset{\sim}{\varepsilon} = \Delta \underset{\sim}{\varepsilon}_e + \Delta \underset{\sim}{\varepsilon}_p \tag{2-2}$$

16

$$\Delta\sigma = \underset{\sim}{D}_e \ \underset{\sim}{\Delta\varepsilon}_e \qquad\qquad (2\text{-}3)$$

where $\underset{\sim}{\Delta\varepsilon}_e$ = elastic strain increment

$\underset{\sim}{D}_e$ = elastic constitutive matrix (Hook's law)

The above equations are universally assumed in all plasticity formulations known to the author, and indeed, are identical to the assumptions employed in the finite element initial strain formulations. In the course of this work some insights into the motivation of these assumptions will be given.

It is important to note that the developments presented herein assume plastic hardening. The special case of no hardening (perfect-plasticity) is easily dealt with once the general equations have been developed on the presumption of hardening.

In addition to the preceding assumptions, plasticity theory is built upon four basic conditions. These conditions are formally defined below and will be clarified in the ensuing discussion.

1. _Yield Condition_. A scalar function signifying when plastic yielding will occur. It is composed of a positive valued "loading function" and a "yield parameter" that is never less than the value of the loading function. Yielding can only occur when the loading function is equal to the yield parameter. The states of stress satisfying this condition form a hypersurface in stress space, termed the yield surface.

2. _Surface Hardening_. A law that "tracks" or measures the move-ment of the yield surface during plastic yielding. Traditionally, yield surface movement is restricted to uniform expansion (isotropic hardening) or "rigid body" translation (kinematic hardening). The former is denoted by an increase in the yield parameter, while the latter is denoted by a translation in stress space of the loading function. The

linear combination of kinematic and isotropic hardening constitutes
"universal hardening." (Note, perfect-plasticity implies no hardening,
i.e., yield surface never changes).

3. <u>Flow Rule</u>. An expression relating increments of plastic strain
to increments of stress. The magnitude of the incremental plastic
strain vector is dependent upon the magnitude of the stress increment
normal to the yield surface and a modulus known as the "hardening
coefficient." The direction of the incremental plastic strain vector
may be assumed normal to the yield surface (associative law), or normal
to some other hypersurface (nonassociative).

4. <u>Hardening Rule</u>. An expression or set of data points that pro-
vides the value of the "hardening coefficient" as a function of some
plastic deformation measure, such as plastic work or effective plastic
strain. (Note, this is distinct from the concept of "surface hardening"
described above because one can specify a hardening rule independent of
the form of surface hardening.)

In order to amplify and clarify these four concepts, a series of
one-dimensional conceptual models are introduced demonstrating the
nature of kinematic, isotropic, and universal surface hardening. For
each of the models, the associated one-dimensional yield condition is
generalized for multidimensional stress states. Also, the corresponding
rules for "tracking" the current location and size of the yield surface
are presented. Although the universal model embraces both the kinematic
and isotropic models, it is instructive to study the kinematic and
isotropic models individually to better appreciate the universal model.

The concept of the "flow rule" and the associated "hardening rule"
is presented after the generalized yield condition with universal hard-
ening. Lastly, having established the four basic concepts of plasticity,
expressions for D_{ep} are developed for the solution algorithms. Supple-
mentary discussions on loading functions and nonassociative flow rules
are given in Appendix A.

PLASTICITY CONCEPTS WITH ONE-DIMENSIONAL MODELS

Plastic deformation is often called frictional deformation because of the similarity between plasticity and the classical Coulomb frictional hypothesis for sliding bodies. To wit, plastic deformation (sliding movement) only occurs when the yield stress (frictional resistance) is exceeded by active loads. Moreover, during plastic deformation, the plastic work (dissipated energy) is independent of the rate of deformation (rate of sliding) and only dependent on the deformation path (sliding path).

This analogy between frictional theory and plasticity theory can be exploited to produce conceptual models that provide a keen insight into the behavior of elastic-plastic materials.

Kinematic Model

Figure 1a represents a one-dimensional elastic-plastic model with kinematic hardening. The sliding block obeys the Coulomb friction hypothesis in that the frictional resistance, σ_f, is a passive resistance, i.e., equal but opposite to the unbalance of active loads acting on the block. In accordance with the frictional hypothesis, the maximum frictional resistance obtainable is the block weight, W, times the coefficient of friction, μ. Without loss of generality, let $W = \sigma_y$ and $\mu = 1$ so that maximum frictional resistance is given by the constant σ_y.

The equilibrium equation of the block is $(\sigma - \sigma_p) - \sigma_f = 0$, where $|\sigma_f| \leq \sigma_y$.

The active load, σ, shall be called the "applied stress" and is transmitted to the block by the linear elastic spring, E_e, representing the elastic portion of the model. Clearly, the applied stress is related to the elastic strain, ε_e, by $\sigma = E_e \varepsilon_e$. The other active load, σ_p, shall be termed the "plastic tracking stress" and is related to the plastic strain, ε_p, by the relation $\sigma_p = E_p \varepsilon_p$. The spring modulus, E_p,
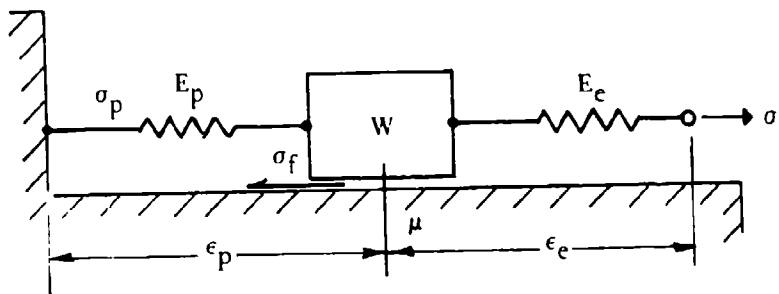
(a) Kinematic.
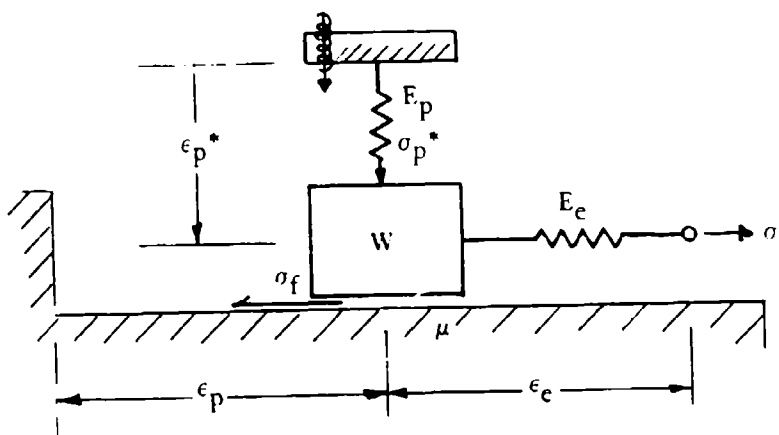
(b) Isotropic.
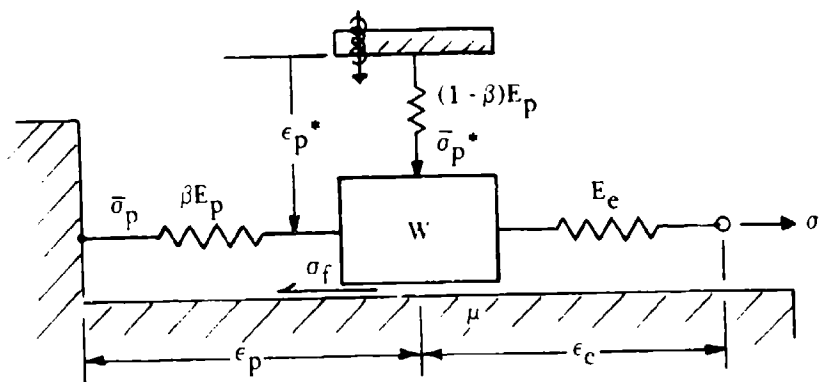
(c) Universal.

Figure 1. Hardening models.

may be assumed constant or considered a function of plastic work or plastic strain. Lastly, it is observed that the model implies that the total strain equals the elastic plus plastic strain; i.e., $\varepsilon = \varepsilon_e + \varepsilon_p$.

With these ground rules, it is instructive to study the model for one cycle of loading over the nominal range $-2.0\sigma_y < \sigma < 1.5\sigma_y$. Beginning with a virgin material specimen, a tensile load is applied. Within the load range $0 < \sigma < \sigma_y$, the model responds elastically as denoted by the segment OA in the stress-strain diagram in Figure 2. Upon further load increase ($\sigma > \sigma_y$), the maximum frictional resistance is exceeded ($\sigma_f = \sigma_y$), and the block moves an amount ε_p such that equilibrium is maintained; i.e., $\sigma_p = \sigma - \sigma_y$. This response implies plastic deformation is occurring and is denoted by the segment AB in Figure 2. The shape of segment AB is dictated by the definition of E_p. For example, if E_p is assumed zero (or nearly zero), the model would depict an elastic-perfectly plastic material, and AB would be a horizontal line. If E_p is assumed a positive constant, AB becomes the upper portion of a bilinear stress-strain curve with a slope equal to $E_p E_e / (E_p + E_e)$. Lastly, if E_p is assumed to be variable, say a function of plastic work, then a variety of shapes is possible as suggested in Figure 2.

After having subjected the model to the maximum load, $\sigma = \sigma_B$, the load is decreased, which produces the intriguing result that unloading is linear elastic; i.e., no block movement, only elastic spring movement. If this characteristic of the model is not obvious to the reader, recall that σ_f is a passive resistance, and reverse movement of the block cannot occur until the frictional resistance is fully reversed to its maximum value, σ_y. Clearly, elastic unloading of this model will always have a stress range of $2\sigma_y$ as typified by the segment BC in Figure 2. Upon further unloading, the block moves, which causes plastic straining in the reverse direction; this is denoted by the segment CD. As before, the shape of CD is dependent on the definition of E_p. Lastly, the load cycle is completed by reversing the load to zero, which produces the elastic response DE shown in Figure 2.
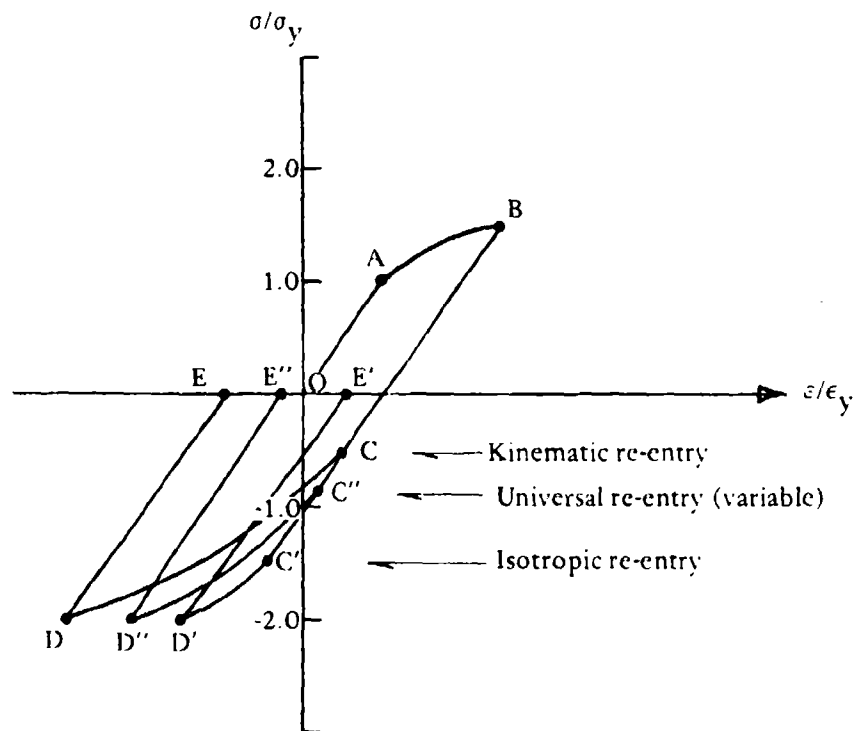
Figure 2.   Stress-strain path for kinematic, isotropic
and universal surface hardening.

Obviously this stress-strain path of the model closely resembles actual experimental data of many ductile materials loaded into the plastic range. Consequently, it is reasonable to describe the concepts of plasticity using the model as a visual aid.

A "yield condition" is described by the scalar function, F, which predicts whether or not the current stress state in the plastic range, that is, on the yield surface. With a little ingenuity, such a function can be found for the one-dimensional model by recalling plastic deformation (block movement) can only occur when the absolute value of the net active loads has mobilized the maximum frictional resistance, i.e.,

$$F(\sigma, \sigma_p) = \sqrt{(\sigma - \sigma_p)^2} - \sigma_y \qquad (2-4)$$

Clearly, F can never be greater than zero, since this would violate the equilibrium of the model. However, F can, and does, equal zero when the active loads have mobilized full frictional resistance, and yielding is occurring or about to occur. Lastly, if F is less than zero, the active loads produce a frictional resistance less than maximum, implying the stress state is in the elastic range. In short, F provides the means of determining whether or not the current state of stress is in the plastic domain (on the yield surface) or in the elastic domain (within the yield surface).

With the above insights in mind, it is possible to generalize the one-dimensional yield condition to a mult...imensional stress state yield condition (kinematic) as follows:

$$F(\underset{\sim}{\sigma}, \underset{\sim}{\sigma}_p) = f(\underset{\sim}{\sigma} - \underset{\sim}{\sigma}_p) - k_o \qquad (2-5)$$

where $f(\underset{\sim}{\sigma} - \underset{\sim}{\sigma}_p)$ = loading function

k_o = yield parameter (constant)

As before, F is the yield condition with the following properties:

F > 0   Impossible. A violation of equilibrium, i.e., inadmissible stress state.   (2-6a)

F = 0   Implies current stress state is on yield surface, i.e., in plastic domain. (All states of stress σ satisfying F = 0 form the current yield surface.)   (2-6b)

F < 0   Implies current stress state is within yield surface, i.e., in elastic domain.   (2-6c)

The loading function $f(\underset{\sim}{\sigma} - \underset{\sim}{\sigma}_p)$ is the single most important concept in plasticity theory. It is a positive-valued scalar function that measures the magnitude of a "select portion" of its argument $\underset{\sim}{\sigma} - \underset{\sim}{\sigma}_p$ that is responsible for plastic yielding. In the one-dimensional example (Equation 2-4) the loading function is given by $\sqrt{(\sigma - \sigma_p)^2}$, which implies the entire argument is responsible for plastic yielding. However, in a general multidimensional stress state, the vector argument of the loading function allows a great deal of freedom in choosing the form of the loading function. For example, some materials, such as ductile metals, exhibit plastic responses due to shearing stresses, but show no plastic response when subjected to hydrostatic stresses. Thus, it would be appropriate to define a loading function that increases with shear

24

stress but not with hydrostatic stress, such as the second invariant of deviatoric stress J_2. Other materials, such as soils, demonstrate plastic responses due to various combinations of the stress invariants.

The literature is full of a wide variety of proposed loading functions for different materials. Several common loading functions are presented in Appendix A. For now, it is only important to appreciate that the loading function acts like a filter in the sense it only increases or decreases its value for some predefined "select portion" of the stress vector considered to be responsible for plastic yielding. All other components of stress are filtered out and do not influence the value of the loading function.

To better appreciate the significance of the loading function, consider Figure 3. Assume $F = 0$, which implies the current state of stress is on the yield surface. Also suppose an arbitrary stress increment, $\Delta \sigma$, is applied to the current stress state. Will this cause plastic deformation? To answer this, it is merely necessary to know if the stress increment has any components in the direction of the outward normal of the loading function, i.e., in the direction that the yield surface moves. The dot product of the stress increment with the loading function gradient (which is in direction of outward normal) provides a simple test with three possible results:

$$f_{\sim 0}^{T} \cdot \Delta\sigma > 0 \qquad \text{Plastic loading; i.e., at least some}$$
portion of $\Delta\sigma$ is colinear with outward
surface normal. Surface moves out. $\qquad$ (2-7a)

$$f_{\sim 0}^{T} \cdot \Delta\sigma = 0 \qquad \text{Neutral loading, no plastic deformation}$$
occurs; i.e., $\Delta\sigma$ is in the tangent plane
of the loading surface. Surface does not
move. $\qquad$ (2-7b)
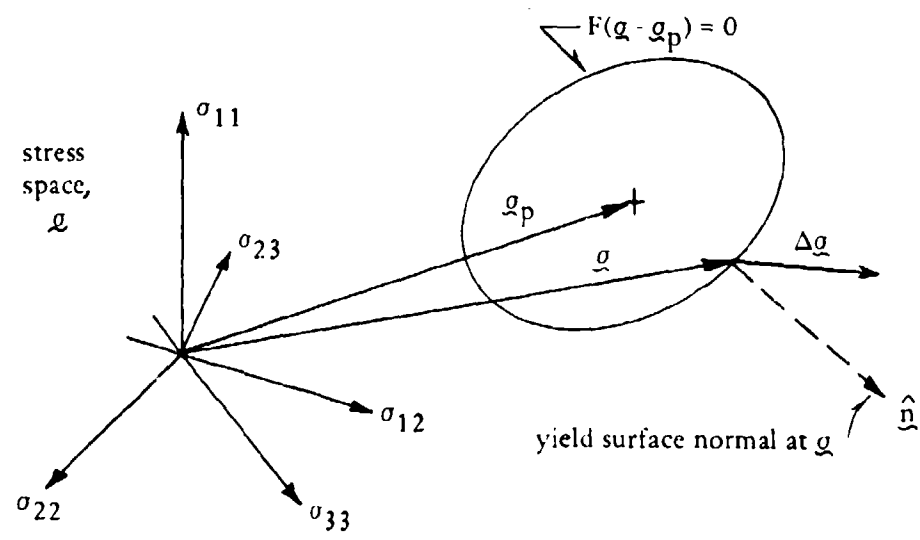
Figure 3.   Yield surface representation.

26

$$\underset{\sim}{f_\sigma}{}^T \cdot \underset{\sim}{\Delta\sigma} < 0 \quad \text{Elastic unloading occurs; i.e., at least}$$

Elastic unloading occurs; i.e., at least
some portion of $\Delta\sigma$ is colinear with the
inward surface normal. Surface does not
move. (2-7c)

where $\underset{\sim}{f_\sigma} = \partial f/\partial\underset{\sim}{\sigma}$ is the loading function gradient, and is in the direction of the outward normal.

Clearly, the importance of the loading function cannot be over-stressed since it dictates what stress increments promote plastic yielding.

The yield parameter, k_o, in Equation 2-5 is a material dependent constant and may be geometrically interpreted as the "radius" of the yield surface. The value of k_o may be determined from any type of standard laboratory test by evaluating the loading function at the stress state producing initial yielding, i.e., $k_o = f(\underset{\sim}{\sigma_y})$, where $\underset{\sim}{\sigma_y}$ is the stress vector producing initial yielding.

In general, "surface hardening" is a simple concept, as it merely pertains to keeping track of the "radius" and "center" of the yield surface (not to be confused with hardening rule for H' discussed later). For the kinematic model under discussion, the radius of the yield surface remains constant, i.e., σ_y for a one-dimensional model, and k_o for the general model. However, the "center" translates every time plastic deformation occurs. The amount of translation can be deduced by considering the total derivative of the yield condition.

To see this, first consider the one-dimensional model. Initially, $\sigma = \sigma_p = 0$, and the radius is σ_y with the center at the origin. As soon as the load σ reaches the yield stress, the yield condition is isfied, i.e., $F = 0$ and the total derivative, $dF = 0$, must also be satisfied. That is, from Equation 2-4:

$$dF = 0 = \Delta\sigma - \Delta\sigma_p \qquad (2-8)$$

In the above $\Delta\sigma$ and $\Delta\sigma_p$ are actually differentials $d\sigma$ and $d\sigma_p$; however, throughout this writing the incremental symbol "Δ" will be used to emphasize numerical approximations. Equation 2-8 simply states that any increment $\Delta\sigma$ of the applied stress is immediately followed by an equal increment $\Delta\sigma_p$ of the plastic tracking stress. This implies the "center" of the elastic range shifts an amount $\Delta\sigma_p$, while the "radius" of the elastic range remains a constant σ_y. Noting σ_p is the sum of its increments, $\sigma_p = \Sigma\Delta\sigma_p$, a geometric interpretation of the plastic tracking stress can be offered. Namely, σ_p is the current center of the elastic range as it translates up or down the stress axis. This concept is demonstrated in Figure 4, wherein the center and radius of the elastic range are shown at various load points corresponding to Figure 2.

This geometric interpretation of the plastic tracking stress also applies to multiaxial stress states in that the yield surface translates rigidly (constant radius k_o) in stress space with its "center" located by σ_p as suggested in Figure 5.

To prove this for the general kinematic case, it is necessary to assume the direction of $\Delta\underset{\sim}{\sigma}_p$ during yielding. In the one-dimensional case, this was not necessary since only one direction was possible. Prager [18] made the assumption that $\Delta\underset{\sim}{\sigma}_p$ is in the direction of the outward normal of the loading function, i.e., in the direction of its gradient.

In light of Equation 2-7b, Prager's assumption has great intuitive appeal since it implies $\Delta\underset{\sim}{\sigma}_p$ is in the direction of the select portion of the applied stress that causes plastic yielding. Therefore, it is assumed:

$$\Delta\underset{\sim}{\sigma}_p = C\,\underset{\sim}{f}_{\sigma}$$
(2-9)

where $\underset{\sim}{f}_{\sigma} = \partial f/\partial\underset{\sim}{\sigma}$, loading function gradient with respect to $\underset{\sim}{\sigma}$

C = scalar constant to be determined
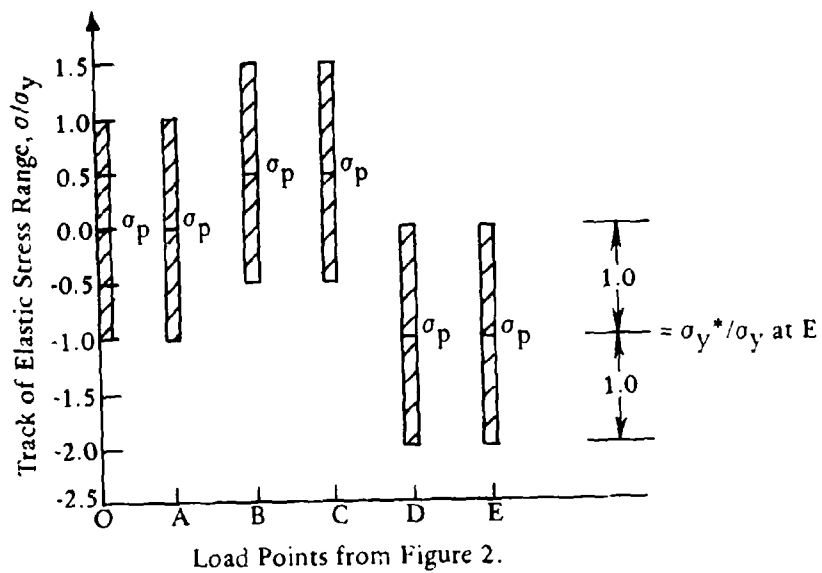
Figure 4.   One-dimensional kinematic surface hardening.
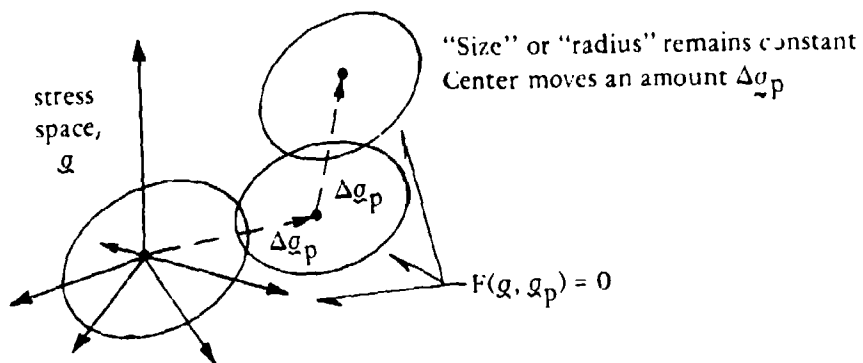
Figure 5.   Multidimensional kinematic surface hardening.

29

The value of C is obtained by taking the total derivative of the yield condition (Equation 2-5) which must be zero during yielding, i.e.,

$$dF = 0 = \underset{\sim}{f}_\sigma^T \cdot \Delta\underset{\sim}{\sigma} + \underset{\sim}{f}_{\sigma_p}^T \cdot \Delta\underset{\sim}{\sigma}_p \qquad (2\text{-}10)$$

where $\underset{\sim}{f}_{\sigma_p} = \partial f / \partial\underset{\sim}{\sigma}_p$, loading function gradient vector with respect to $\underset{\sim}{\sigma}_p$.

Because the argument of the loading function has the special form, $\underset{\sim}{\sigma} - \underset{\sim}{\sigma}_p$, it is trivial to show that $\underset{\sim}{f}_\sigma = -\underset{\sim}{f}_{\sigma_p}$ for any function f. Therefore, Equation 2-9 can be combined with 2-10 to give:

$$C = (\underset{\sim}{f}_\sigma^T \cdot \Delta\underset{\sim}{\sigma}) / (\underset{\sim}{f}_\sigma^T \cdot \underset{\sim}{f}_\sigma)$$

Returning to Equation 2-9, the desired relationship is obtained:

$$\Delta\underset{\sim}{\sigma}_p = (\hat{\underset{\sim}{n}}^T \Delta\underset{\sim}{\sigma})\hat{\underset{\sim}{n}} \qquad (2\text{-}11)$$

$$\hat{\underset{\sim}{n}} = \underset{\sim}{f}_\sigma / \sqrt{\underset{\sim}{f}_\sigma^T \underset{\sim}{f}_\sigma} \qquad (2\text{-}12)$$

where $\hat{\underset{\sim}{n}}$ is the unit outward normal of the loading function.

Equation 2-11 provides the rule for determining the increment of plastic tracking stress for every applied stress increment $\Delta\underset{\sim}{\sigma}$. The total sum of the plastic tracking stress increments, i.e., $\underset{\sim}{\sigma}_p = \Sigma\Delta\underset{\sim}{\sigma}_p$, provides the coordinates for tracking the "center" of the yield surface as was suggested in Figure 5.

This completes the general development for the kinematic yield condition and surface tracking rules. Next, isotropic hardening is examined.

Isotropic Model

Figure 1b is a one-dimensional representation of an elastic-plastic model with isotropic hardening. All of the ground rules previously described for the kinematic model still hold. The only difference is that the spring E_p has been moved to act vertically on the block as shown. Furthermore, it is imagined some servo-mechanism compresses this spring an amount $|\varepsilon_p|$ everytime the block moves a distance ε_p in either direction. The accumulation of all plastic strain movements is denoted by ε_p^*; i.e., $\varepsilon_p^* = \Sigma|\varepsilon_p|$.

The significant consequence of this new model is that the load σ_p has been transformed from the status of an active load into a passive frictional resistance and is hereby renamed as σ_p^*. Accordingly, the maximum frictional resistance is no longer constant, but rather is given by $\sigma_{f_{max}} = \sigma_y + \sigma_p^*$, where $\sigma_p^* = E_p \varepsilon_p^*$. Equilibrium of the model is given by $\sigma - \sigma_f = 0$, where $\sigma_f \leq \sigma_{f_{max}}$.

With the above in mind, it is instructive to trace the performance of the new model through a loading cycle as was previously done for the kinematic model. Beginning with a virgin specimen and referring back to Figure 2, the initial elastic loading follows the same path OA as the kinematic model. Furthermore, the identical curve AB is traced with a loading above σ_y. This is because $\varepsilon_p^* = \varepsilon_p$, which implies $\sigma_p^* = \sigma_p$, and, hence, both models have identical equilibrium equations. At point B unloading begins. The block cannot move backward until the applied stress σ completely reverses the current maximum frictional resistance $(\sigma_{f_{max}} = \sigma_B)$. Therefore, elastic unloading continues to point C', where $\sigma = -\sigma_B$. With additional negative loading the curve C'D' is traced. Note C'D' has the same shape as CD; however, it is rigidly shifted along the elastic unloading path an amount $C'C = 2(\sigma_B - \sigma_y)$.

It is evident that the kinematic and isotropic models will produce extraordinarily different results after a few loading cycles even though E_p and E_e are the same for both models. However, the models will give identical results as long as the load is monotonically increasing.

The yield condition for the one-dimensional isotropic model can be written as:

$$F(\sigma, \sigma_y^*) = \sqrt{\sigma^2} - \sigma_y^* \qquad (2\text{-}13)$$

where $\sigma_y^* = \sigma_y + \sigma_p^*$, the yield stress parameter.

Generalizing the isotropic yield condition to multidimensional stress states gives:

$$F(\underset{\sim}{\sigma}, k^*) = f(\underset{\sim}{\sigma}) - k^* \qquad (2\text{-}14)$$

where $f(\underset{\sim}{\sigma})$ = loading function

k^* = yield parameter (increases with plastic deformation)

As before, the yield condition, F, denotes whether the current state of stress is in the elastic or plastic domain, and has the properties given by Equations 2-6a, 2-6b. and 2-6c.

The concept of the loading function is the same as described for the kinematic model, and it has the properties given by Equations 2-7a, 2-7b, and 2-7c. The only difference is that the argument is composed of the stress vector $\underset{\sim}{\sigma}$ rather than the stress vector difference $\underset{\sim}{\sigma} - \underset{\sim}{\sigma}_p$; consequently, the "center" of the yield surface remains fixed at the origin of stress space.

32

The "radius" of the yield surface is measured by the yield parameter $k*$ which increases with plastic deformation. A pictorial representation of isotropic surface hardening for the one-dimensional load cycle is shown in Figure 6, whereas Figure 7 illustrates isotropic hardening in a multidimensional stress state.

To determine the amount the yield surface expands for every applied stress increment causing plastic deformation, the total derivative of Equation 2-14 is set to zero to give:

$$dF = 0 = \underset{\sim}{f_\sigma}^T \cdot \underset{\sim}{\Delta\sigma} - \Delta k* \qquad (2-15)$$

Equation 2-15 provides the surface hardening rule for updating the "radius" of the yield surface after every increment of applied stress. Specifically, $k* = k_o + \Sigma\Delta k*$, where k_o is the initial yield parameter (radius) and $\Delta k* = \underset{\sim}{f_\sigma}^T \cdot \underset{\sim}{\Delta\sigma}$.

Universal Model

The kinematic and isotropic responses, as displayed in Figure 2, represent two extreme predictions for re-entry into the plastic domain. Most ductile materials exhibit a re-entry point "C" somewhere between the points C and C'. Clearly, it would be desirable to choose a surface hardening model that allows some flexibility in selecting the "radius" and "center" of the yield surface.

The "universal surface hardening" concept provides this flexibility by taking a linear combination of the kinematic and isotropic models. Figure 1c illustrates this concept with a one-dimensional model, wherein β is a weighting parameter ($0 < \beta < 1$) applied to the vertical load, σ_p*, and the remaining weight $1-\beta$ is applied to the horizontal load, σ_p. If $\beta = 0$, the universal model reduces to the isotropic form; if $\beta = 1$,
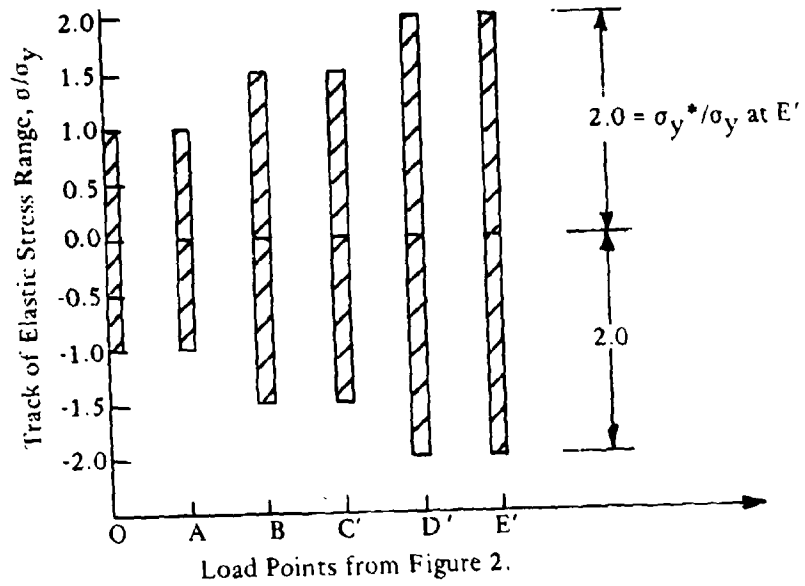
Figure 6.   One-dimensional isotropic surface hardening.
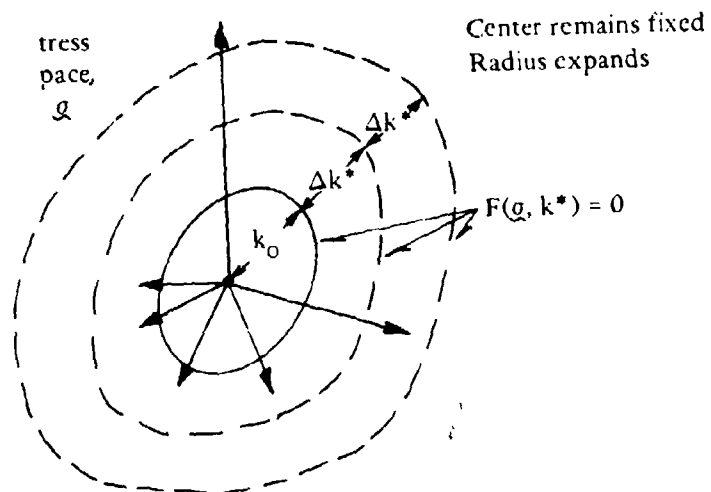
Figure 7.   Multidimensional isotropic surface hardening.

34

the kinematic form is attained. Any other value of β combines the characteristics of both models so that both radius and center of the yield surface change during plastic deformation. For example, the universal model will re-enter the plastic range at point C" in Figure 2 if β is chosen as the ratio: $\beta = CC''/CC'$.

The ground rules for this one-dimensional model are the same as stated for the kinematic and isotropic models; therefore, during initial monotonic loading, the stress-strain curve of this model follows the same path OAB in Figure 2 for any value of β. However, after elastic unloading and re-entry into the plastic domain at point C" the stress-strain path for all future load cycles is a unique function of β. (Note, for added generality, β could be specified as a function of the number of load cycles, $\beta = \beta(n)$, thereby allowing the model to shift from isotropic to kinematic or vice-versa during load cycling.)

Equilibrium of the universal model can easily be deduced as:

$$(\sigma - \beta \sigma_p) - \sigma_f = 0$$

where
$$\sigma_{f_{max}} = \sigma_y + (1 - \beta)\dot{\sigma}_p{}^*$$

$$|\sigma_f| \leq \sigma_{f_{max}}$$

The corresponding one-dimensional yield condition is given by:

$$F(\sigma,\bar{\sigma}_p,\bar{\sigma}_y{}^*) = \sqrt{(\sigma - \bar{\sigma}_p)^2} - \bar{\sigma}_y{}^* \qquad (2\text{-}16)$$

where $\quad \bar{\sigma}_p = \beta\, \sigma_p$

$\quad\quad\quad \bar{\sigma}_y{}^* = \sigma_y + (1 - \beta)\sigma_p{}^*$

Generalizing the universal yield condition to multidimensional stress states gives:

$$F(\underset{\sim}{\sigma}, \underset{\sim}{\bar{\sigma}}_p, \bar{k}^*) \;=\; f(\underset{\sim}{\sigma} - \underset{\sim}{\bar{\sigma}}_p) \;-\; \bar{k}^* \qquad\qquad (2\text{-}17)$$

where $\quad \underset{\sim}{\bar{\sigma}}_p = \beta\, \underset{\sim}{\sigma}_p$, "weighted" plastic tracking stress

$\quad\quad\quad \bar{k}^* = k_o + (1 - \beta)k^*$, weighted yield parameter

As always, F is the yield condition with the properties denoted in Equations 2-6a, 2-6b, and 2-6c, and f is the specified loading function whose gradient can be used for the plastic yielding test denoted by Equations 2-7a, 2-7b, and 2-7c.

The vector $\underset{\sim}{\bar{\sigma}}_p$ and the scalar $\bar{k}^*$ specify the origin and the radius, respectively, of the universal yield surface. Figure 8 demonstrates the concept of universal hardening for the one-dimensional load cycling, while Figure 9 portrays an example evolution of the yield surface in multidimensional stress space.

To determine the amount of radius expansion $\Delta\bar{k}^*$ and center shift $\Delta\underset{\sim}{\bar{\sigma}}_p$ for any applied stress increment causing plastic deformation (F = 0), the total derivative of Equation 2-17 could be set to zero to permit solving for $d\underset{\sim}{\bar{\sigma}}_p$ and $d\bar{k}^*$ in terms of $\underset{\sim}{f}{}_\sigma{}^T$ and $d\underset{\sim}{\sigma}$. However, it is far simpler to directly use the definitions of $\bar{\sigma}_p$ and $\bar{k}^*$ from Equation 2-17 to determine the derivatives; i.e., $\Delta\bar{k}^* = (1 - \beta)\Delta k^*$ and $\Delta\underset{\sim}{\bar{\sigma}}_p = \beta\,\Delta\underset{\sim}{\sigma}_p$. With the aid of Equations 2-11, 2-12, and 2-15, the increments of the radius and center of the universal yield surface are:

$$\Delta \bar{k}^* = (1 - \beta) f_{\sim\sigma}^T \Delta\sigma \qquad (2\text{-}18)$$

$$\Delta\bar{\sigma}_{\sim F} = \beta(\hat{n}_{\sim}^T \cdot \Delta\sigma_{\sim})\hat{n}_{\sim} \qquad (2\text{-}19)$$

Thus, the universal surface hardening rule may be written as:

$$\bar{k}^* = k_o + \sum \Delta\bar{k}^* \qquad (2\text{-}20)$$

$$\bar{\sigma}_p = \sum \Delta\bar{\sigma}_{\sim p} \qquad (2\text{-}21)$$

where $\bar{k}^*$ is the current "radius" of the yield surface, and $\bar{\sigma}_p$ is the current vector from the origin of stress space to the "center" of the yield surface.

Flow Rule

The purpose of a flow rule is to define increments of plastic strain accompanying an increment of applied stress during plastic yielding ($F = 0$). For any and all of the one-dimensional models this is a straight-forward application of the ground rules, and it is easy to deduce the flow rule to be:

$$\Delta\varepsilon_p = \frac{1}{E_p'} \Delta\sigma \qquad (2\text{-}22)$$
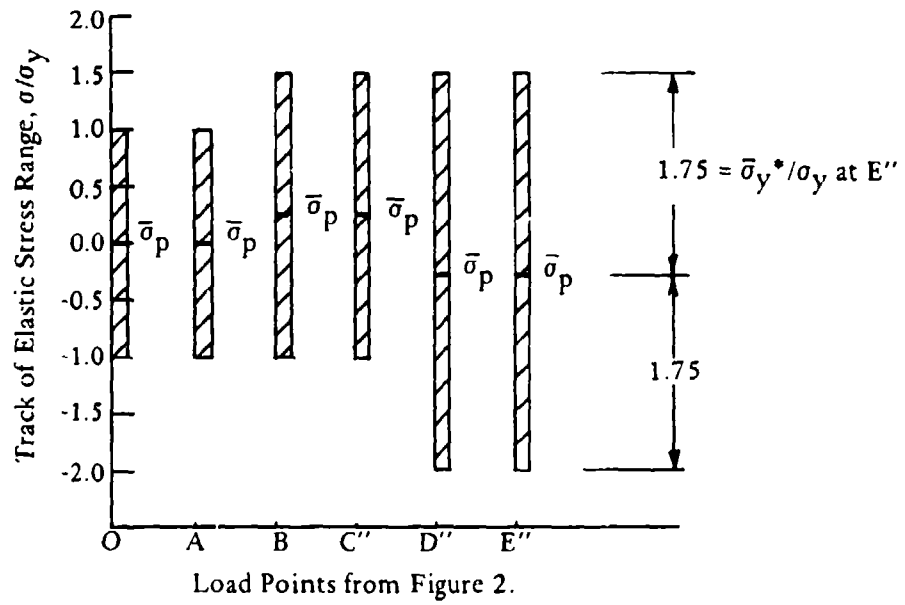
Figure 8.   One-dimensional universal hardening with
            $\beta = 1/2$.
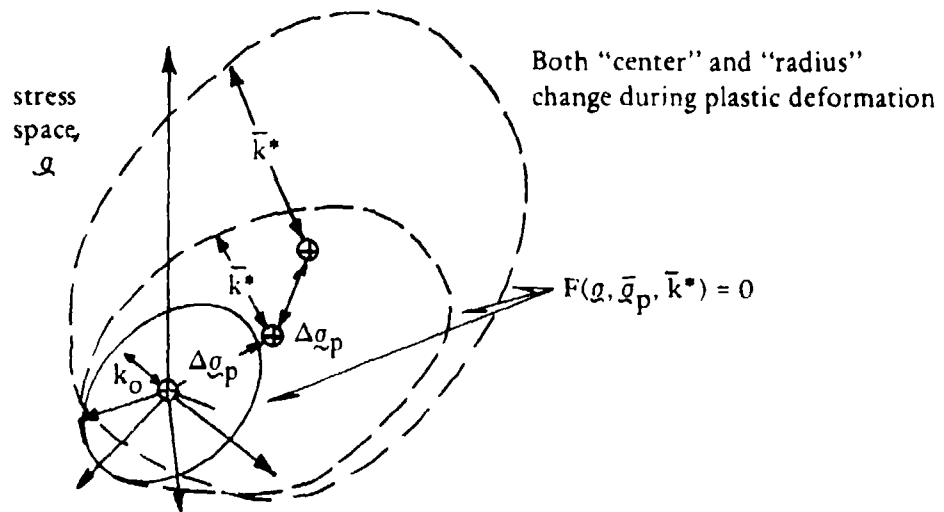
Figure 9.   Multidimensional universal surface hardening.

where E_p' is the tangent value of the uniaxial curve relating total plastic strain to total stress as illustrated in Figure 10.

When the flow rule is generalized to multidimensional stress-strain states, the development is not quite as simple. The complication is due to the fact that now the plastic strain increment is a vector; therefore, it must be defined with respect to direction as well as to magnitude. (Note, in the one-dimensional idealization, direction and magnitude were one.)

Thus, for the general case, the plastic strain increment vector may be described by

$$\Delta \varepsilon_{\sim p} = d\lambda \; \hat{\underset{\sim}{m}} \tag{2-23}$$

where $\hat{\underset{\sim}{m}}$ is some directional vector (in stress or strain space) of unit magnitude, and $d\lambda$ is a scalar denoting the magnitude of the plastic strain increment. To determine $d\lambda$ and $\hat{\underset{\sim}{m}}$ require assumptions similar to the assumptions made for the plastic tracking stress vector.

The first assumption is based on the observation that the magnitude of the plastic strain increment should be proportional to the magnitude of the applied stress increment which is colinear with the outward normal $(\hat{\underset{\sim}{n}})$ of the loading function; i.e.,

$$d\lambda = \frac{1}{H'} \; (\hat{\underset{\sim}{n}}^T \, \Delta\sigma) \tag{2-24}$$

The inner product, $\hat{\underset{\sim}{n}}^T \Delta\sigma$, is the scalar measure of stress that pushes the yield surface outward, and H' is a hardening coefficient (modulus) determined from experimental tests. H' will be discussed further in the hardening rule.
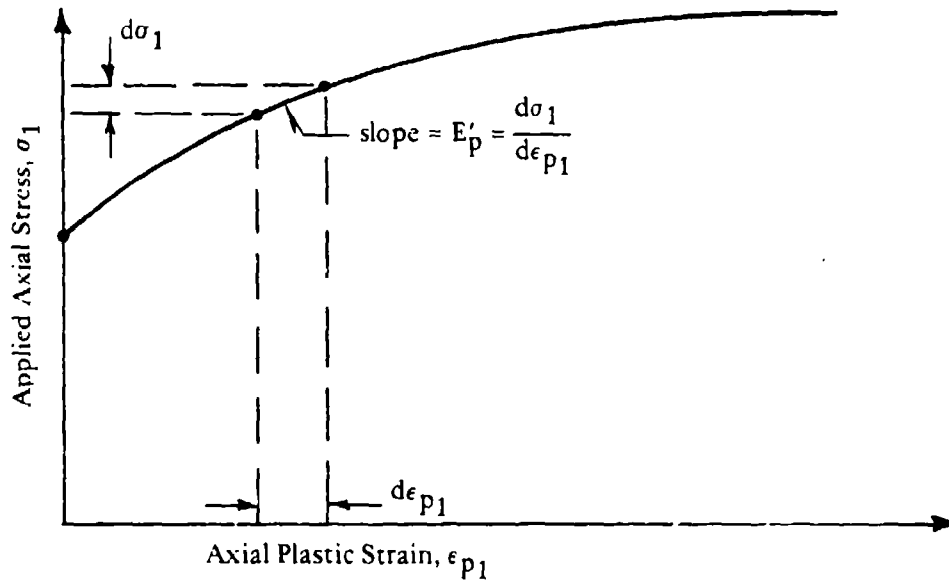
Figure 10. Shape of stress-plastic strain curve.

With regard to the direction $\hat{\underset{\sim}{m}}$ of the plastic strain increment, two assumptions are available. By far the most common is the so-called "associative flow rule assumption." Here, the idea is that plastic straining occurs in the same direction as the outward normal of the loading function. Although this may be aesthetically pleasing, it is still only an assumption. Other plastic potential functions (loading functions) could just as well be used to predict the direction of the plastic strain. In such cases, the procedure is termed "nonassociative flow rule assumption."

In short, the direction $\hat{\underset{\sim}{m}}$ has two possibilities:

$$\hat{\underset{\sim}{m}} = \hat{\underset{\sim}{n}} \qquad \text{associative flow law} \qquad (2\text{-}25a)$$

$$\hat{\underset{\sim}{m}} \neq \hat{\underset{\sim}{n}} \qquad \text{nonassociative flow law} \qquad (2\text{-}25b)$$

More on nonassociative flow rules is given in Appendix B.

Inserting Equation 2-24 into Equation 2-23 and with the understanding of Equation 2-25, the general flow rule is:

$$\Delta\underset{\sim}{\varepsilon}_p = \frac{1}{H'} (\hat{\underset{\sim}{n}}^T \Delta\underset{\sim}{\sigma})\hat{\underset{\sim}{m}} \qquad (2\text{-}26)$$

Hardening Rule

The hardening coefficient, H', is the only quantity that remains to be defined. The value of H' must be determined from experimental results consistent with Equation 2-26. That is, H' is dependent on $\hat{\underset{\sim}{n}}$ and $\hat{\underset{\sim}{m}}$ as well as $\underset{\sim}{c}$ and $\underset{\sim}{\varepsilon}$. As an example, suppose it is decided to determine H'

41

by means of a simple tension test. Let the curve in Figure 10 represent axial stress versus plastic strain (i.e., elastic strains have been subtracted from total strains). Since all components of stress are zero except σ_1, the inner product in Equation 2-26 is simply $\Delta\sigma_1 n_1$. Also, Equation 2-26 is valid for every component of plastic strain, in particular, it is valid for $\Delta\epsilon_{p_1}$. Therefore, $H' = m_1 n_1 (\Delta\sigma_1 / \Delta\epsilon_{p_1})$, or using Equation 2-22 the hardening coefficient determined from a tensile (or compression) test is:

$$H' = m_1 \, n_1 \, E_p' \qquad (2-27)$$

For the special case where a Von Mises loading function and an associative flow rule is assumed, $n_1 = m_1 = 2/\sqrt{6}$, and $H' = 2/3\ E_p'$.

Furthermore, it is emphasized that the determination of H' is not restricted to tensile tests. Any type of experimental data can be used to determine H' providing Equation 2-26 is used consistently.

In the event H' is constant throughout the loading path, no additional assumptions are necessary, and the flow rule is well defined for all stress states. However, in general, H' varies throughout the load path as implied in Figure 10. This gives rise to the need of a "hardening rule," wherein H' is assumed to be a function of some plastic response. The first inclination is to consider H' a function of the magnitude of plastic strain, i.e., $H' = \epsilon_p^o$, where ϵ_p^o is plastic strain magnitude given by $\epsilon_p^o = \sqrt{\epsilon_{\sim p}^T \cdot \epsilon_{\sim p}}$. Although this assumption is adequate for a monotonic radial loading, for general loadings it produces results unrepresentative of actual material behavior. For example, consider the response of the one-dimensional kinematic model shown in Figure 2. If $E_p' = E_p'(\epsilon_p^o)$, then, during the reverse loading phase, the value of ϵ_p^o reduces. This results in an increased value of E_p', and the shape of segment CD is concave up rather than concave down as desired.

42

To avoid this anomaly, the hardening rule must be based on some nondecreasing measure of plastic response. Two such measures are commonly employed: plastic work and "total" plastic strain. The former is known as the "work hardening rule" and simply asserts that H' is a function of the plastic work per unit volume, W_p:

$$H' = H'(W_p) \qquad (2\text{-}28)$$

where $\quad W_p = \int \underset{\sim}{\sigma}^T \, d\underset{\sim}{\varepsilon}_p$

The second method is known as "strain hardening," wherein it is assumed that H' is a function of the "total path" of the plastic strain magnitude, $\varepsilon_p{}^*$:

$$H' = H'(\varepsilon_p{}^*) \qquad (2\text{-}29)$$

where $\quad \varepsilon_p{}^* = \sum \Delta \varepsilon_p{}^o$

Note: $\varepsilon_p{}^*$ is not the same measure as $\varepsilon_p{}^o$, since $\varepsilon_p{}^*$ increases with every increment $\Delta\varepsilon_p$; however, $\varepsilon_p{}^o$ is the measure of current plastic strain magnitude regardless of the path.

The choice of one hardening rule over the other is largely a matter of computational convenience. By either rule, H' is generally not known as a continuous function, but rather as discrete points of the plastic work or total plastic strain as suggested in Figure 11. It is a trivial matter to store the discrete points in the computer and interpolate to find the current value of H'.

43
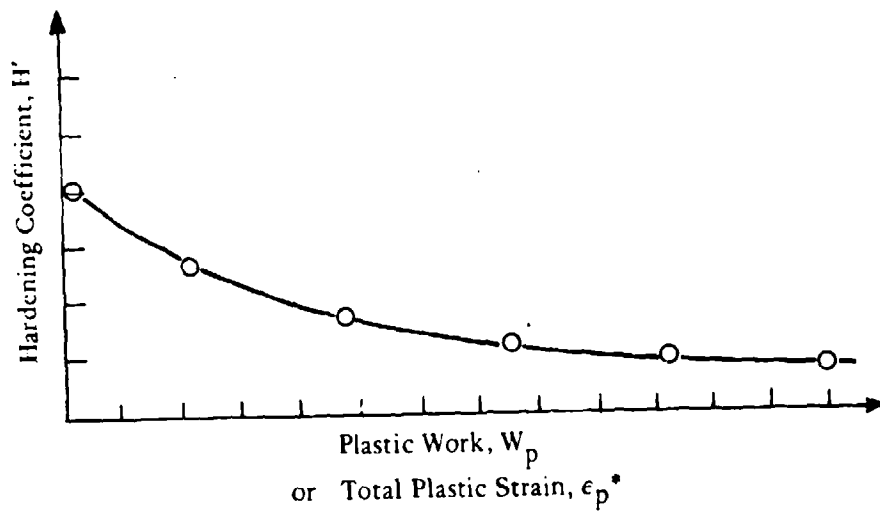
Figure 11. Hardening coefficient versus plastic
work or total plastic strain.

INCREMENTAL PLASTICITY RELATIONS

The four basic concepts of plasticity have been presented. The remaining job is to pull the pieces together to find the matrix quantity D_{ep} denoted in Equation 2-1.

Beginning with the combination of Equations 2-2 and 2-3, $\Delta\sigma$ is given as:

$$\Delta\sigma = D_e(\Delta\varepsilon - \Delta\varepsilon_p) \tag{2-30}$$

Taking the dot product of Equation 2-30 with respect to the unit gradient of the loading function $\hat{n}^T$, and replacing $\Delta\varepsilon_p$ by Equation 2-26, the scalar quantity $(\hat{n}^T \Delta\sigma)$ can be determined as:

$$\hat{n}^T \Delta\sigma = \frac{\hat{n}^T D_e \Delta\varepsilon}{1 + (\hat{n}^T D_e \hat{m})/H'} \tag{2-31}$$

Using Equation 2-31 in Equation 2-26, the plastic strain increment is related to the total strain increment by:

$$\Delta\varepsilon_p = C_p D_e \Delta\varepsilon \tag{2-32}$$

$$\text{where} \quad C_p = \frac{\hat{m} \hat{n}^T}{H' + (\hat{n}^T D_e \hat{m})}$$

Lastly, inserting Equation 2-32 into Equation 2-30, the desired stress-strain relationship is achieved:

$$\Delta\underset{\sim}{\sigma} = (\underset{\sim}{D}_e - \underset{\sim}{D}_p)\Delta\underset{\sim}{\varepsilon} \qquad (2\text{-}33)$$

where $\underset{\sim}{D}_p = \underset{\sim}{D}_e \underset{\sim}{C}_p \underset{\sim}{D}_e$

Equation 2-33 is the key incremental stress-strain relationship for use in elastic-plastic boundary value problems. The plasticity matrix, $\underset{\sim}{D}_p$, is dependent on the variables H' and $\hat{\underset{\sim}{n}}$ (and $\hat{\underset{\sim}{m}}$ for nonassociative law). Traditionally, these quantities are updated at the beginning of each load step and are assumed to be constant over the load increment. These concepts will be discussed later when the plasticity relationships are incorporated into a finite element formulation. For now, the plasticity constitutive theory is reviewed.

SUMMARY OF CONSTITUTIVE THEORY OF PLASTICITY

For easy reference, the pertinent plasticity relationships for universal hardening are listed below.

The universal yield condition is:

$$F(\underset{\sim}{\sigma},\bar{\underset{\sim}{\sigma}}_p,\bar{k}^*) = f(\underset{\sim}{\sigma} - \bar{\underset{\sim}{\sigma}}_p) - \bar{k}^* \qquad (2\text{-}34)$$

F is the yield function, such that F = 0 implies yielding. $\underset{\sim}{\sigma}$ is the total stress vector, $\bar{\underset{\sim}{\sigma}}_p$ is the plastic tracking stress locating the

"center" of the yield surface, and $\bar{k}*$ is a scalar stress measure defining "radius" of the yield surface. The function f is the prescribed loading function.

The surface hardening law is given by:

$$\Delta\bar{k}* \;=\; (1 - \beta)\underset{\sim\sigma}{f}^{T}\,\Delta\underset{\sim}{\sigma} \tag{2-35}$$

$$\Delta\underset{\sim p}{\bar{\sigma}} \;=\; \beta(\underset{\sim}{\hat{m}}\cdot\Delta\underset{\sim}{\sigma})\underset{\sim}{\hat{n}} \tag{2-36}$$

where

$$\underset{\sim\sigma}{f} \;=\; \frac{\partial f}{\partial\underset{\sim}{\sigma}} \tag{2-37}$$

$$\underset{\sim}{\hat{n}} \;=\; \frac{\underset{\sim\sigma}{f}}{\underset{\sim\sigma}{f}^{T}\cdot\underset{\sim\sigma}{f}} \tag{2-38}$$

Equations 2-35 and 2-36 give the rule for keeping track of the yield surface, i.e., $k* = k_o + \Sigma\Delta k*$ and $\bar{\underset{\sim p}{\sigma}} = \Sigma\Delta\bar{\underset{\sim p}{\sigma}}$. β is the universal hardening parameter $(0 < \beta < 1)$, where $\beta = 0$ implies isotropic hardening, $\beta = 1$ implies kinematic hardening, and other values of β imply a linear combination of kinematic and isotropic hardening. In Equation 2-37 $\underset{\sim\sigma}{f}$ is the gradient of the loading function and is, by definition, in the direction of the outward normal of the yield surface. Accordingly, $\underset{\sim}{\hat{n}}$ in Equation 2-38 is the unit outward normal.

The hardening rule is:

$$H' \;=\; H'(\varepsilon_p*) \tag{2-39}$$

47

$$\varepsilon_p^* \;=\; \sum \Delta\varepsilon_p^* \qquad\qquad (2\text{-}40)$$

$$\Delta\varepsilon_p^* \;=\; \sqrt{\Delta\varepsilon_{\sim p}^{T} \cdot \Delta\varepsilon_{\sim p}} \qquad\qquad (2\text{-}41)$$

Here H' is known as the hardening coefficient to be used in the flow rule. It is assumed H' is a function of the accumulated plastic strain norm, ε_p^*. The function $H'(\varepsilon_p^*)$ is prescribed material data.

The flow rule is given by:

$$\Delta\varepsilon_{\sim p} \;=\; \frac{1}{H'} \, (\hat{\underset{\sim}{n}}^{T}\, \Delta\sigma)\hat{\underset{\sim}{m}} \qquad\qquad (2\text{-}42)$$

The direction vector, m, is the direction of plastic straining. If $\hat{\underset{\sim}{m}} = \hat{\underset{\sim}{n}}$, Equation 2-42 is termed an "associative" flow rule. If $\hat{\underset{\sim}{m}}$ is defined from some other potential function, Equation 2-42 is termed "nonassociative." In either case, the flow rule can be used to determine the incremental plastic constitutive law:

$$\Delta\sigma \;=\; (\underset{\sim e}{D} - \underset{\sim p}{D})\Delta\varepsilon_{\sim} \qquad\qquad (2\text{-}43)$$

$$\underset{\sim p}{D} \;=\; \frac{\underset{\sim e}{D}\,\hat{\underset{\sim}{m}}\,\hat{\underset{\sim}{n}}^{T}\,\underset{\sim e}{D}}{H' + (\hat{\underset{\sim}{n}}^{T}\,\underset{\sim e}{D}\,\hat{\underset{\sim}{m}})} \qquad\qquad (2\text{-}44)$$

Equations 2-34 through 2-44 summarize the incremental laws of plasticity. In the next section these laws will be incorporated into a finite element formulation.

PLASTICITY FINITE ELEMENT FORMULATION

From the previous finite element development, the general equilib-
rium equation (Equation 1-6) was given as:

$$\sum \int_V \underset{\sim}{B}^T \, \Delta\underset{\sim}{\sigma} \, dv \; = \; \Delta\underset{\sim}{P} \tag{2-45}$$

In the above, $\underset{\sim}{B}$, is the strain-to-nodal displacement matrix, $\Delta\underset{\sim}{P}$ is the
external load increment, and the symbol $\sum$ implies the ordered summation
of the element volume integrations.

Inserting the constitutive law, Equation 2-43, into the equilibrium
equations, and using $\Delta\underset{\sim}{\varepsilon} = \underset{\sim}{B} \, \Delta\hat{\underset{\sim}{u}}$, Equation 2-45 can be written as:

$$(\underset{\sim}{K}_e - \underset{\sim}{K}_p)\Delta\hat{\underset{\sim}{u}} \; = \; \Delta\underset{\sim}{P} \tag{2-46}$$

$$\underset{\sim}{K}_e \; = \; \sum \int_V \underset{\sim}{B}^T \, \underset{\sim}{D}_e \, \underset{\sim}{B} \, dv \tag{2-47}$$

$$\underset{\sim}{K}_p \; = \; \sum \int_V \underset{\sim}{B}^T \, \underset{\sim}{D}_p \, \underset{\sim}{B} \, dv \tag{2-48}$$

In the above, $\underset{\sim}{K}_e$ is the global elastic stiffness matrix which remains
constant throughout the loading schedule. $\underset{\sim}{K}_p$ is the global plastic
stiffness (reduction) matrix which is dependent on stress state. Note,
$\underset{\sim}{K}_p = 0$ whenever the stress state is within the yield surface. As dis-
played in Equation 2-46, the equilibrium equations are in the proper

49

form for a direct solution by the tangent stiffness method. This method requires the combined stiffness matrix $\underset{\sim e}{K} - \underset{\sim p}{K}$ to be triangularized at least once for each load step in which plastic deformation occurs. Although this method may be inefficient, many researchers prefer this to the uncertainties of iterative techniques.

Alternatively, to obtain the proper form for the initial strain method, Equation 2-46 is written as:

$$\underset{\sim e}{K} \; \Delta \underset{\sim}{u} \; = \; \Delta \underset{\sim}{P} \; + \; \Delta \underset{\sim p}{F} \qquad\qquad (2\text{-}49)$$

where

$$\Delta \underset{\sim p}{F} \; = \; \sum \int_V \underset{\sim}{B}^T \; \underset{\sim p}{D} \; \underset{\sim}{B} \; dv \; \Delta \underset{\sim}{\hat{u}} \qquad\qquad (2\text{-}50)$$

In Equation 2-49, $\underset{\sim e}{K}$ needs only to be triangularized once. All non-linearities are introduced through the unknown force vector $\Delta \underset{\sim p}{F}$, and an iterative method is employed.

Both solution procedures are outlined in the following pages.

Tangent Stiffness Method

It is assumed the following quantities are known at load step "n": $\underset{\sim n}{\hat{u}}$, $\underset{\sim n}{\sigma}$, and $\underset{\sim n}{\varepsilon}$, along with the current plastic measures $\underset{\approx p}{D}$, $k_n{}^*$, $\varepsilon_{p_n}{}^*$, and $\underset{\sim p_n}{\bar{\sigma}}$. The objective is to find the increments of the above quantities from load step n to n + 1; i.e., $\Delta \underset{\sim}{\hat{u}}$, $\Delta \underset{\sim}{\sigma}$, $\Delta \underset{\sim}{\varepsilon}$, etc., and to update the plastic measures.

1. Determine load increment ΔP.

2. Assemble $\underset{\approx e}{K} - \underset{\approx p}{K}$ from Equations 2-47 and 2-48, where $\underset{\approx p}{K}$ is based on $\underset{\approx p}{D}$ at the beginning of the step.

3. Solve $(\underset{\sim}{K}_e - \underset{\sim}{K}_p)\Delta\hat{\underset{\sim}{u}} = \Delta\underset{\sim}{P}$, for $\Delta\hat{\underset{\sim}{u}}$.

4. Compute stress and strain increments for each element (or each integration point); i.e.,

   a. $\Delta\underset{\sim}{\varepsilon} = \underset{\sim}{B}\,\Delta\hat{\underset{\sim}{u}}$

   b. $\Delta\underset{\sim}{\sigma} = (\underset{\sim}{D}_e - \underset{\sim}{D}_p)\Delta\underset{\sim}{\varepsilon}$

5. Monitor each element (or integration point) to determine if the current stress state is in the plastic region or elastic region:

   a. Compute $F = f(\underset{\sim}{\sigma}_{n+1} - \bar{\underset{\sim}{\sigma}}_{p_n}) - k_n^*$

   b. If $F < 0$, stress state is elastic. Set $\underset{\sim}{D}_p = 0$ and go to Step 8.

   c. If $F > 0$, stress state is plastic. Go to Step 6.

6. Update yield surface measures:

   a. $\bar{\underset{\sim}{\sigma}}_{p_{n+1}} = \bar{\underset{\sim}{\sigma}}_{p_n} + \Delta\bar{\underset{\sim}{\sigma}}_p$, where $\Delta\bar{\underset{\sim}{\sigma}}_p = \beta(\hat{\underset{\sim}{n}}^T \Delta\underset{\sim}{\sigma})\hat{\underset{\sim}{n}}$

   b. $\bar{k}_{n+1}^* = f(\underset{\sim}{\sigma}_{n+1} - \bar{\underset{\sim}{\sigma}}_{p_{n+1}})$

7. Update plastic flow law:

   a. $\hat{\underset{\sim}{n}} = \underset{\sim}{f}_\sigma / \sqrt{\underset{\sim}{f}_\sigma^T \cdot \underset{\sim}{f}_\sigma}$, where $\underset{\sim}{f}_\sigma$ is evaluated at stress state $n + 1$.

   b. $\hat{\underset{\sim}{m}} = \hat{\underset{\sim}{n}}$ for associative flow rule; otherwise compute $\hat{\underset{\sim}{m}}$ from nonassociative function.

   c. $H' = H'(\varepsilon_{p_{n+1}}^*)$, where $\varepsilon_{p_{n+1}}^* = \varepsilon_{p_n}^* + \Delta\varepsilon_p^*$,

   $\Delta\varepsilon_p^* = \sqrt{\Delta\underset{\sim}{\varepsilon}_p^T \cdot \Delta\underset{\sim}{\varepsilon}_p}$, and $\Delta\underset{\sim}{\varepsilon}_p = \underset{\sim}{D}_e^{-1}\,\underset{\sim}{D}_p\,\Delta\underset{\sim}{\varepsilon}$

d. $\underset{\sim}{D}_p = \underset{\sim}{D}_e \, \hat{\underset{\sim}{m}} \, \hat{\underset{\sim}{n}}^T \, \underset{\sim}{D}_e / [H' + (\hat{\underset{\sim}{n}}^T \, \underset{\sim}{D}_e \, \hat{\underset{\sim}{m}})]$

3. Print out desired results, and return to Step 1 for next load increment.

The preceding algorithm is a relatively straightforward procedure; however, it is not computationally efficient. Worse still, the transition error may require additional matrix triangularizations within the load step. It is assumed the matrix $\underset{\sim}{D}_p$ remains constant (chord value) during a given load step. This assumption is reasonable providing the element is in the plastic region at the beginning and end of the load step, or it is in the elastic region at the beginning and end of the load step. However, when an element shifts from the elastic zone to the plastic zone or vice versa (the transition region), it must be treated with special care. In these cases, $\underset{\sim}{D}_p$ actually abruptly changes from zero to some finite value as the element transcends from an elastic state to a plastic state, or conversely, from a finite value to zero for the reverse transition.

To account for these transitions in the above algorithm, two basic approaches are available. First, and simplest, is to divide the load into sufficiently small increments so that the transition error can be ignored. By this method, the algorithm lags the transition responses by one load step.

The alternative approach is to modify $\underset{\sim}{D}_p$ is some way to account for transition and resolve the problem. In the case of the transition from plastic to elastic zone, $\underset{\sim}{D}_p$ should be set to zero because all unloading is elastic. However, when the transition is from the elastic to the plastic zone, the first part of the load step is in the elastic zone as the stress path moves from some point within the yield surface to the yield surface. The second part of the load step is in the plastic zone as the stress path moves with the yield surface. To reflect the abrupt change of $\underset{\sim}{D}_p$ during the load step, it is convenient to take a weighted average based on the proportion of the load increment in the plastic zone as measured by the ratio:

$$r = \frac{f(\underset{\sim}{\sigma}_{i+1} - \overline{\underset{\sim}{\sigma}}_{r_i}) - \overline{k}_i^*}{f(\underset{\sim}{\sigma}_{i+1} - \overline{\underset{\sim}{\sigma}}_{p_i}) - f(\underset{\sim}{\sigma}_i - \overline{\underset{\sim}{\sigma}}_{p_i})} \qquad (2\text{-}51)$$

Thus, in the algorithm, each element is checked to see if it underwent a transition phase. If so, the load step is repeated, wherein $\underset{\sim}{D}_p$ for each transition element is re-estimated as follows. For an unload transition, set $\underset{\sim}{D}_p = 0$. For loading, the transition ratio, r, is computed from Equation 2-51, and the stress state at the yield surface is $\underset{\sim}{\sigma} = \underset{\sim}{\sigma}_{n_i} + (1 - r)\Delta\underset{\sim}{\sigma}$. Next, $\underset{\sim}{D}_p$ is calculated at the stress state $\underset{\sim}{\sigma}$ and then reduced by the factor r. The reduced value of $\underset{\sim}{D}_p$ is used for calculating the plastic stiffness $\underset{\sim}{K}_p$, and the algorithm proceeds as before.

The computational inefficiencies of the tangent stiffness method are clearly evident, since the combined stiffness matrix must be assembled and triangularized, not only for each load step, but also again within a load step when element transitions occur. The advantages of the initial strain method are demonstrated in the next section.

Initial Strain Method

Equation 2-49 represents the governing equations for the initial strain method. It may be observed that it differs from tangent stiffness formulation only in that the plastic contributions have been moved to the right-hand side, i.e., $\Delta\underset{\sim}{F}_p = \underset{\sim}{K}_p \Delta\underset{\sim}{u}$, leaving $\underset{\sim}{K}_e$ as a constant global stiffness matrix that requires only one triangularization. To achieve the same accuracy as the tangent stiffness method, it is necessary to iterate within each load step. Many of the calculations are the same for both methods, and only the differences are emphasized here.

As before, it is assumed all quantities are known at time step n, and the objective is to determine the quantities at time step n + 1.

1. Determine load increment $\Delta \underset{\sim}{P}$; let $\hat{\underset{\sim}{u}}_n = \hat{\underset{\sim}{u}}_{n-1}$

2. Estimate $\Delta \underset{\sim}{F}_p = \sum \int_v (\underset{\sim}{B}^T \underset{\sim}{D}_p \underset{\sim}{B} \, dv)_n \, \Delta \underset{\sim}{u}_n$

3. Solve $\underset{\sim}{K}_e \, \Delta \hat{\underset{\sim}{u}}_n = \Delta \underset{\sim}{P} + \Delta \underset{\sim}{F}_p$. If $\Delta \hat{\underset{\sim}{u}}_n \approx \Delta \underset{\sim}{u}_{n-1}$, go to Step 4; other-
wise, go to Step 2.

4 through 8. Same as tangent stiffness method.

The heart of the initial strain method is embedded in the iteration
loop within the load step, i.e., steps 2 and 3. As illustrated in the
above algorithm, $\Delta \underset{\sim}{F}_p$ is reconstructed on each iteration based on the new
estimate for $\Delta \hat{\underset{\sim}{u}}_n$. However, there is no reason $\underset{\sim}{D}_p$ cannot also be changed
simultaneously on each iteration to reflect abrupt changes in transition
zones or even subtle changes in $\underset{\sim}{D}_p$ over the time interval. Herein lies
the advantages of the initial strain method. To wit, after the initial
triangularization of $\underset{\sim}{K}_e$, each solution merely requires modifying the
right-hand side and performing a back substitution. Moreover, each
estimate of $\Delta \underset{\sim}{F}_p$ can simultaneously consider variations in $\underset{\sim}{D}_p$ as well as
$\Delta \hat{\underset{\sim}{u}}$ in obtaining a convergent solution.

This concludes the development and implementation of plasticity
theory. In Appendix A some common loading functions are presented
together with some fine points on flow laws and hardening rules.

Chapter 3

LINEAR VISCOELASTICITY

In this section a general three-dimensional isotropic viscoelastic
constitutive formulation will be developed that is compatible with the
finite element formulation previously presented. To this end, a brief
review of viscoelastic constitutive theory will be given, beginning with
simple one-dimensional concepts followed by a generalization of multi-
dimensional stress-strain states. For a comprehensive introduction into
viscoelastic theory, the reader is referred to Flugge [19] and Christensen
[20].

BASIC CONCEPTS

Viscoelastic materials are often called "memory" materials, that
is, the stress in the material is determined not only by the current
state of deformation, but also by all past deformation states. More-
over, the "memory" exhibits a fading phenomenon in that past deformation
states influence the current stress state to a lesser degree than do
more recent deformation states. As a consequence of this memory phenom-
enon, viscoelastic materials dissipate energy during deformation; thus,
the external work put into the system cannot be completely recovered.

ONE-DIMENSIONAL MODELS

The above characteristics of linear viscoelasticity can be exhibited by one-dimensional mechanical models composed of an assemblage of springs and dashpots, where the springs denote a linear relationship between stress and deformation while dashpots denote a linear relationship between stress and rate of deformation. Mechanical models provide an insight into the nature of viscoelastic behavior and also provide a basis for defining a differential equation relating stress and strain.

Differential Equations

Consider the one-dimensional model shown below, which is known as the standard linear solid.
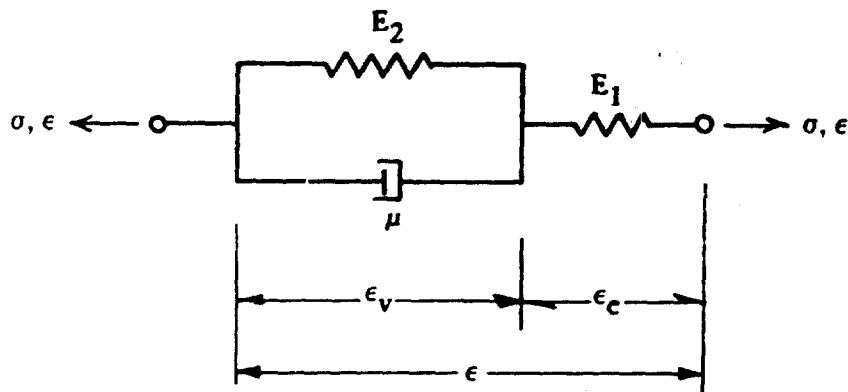
σ = total stress, ε = total strain, ε_e = elastic strain, ε_v = viscous strain, E_1, E_2 = spring constants, and μ = dashpot constant. Using simple concepts of equilibrium, it is easy to deduce $\sigma = E_1 \, \varepsilon_e$ in the elastic spring and $\sigma = \mu \, \dot{\varepsilon}_v + E_2 \, \varepsilon_v$ in the parallel assembly, where ($\dot{}$) denotes a time derivative. As implied by the model, the total strain is given by $\varepsilon = \varepsilon_e + \varepsilon_v$. Combining these three relationships, a differential equation relating total stress to total strain is obtained as:

$$\left(\frac{E_1 + E_2}{E_1}\right) \sigma \ + \ \frac{\mu}{E_1} \ \dot{\sigma} \ = \ E_2 \ \varepsilon \ + \ \mu \ \dot{\varepsilon} \qquad (3\text{-}1)$$

To use the mechanical model as a visual aid, it is noted that the dashpot cannot move instantaneously. Thus, at the first instance of deformation (from $t = 0^-$ to $t = 0^+$) only the spring E_1 can deform; hence, $\sigma(0) = E_1 \varepsilon(0)$. Furthermore, if the load is maintained for an extended period of time, the dashpot will finally come to rest, shifting all the load to spring E_2 in series with E_1. Hence, at $t = \infty$,

$$\sigma(\infty) \ = \ \frac{E_1 \ E_2}{E_1 + E_2} \ \varepsilon(\infty)$$

These concepts are often useful in interpreting viscoelastic responses.

Equation 3-1 represents a one-dimensional viscoelastic relationship for a particular model. If the strain were prescribed over some time interval $0 \le \tau \le t$, where t is the current time, then it would be possible to solve for the stress response. For example, suppose the strain is input by a Heavyside step function, such that $\varepsilon(t) = \varepsilon_o \ h(t)$, where ε_o is a constant strain magnitude and $h(t)$ is the unit Heavyside function (i.e., $h(t) = 0$ for $t < 0$, and $h(t) = 1$ for $t \ge 0$), then the solution of Equation 3-1 is:

$$\sigma(t) \ = \ \left\{ \frac{E_1 \ E_2}{E_1 + E_2} \ + \ \frac{E_1^2}{E_1 + E_2} \ \exp[-t(E_1 + E_2)/\mu] \right\} \ \varepsilon_o \qquad (3\text{-}2)$$

where the initial condition $\sigma(0) = E_1 \epsilon_0$ was used to determine the constant of integration.

In a manner similar to the above example, more complicated one-dimensional models can be constructed by adding springs and dashpots in series and/or parallel that will always result in a linear differential equation of the form:

$$P_0 \, \sigma_0 \; + \; p_1 \, \dot{\sigma} \; + \; p_2 \, \ddot{\sigma} \; + \; \ldots \; = \; q_0 \, \epsilon \; + \; q_1 \, \dot{\epsilon} \; + \; q_2 \, \ddot{\epsilon} \; + \; \ldots \quad (3\text{-}3)$$

where p_0, p_1, p_2, $\ldots$, q_0, q_1, q_2, $\ldots$ are constants composed of the parameters of the springs and dashpots.

Equation 3-3 may be considered as a general linear viscoelastic constitutive relationship for a one-dimensional problem. However, it is not a particularly useful form for solving boundary value problems because both stress and strain are expressed in terms of their derivatives.

Integral Equations

A more useful form can be obtained by expressing Equation 3-3 in an integral form in the following manner. First, assume the strain is prescribed by a Heavyside step function; i.e., $\epsilon(t) = \epsilon_0 \, h(t)$, where ϵ_0 is some constant strain amplitude and $h(t) = 0$ for $t < 0$ or $h(t) = 1$ for $t > 0$. With this prescription for strain, the right-hand side of Equation 3-3 reduces to the constant $q_0 \, \epsilon_0$ for all $t > 0$. Therefore, Equation 3-3 represents an ordinary linear differential equation in terms of stress for which a solution is always possible. Symbolically, this solution can be expressed as:

$$\sigma(t) \; = \; Y(t) \, \epsilon_0 \quad\quad (3\text{-}4)$$

Here $Y(t)$ is termed the relaxation function and is an intrinsic charac-
teristic of the material model because it describes the nature of the
stress response due to a prescribed strain equal to unity. Implicit in
the definition of a relaxation function is $Y(t) = 0$ when $t < 0$; i.e.,
there is no stress response prior to application of strain. As an
example, the relaxation function for the standard linear solid is
enclosed in braces in Equation 3-2.

Next, to extend the solution of Equation 3-4 to apply to an arbi-
trary strain input, linearity and superposition are exploited as follows.
Consider an arbitrary strain input $\varepsilon(t)$, shown in Figure 12, along with
a step-wise approximation to this curve given by

$$\varepsilon(t) = \varepsilon_o \, h(t) + \sum_{k=1}^{n} \Delta\varepsilon_k \, h(t - k \, \Delta t)$$

where $\Delta\varepsilon_k$ is an increment of strain applied at the time $t = k \, \Delta t$.

Because of linearity the solution given by Equation 3-4 applies to
each strain increment corresponding to the time it makes its contribu-
tion; i.e., $\Delta\sigma_k = Y(t - k \, \Delta t)\Delta\varepsilon_k$. Thus, the solution for stress is
given by the superposition of solutions as:

$$\sigma(t) \approx Y(t) \, \varepsilon_o + \sum_{k=1}^{n} Y(t - k \, \Delta t) \, \Delta\varepsilon_k \qquad (3-5)$$

where $t = n \, \Delta t$. In the limit, as $n \to \infty$, $\Delta t \to 0$, and t is current time.
The stress is given exactly by the integral form:
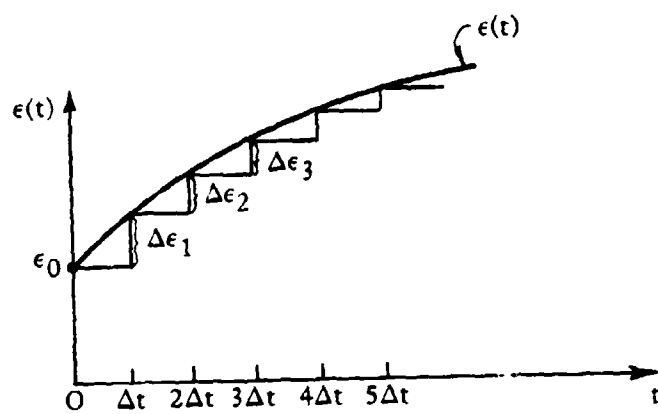
Figure 12.   Stepwise strain approximation.

$$\sigma(t) = Y(t)\, \varepsilon_o + \int_0^t Y(t - \tau)\, \frac{\partial \varepsilon(\tau)\, d\tau}{\partial \tau} \qquad (3\text{-}6a)$$

For simplicity it is convenient to adopt the shorthand notation of convolution algebra, wherein Equation 3-6a is written equivalently as:

$$\sigma(t) = Y^* \, d\varepsilon \qquad (3\text{-}6b)$$

where $*$ is called a convolution operator.

Equation 3-6a or 3-6b is known as a heredity integral and is physically and mathematically equivalent to the differential form given by Equation 3-3. However, the heredity integral provides an expression for stress without stress derivatives, thereby facilitating displacement formulations for boundary value problems. Moreover, many investigators assert that the heredity integral is the proper definition for the linear viscoelastic constitutive law, and, thus, there is no need to concoct mechanical models or their associated differential equations. When this viewpoint is adopted, the relaxation function $Y(t)$ need not be considered related to any particular mechanical model, but rather may be considered as some monotonically decreasing function that predicts the stress response (relaxation) which occurs from an imposed unit of strain.

In the remainder of the study, the relaxation function will be assumed to be given by an exponential series, i.e.,

$$Y(t) = E_\infty + \sum_{i=1}^{N} E_i \exp\left(-t/\lambda_i\right) \qquad (3\text{-}7)$$

where E_∞, E_1, E_2, ... are relaxation moduli, and λ_1, λ_2, λ_3, ... are relaxation times. Specification of these non-negative material constants is all that is required to completely define the relaxation function which in turn can be used in the heredity integral to form a one-dimensional viscoelastic constitutive law.

It can be shown that the exponential series form of the relaxation function will always correspond to some mechanical model; thus, it is left to the discretion of the reader as to whether or not he will accept the relaxation function at face value, as given in Equation 3-7, or interpret the relaxation function in terms of a mechanical model.

To summarize the discussion thus far, Equation 3-6a or 3-6b represents a general one-dimensional viscoelastic constitutive relationship, wherein $Y(t)$ is a relaxation function characterized by an exponential series, Equation 3-7. The parameters of the exponential series may be determined directly from experimental data or interpreted from mechanical models. In the next section, multidimensional stress-strain models will be discussed.

MULTIDIMENSIONAL MODELS

General Viscoelastic Constitutive Law

Extending the constitutive relaxation from one dimension to multi-dimensional stress states follows reasoning directly analogous o the generalized Hook's law for elastic materials. Namely, each component of stress is coupled in some fashion to various components of the strain vector through a constitutive matrix, i.e.,:

$$\underset{\sim}{\sigma} = \underset{\approx}{D^*} \, d\underset{\sim}{\varepsilon} \qquad (3\text{-}8)$$

where the convolution symbol, *, denotes the integral relationships given by Equation 3-6b. In general, the matrix D may contain 21 independent relaxation functions for describing anisotropic materials; however, for isotropic materials, only two independent relaxation functions are required.

In this writing, only the isotropic form will be pursued. It is convenient in solving boundary value problems to choose the isotropic relaxation functions as the response due to bulk and shear deformations. That is, the bulk relaxation function, $K(t)$, is defined as the hydrostatic stress response due to a prescribed unit of volume change by a Heavyside step function. Similarly, the shear relaxation function, $G(t)$, is defined as the shear stress response due to a prescribed unit of shear strain by a Heavyside step function.

Thus, for isotropic viscoelastic materials, Equation 3-8 has the following expanded form, where K and G represent the independent relaxation functions:

$$
\begin{Bmatrix} \sigma_{11} \\ \sigma_{22} \\ \sigma_{33} \\ \sigma_{12} \\ \sigma_{13} \\ \sigma_{23} \end{Bmatrix} = \begin{bmatrix} K+(4G/3) & K-(2G/3) & K-(2G/3) & 0 & 0 & 0 \\ K-(2G/3) & K+(4G/3) & K-(2G/3) & 0 & 0 & 0 \\ K-(2G/3) & K-(2G/3) & K+(4G/3) & 0 & 0 & 0 \\ 0 & 0 & 0 & 2G & 0 & 0 \\ 0 & 0 & 0 & 0 & 2G & 0 \\ 0 & 0 & 0 & 0 & 0 & 2G \end{bmatrix} * d \begin{Bmatrix} \varepsilon_{11} \\ \varepsilon_{22} \\ \varepsilon_{33} \\ \varepsilon_{12} \\ \varepsilon_{13} \\ \varepsilon_{23} \end{Bmatrix} \quad (3-9)
$$

Equation 3-9 is the general viscoelastic constitutive law for isotropic materials and has a strong resemblance to the analogous elastic constitutive law. However, it must be kept in mind that K and G are functions of time, and the convolution operator, *, denotes an integral relationship. For example,

$$
Y* d\varepsilon = Y(t)\, \varepsilon(o) + \int_0^t Y(t - \tau)\, \frac{\partial \varepsilon(\tau)}{\partial \tau}\, d\tau
$$

63

By integration of parts, it can be demonstrated that the convolution operator is communicative, i.e., $Y* \, d\varepsilon = \varepsilon* \, dY$. Also, the convolution operator is linear in the sense that if $Y = Y_K + Y_G$, then $\varepsilon* \, dY = \varepsilon* \, dY_K + \varepsilon* \, dY_G$. Therefore, Equation 3-9 may be uncoupled in shear and bulk and written as:

$$\underset{\sim}{\sigma} = \underset{\sim}{D}_K(\underset{\sim}{\varepsilon}* \, dK) + \underset{\sim}{D}_G(\underset{\sim}{\varepsilon}* \, dG) \tag{3-10}$$

This may be written in expanded form as:

$$\underset{\sim}{\sigma} = \underset{\sim}{D}_e \, \underset{\sim}{\varepsilon}(t) - \underset{\sim}{D}_K \int_{0+}^{t} \underset{\sim}{\varepsilon}(t) \, \frac{\partial K(t - \tau)}{\partial \tau} \, d\tau$$

$$- \underset{\sim}{D}_G \int_{0+}^{t} \underset{\sim}{\varepsilon}(\tau) \, \frac{\partial G(t - \tau)}{\partial \tau} \, d\tau \tag{3-11}$$

where $\underset{\sim}{D}_K = \begin{bmatrix} 1 & 1 & 1 & 0 & 0 & 0 \\ 1 & 1 & 1 & 0 & 0 & 0 \\ 1 & 1 & 1 & 0 & 0 & 0 \\ 0 & 0 & 0 & 0 & 0 & 0 \\ 0 & 0 & 0 & 0 & 0 & 0 \\ 0 & 0 & 0 & 0 & 0 & 0 \end{bmatrix}$

$$\underset{\sim}{D}_G = (2/3) \begin{bmatrix} 2 & -1 & -1 & 0 & 0 & 0 \\ -1 & 2 & -1 & 0 & 0 & 0 \\ -1 & -1 & 2 & 0 & 0 & 0 \\ 0 & 0 & 0 & 3 & 0 & 0 \\ 0 & 0 & 0 & 0 & 3 & 0 \\ 0 & 0 & 0 & 0 & 0 & 3 \end{bmatrix}$$

$$\underset{\sim}{D}_e = K(o) \, \underset{\sim}{D}_K + G(o) \, \underset{\sim}{D}_G$$

In the above, D_K and D_G are constant dimensionless matrices for bulk and shear, respectively, whereas D_e is the familiar constant elastic constitutive matrix representing the instantaneous response of the viscoelastic model.

Viscoelastic Law With Exponential Series

As previously discussed, the relaxation functions can be represented by an exponential series with no serious degradation of generality. Accordingly, the bulk and shear relaxation functions are taken as:

$$K(t) = K_\infty + \sum_{i=1}^{N_K} K_i \exp(-t/\beta_i) \qquad (3-12)$$

$$G(t) = G_\infty + \sum_{i=1}^{N_G} G_i \exp(-t/\gamma_i) \qquad (3-13)$$

where K_∞, K_1, K_2, ... K_{N_K} and G_∞, G_1, G_2, ... G_{N_G} are relaxation moduli for bulk and shear, respectively, and β_1, β_2, ... β_{N_K} and γ_1, γ_2, ... γ_{N_G} are relaxation times for bulk and shear, respectively. Determination of these parameters is discussed in Appendix B of this report and elsewhere [21]. For now it is assumed these parameters are known, and the relaxation functions e completely defined.

Inserting the relaxation functions, i.e., Equations 3-12 and 3-13, into the general constitutive law, Equation 3-11, the following relationship may be written:

65

$$\underset{\sim}{\sigma}(t) = \underset{\sim}{D}_e \, \underset{\sim}{\varepsilon}(t) + \underset{\sim}{D}_K \sum_{i=1}^{N_K} K_i \, \underset{\sim}{k}_i + \underset{\sim}{D}_G \sum_{i=1}^{N_G} G_i \, \underset{\sim}{g}_i \qquad (3\text{-}14)$$

where

$$\underset{\sim}{k}_i = -\int_0^t \underset{\sim}{\varepsilon}(\tau) \frac{1}{\beta_i} \exp[-(t - \tau)/\beta_i]d\tau \qquad (3\text{-}15)$$

$$\underset{\sim}{g}_i = -\int_0^t \underset{\sim}{\varepsilon}(\tau) \frac{1}{\gamma_i} \exp[-(t - \tau)/\gamma_i]d\tau \qquad (3\text{-}16)$$

The vector sets, $\underset{\sim}{k}_i$ and $\underset{\sim}{g}_i$, are often called "hidden coordinates" or "internal variables" [22,23] for bulk and shear, respectively. The motivation for introducing these internal variables will become evident in subsequent derivations. It will be shown that incremental recursion relationships for $\underset{\sim}{k}_i$ and $\underset{\sim}{g}_i$ can be used to great advantage in circumventing the need for storing the complete history of deformation [21,24].

Incremental Viscoelastic Law

In anticipation of using an incremental solution procedure, the constitutive law can be cast in incremental form by defining the current time increment as $\Delta t = t_{n+1} - t_n$ and $\Delta \underset{\sim}{\sigma}$, $\Delta \underset{\sim}{\varepsilon}$, $\Delta \underset{\sim}{k}_i$, and $\Delta \underset{\sim}{g}_i$ as $\Delta \underset{\sim}{\sigma} = \underset{\sim}{\sigma}(t_{n+1}) - \underset{\sim}{\sigma}(t_n)$, etc. With these definitions, Equation 3-14 can be directly written in incremental form as:

$$\Delta \underset{\sim}{\sigma} = \underset{\sim}{D}_e \, \Delta \underset{\sim}{\varepsilon} + \underset{\sim}{D}_K \sum_{i=1}^{N_K} K_i \, \Delta \underset{\sim}{k}_i + \underset{\sim}{D}_G \sum_{i=1}^{N_G} G_i \, \Delta \underset{\sim}{g}_i \qquad (3\text{-}17)$$

To obtain corresponding incremental relationships for the internal variables given by Equations 3-15 and 3-16, the time integrals are subdivided into $n + 1$ time intervals, not necessarily of constant size. Then, using the definition $\Delta k_i = k_i(t_{n+1}) - k_i(t_n)$, and $\Delta g_i = g_i(t_{n+1}) - g_i(t_n)$, the following recursive relationship can be found:

$$\Delta \underset{\sim}{k}_i = -\int_{t_n}^{t_{n+1}} \underset{\sim}{\varepsilon}(\tau) \frac{1}{\beta_i} \exp[-(t_{n+1} - \tau)/\beta_i] d\tau + \bar{r}_i \underset{\sim}{k}_i(t_n) \quad (3\text{-}18)$$

where $\bar{r}_i = 1 - \exp(-\Delta t/\beta_i)$

and

$$\Delta \underset{\sim}{g}_i = -\int_{t_n}^{t_{n+1}} \underset{\sim}{\varepsilon}(\tau) \frac{1}{\gamma_i} \exp[-(t_{n+1} - \tau)/\gamma_i] d\tau + \bar{q}_i \underset{\sim}{g}_i(t_n) \quad (3\text{-}19)$$

where $\bar{q}_i = 1 - \exp(-\Delta t/\gamma_i)$

It is significant to note that $\Delta \underset{\sim}{k}_i$ and $\Delta \underset{\sim}{g}_i$ can be determined by just integrating over the current time step, t_n to t_{n+1}, rather than the entire time history. The time history effect is given by the recursive terms $\bar{r}_i \underset{\sim}{k}_i(t_n)$ and $\bar{q}_i \underset{\sim}{g}_i(t_n)$.

As yet, no numerical approximations have been made. However, in order to evaluate the integral in Equations 3-18 and 3-19, it will be assumed the strain vector varies linearly over the time step. That is, in the time interval $t_n \le \tau \le t_n + \Delta t$, let:

$$\underset{\sim}{\varepsilon}(t) = \underset{\sim}{\varepsilon}(t_n) + \frac{\tau - t_n}{\Delta t} \Delta \underset{\sim}{\varepsilon}$$

Then Equation 3-18 can be evaluated as:

$$\Delta \underset{\sim}{k}_i = -r_i \Delta \underset{\sim}{\varepsilon} - \overline{r}_i [\underset{\sim}{\varepsilon}(t_n) - \underset{\sim}{k}_i(t_n)] \qquad (3\text{-}20)$$

where $\quad \overline{r}_i = 1 - \exp(-\Delta t/\beta_i)$

$$r_i = 1 - \frac{\beta_i}{\Delta t} \overline{r}_i$$

In an identical fashion, an incremental recursion relationship for $\Delta \underset{\sim}{g}_i$ can be deduced as:

$$\Delta \underset{\sim}{g}_i = -q_i \Delta \underset{\sim}{\varepsilon} - \overline{q}_i [\underset{\sim}{\varepsilon}(t_n) - \underset{\sim}{g}_i(t_n)] \qquad (3\text{-}21)$$

where $\quad \overline{q}_i = 1 - \exp(-\Delta t/\gamma_i)$

$$q_i = 1 - \frac{\gamma_i}{\Delta t} \overline{q}_i$$

Inserting Equations 3-20 and 3-21 into Equation 3-17 and separating the
current strain increment from history terms, the following incremental
constitutive law is achieved:

$$\Delta \underset{\sim}{\sigma} = (\underset{\sim}{D}_e - \underset{\sim}{D}_v)\Delta \underset{\sim}{\varepsilon} - \bar{\underset{\sim}{\sigma}}_v \qquad (3\text{-}22)$$

where $\quad \underset{\sim}{D}_v = \alpha_K \underset{\sim}{D}_K + \alpha_G \underset{\sim}{D}_G$

$$\alpha_K = \sum_{i=1}^{N_K} K_i \, r_i$$

$$\alpha_G = \sum_{i=1}^{N_G} G_i \, q_i$$

$\bar{\underset{\sim}{\sigma}}_v =$ stress-history influence vector

Note that $\underset{\sim}{D}_v$ is composed of the constant, dimensionless matrices $\underset{\sim}{D}_K$ and
$\underset{\sim}{D}_G$, and the scalar multiples α_K and α_G that are only dependent on time-
step size Δt and not the time t. Therefore, $\underset{\sim}{D}_v$ only changes its value
when the size of the time step is changed.

The term $\bar{\underset{\sim}{\sigma}}_v$ will be called the viscoelastic stress-history influence
vector and is given by:

$$\bar{\underset{\sim}{\sigma}}_v(t_n) = \underset{\sim}{D}_K \sum_{i=1}^{N_K} K_i \, \bar{r}_i [\underset{\sim}{\varepsilon}(t_n) - \underset{\sim}{k}_i(t_n)]$$

$$+ \underset{\sim}{D}_G \sum_{i=1}^{N_G} G_i \, \bar{q}_i [\underset{\sim}{\varepsilon}(t_n) - \underset{\sim}{g}_i(t_n)] \qquad (3\text{-}23)$$

The stress-history influence vector accounts for the influence of all past deformation states on the current stress increment given in Equation 3-22. It should be observed that $\bar{\sigma}_v$ is not dependent on the current time interval t_n to t_{n+1}; therefore, $\bar{\sigma}_v$ is a known quantity at the beginning of each time step and can be treated as an initial stress.

In computational practice it is convenient to compute $\bar{\sigma}_v$ at the end of a time step in preparation for the next step. Summarized below are the necessary relationships to update $\bar{\sigma}_v$ after the time step t_n to t_{n+1}:

1. $\Delta k_i = - r_i \Delta \varepsilon - \bar{r}_i [\varepsilon(t_n) - k_i(t_n)]$

2. $\Delta g_i = - q_i \Delta \varepsilon - \bar{q}_i [\varepsilon(t_n) - g_i(t_n)]$

3. $k_i(t_{n+1}) = k_i(t_n) + \Delta k_i$

4. $g_i(t_{n+1}) = g_i(t_n) + \Delta g_i$

5. $\varepsilon(t_{n+1}) = \varepsilon(t_n) + \Delta \varepsilon$

6. $\displaystyle \bar{\sigma}_v(t_{n+1}) = D_K \sum_{i=1}^{N_K} K_i \bar{r}_i [\varepsilon(t_{n+1}) - k_i(t_{n+1})]$

$\displaystyle + D_G \sum_{i=1}^{N_G} G_i \bar{q}_i [\varepsilon(t_{n+1}) - g_i(t_{n+1})]$

In summary, Equation 3-22 is the general viscoelastic constitutive relationship to be incorporated into the boundary value problem, and the above relationships provide the algorithm for updating $\bar{\sigma}_v$. In the next sections the constitutive relationship is introduced into a finite element formulation and a step-by-step procedure is outlined for the solution.

VISCOELASTIC FINITE ELEMENT FORMULATION

For convenience, the general equilibrium equations previously derived in the finite element development are repeated here;

$$\sum \int_v \underset{\sim}{B}^T \Delta\underset{\sim}{\sigma} \, dv = \Delta\underset{\sim}{P} \tag{3-24}$$

where it will be recalled that $\underset{\sim}{B}$ is the strain-to-nodal point displacement matrix, $\Delta\underset{\sim}{P}$ is the external load increment, and the symbol $\sum$ denotes the ordered summation of each finite element volume integration into its correct location of the global stiffness matrix. Replacing $\Delta\underset{\sim}{\sigma}$ by the viscoelastic constitutive law, Equation 3-22, and using the strain-to-node displacement relationship, $\Delta\underset{\sim}{\varepsilon} = \underset{\sim}{B} \Delta\underset{\sim}{\hat{u}}$, Equation 3-24 may be written as:

$$(\underset{\sim}{K}_e - \underset{\sim}{K}_v)\Delta\underset{\sim}{\hat{u}} = \Delta\underset{\sim}{P} + \underset{\sim v}{\bar{F}} \tag{3-25}$$

where

$$\underset{\sim}{K}_e = \sum \int_v \underset{\sim}{B}^T \underset{\sim e}{D} \underset{\sim}{B} \, dv \tag{3-26}$$

$$\underset{\sim}{K}_v = \sum \int_v \underset{\sim}{B}^T \underset{\sim v}{D} \underset{\sim}{B} \, dv \tag{3-27}$$

71

$$\bar{\mathbf{F}}_{\mathbf{v}} = \sum \int_{v} \mathbf{B}^{T} \bar{\sigma}_{\mathbf{v}} \, dv \qquad (3\text{-}28)$$

Equation 3-25 represents the familiar set of linear algebraic equations common to step-by-step methods. $\mathbf{K}_{e}$ is the constant, elastic, global stiffness matrix, and $\mathbf{K}_{\mathbf{v}}$ is the global viscous stiffness matrix which is independent of time, t, and is only dependent on the current size of the time step, Δt. $\bar{\mathbf{F}}_{\mathbf{v}}$ represents the viscoelastic force history vector which is independent of the current time interval, t_{n} to t_{n+1}, and, therefore, is known at the beginning of each time step.

The solution procedure for Equation 3-25 can be handled in a straightforward manner. However, caution must be followed with regard to the calculation of $\bar{\mathbf{F}}_{\mathbf{v}}$. Note the volume integral in Equation 3-28 requires that the spatial distribution of $\bar{\sigma}_{\mathbf{v}}$ be known within each element. Unfortunately, it is not known in a continuous fashion. Therefore, in order to perform the volume integration, several approaches are possible. First, it may be assumed that $\bar{\sigma}_{\mathbf{v}}$ is constant within the element. Thus, $\bar{\sigma}_{\mathbf{v}}$ is determined at the element center. Second, $\bar{\sigma}_{\mathbf{v}}$ may be computed at the numerical integration points (Gauss points), thereby facilitating a direct numerical integration. Although this second approach is accurate, it may require excessive auxiliary storage because the calculation of $\bar{\sigma}_{\mathbf{v}}$ requires the storage of all the internal variables $\mathbf{k}_{i}$ and $\mathbf{g}_{i}$ for each integration point (see Equation 3-23).

A third and last approach is the most consistent. Basically, the idea is to develop an updating procedure for $\bar{\mathbf{F}}_{\mathbf{v}}$ based on a recursion scheme. To this end, Equations 3-23 and 3-28 are combined to express $\bar{\mathbf{F}}_{\mathbf{v}}$ in the following manner:

$$\bar{\mathbf{F}}_{\mathbf{v}} = \sum \left(\sum_{i=1}^{N_{K}} \mathbf{h}_{\mathbf{K}_{i}} + \sum_{i=1}^{N_{G}} \mathbf{h}_{\mathbf{G}_{i}} \right) \qquad (3\text{-}29)$$

where

$$h_{\underset{\sim}{K_i}} = K_i \, \bar{r}_i \int_v B^T \, D_{\underset{\sim}{K}} [\underset{\sim}{\varepsilon}(t_n) - \underset{\sim}{k}_i(t_n)] dv \qquad (3\text{-}30)$$

$$h_{\underset{\sim}{G_i}} = G_i \, \bar{q}_i \int_v B^T \, D_{\underset{\sim}{G}} [\underset{\sim}{\varepsilon}(t_n) - \underset{\sim}{g}_i(t_n)] dv \qquad (3\text{-}31)$$

In the above equations, $h_{\underset{\sim}{K_i}}$ and $h_{\underset{\sim}{G_i}}$ represent viscoelastic force history vectors for bulk and shear within each element.

As expressed in Equations 3-29, 3-30, and 3-31, the calculation of $h_{\underset{\sim}{K_i}}$ and $h_{\underset{\sim}{G_i}}$ and then $\bar{F}_{\underset{\sim}{v}}$ does not provide any advantage over the calculation for $\bar{F}_{\underset{\sim}{v}}$ as given previously in Equation 3-28. However, if Equations 3-30 and 3-31 are written in incremental form (that is, $\Delta h_{\underset{\sim}{K_i}} = h_{\underset{\sim}{K_i}}(t_n) - h_{\underset{\sim}{K_i}}(t_{n-1})$ and $\Delta h_{\underset{\sim}{G_i}} = h_{\underset{\sim}{G_i}}(t_n) - h_{\underset{\sim}{G_i}}(t_{n-1})$, if $\Delta\underset{\sim}{\varepsilon}$ is replaced by $\underset{\sim}{B}\, \Delta\underset{\sim}{u}$, and if $\Delta\underset{\sim}{k}_i$ and $\Delta\underset{\sim}{g}_i$ are replaced by their recursion relationships given by Equations 3-20 and 3-21, then the following recursive relationships are found for $\Delta h_{\underset{\sim}{K_i}}$ and $\Delta h_{\underset{\sim}{G_i}}$.

$$\Delta h_{\underset{\sim}{K_i}} = K_i \, \bar{r}_i (1 + r_i) S_{\underset{\sim}{K}} \, \Delta\hat{\underset{\sim}{u}} + \bar{r}_i \, h_{\underset{\sim}{K_i}} \qquad (3\text{-}32)$$

$$\Delta h_{\underset{\sim}{G_i}} = G_i \, \bar{q}_i (1 + q_i) S_{\underset{\sim}{G}} \, \Delta\hat{\underset{\sim}{u}} + \bar{q}_i \, h_{\underset{\sim}{G_i}} \qquad (3\text{-}33)$$

where $S_{\underset{\sim}{K}} = \int_v B^T \, D_{\underset{\sim}{K}} \, B \, dv$, dimensionless bulk stiffness

$S_{\underset{\sim}{G}} = \int_v B^T \, D_{\underset{\sim}{G}} \, B \, dv$, dimensionless shear stiffness

At the end of each time step, Equations 3-32 and 3-33 provide a simple and consistent method of determining the force history increments Δh_{K_i} and Δh_{G_i} for each element by making use of the known displacement increment Δu and the accumulated force history vectors, h_{K_i} and h_{G_i}. It should be observed that the volume integrations are consistently defined by the dimensionless element stiffness matrices, S_K and S_G. Furthermore, S_K and S_G are independent of time and time step; therefore, they need only be computed once for each element and stored.

The foregoing viscoelastic finite element formulation is summarized in the following step-by-step solution procedure. Equation 3-25 is the governing equilibrium equation to be solved at each time step. To present the solution strategy, it is assumed that all quantities have been calculated at time t_n, i.e., $\hat{u}(t_n)$, $h_{K_i}(t_n)$, and $h_{G_i}(t_n)$. The objective is to find the increments $\Delta\hat{u}$, Δh_{K_i}, and Δh_{G_i} from time t_n to t_{n+1}.

1. Form new load increment ΔP.

2. Assemble force history vector, $\bar{F}_v$, from Equation 3-29.

3. Assemble total stiffness matrix, $K_e - K_v$, from Equations 3-26 and 3-27 (only required if time-step size changes).

4. Solve $(K_e - K_v)\Delta\hat{u} = \Delta P + \bar{F}_v$ for $\Delta\hat{u}$.

5. Evaluate Δh_{G_i} and Δh_{K_i} from Equations 3-32 and 3-33.

6. Update all quantities: $\hat{u}(t_{n+1})$, $h_{G_i}(t_{n+1})$, $h_{K_i}(t_{n+1})$.

7. Print results, and return to Step 1. (Note stresses may be calculated from Equations 3-22 and 3-23.)

To start the above algorithm, it is assumed the body is undeformed prior to loading so that initially $\hat{u}(o) = h_{K_i}(o) = h_{G_i}(o) = 0$. For the initial instantaneous elastic solution over the time interval $t = 0^-$ to 0^+, we have $\Delta t = 0$, which implies $K_v = 0$, $\Delta h_{K_i} = \Delta h_{G_i} = 0$, and $\bar{F}_v = 0$.

Therefore, the first solution at $t = 0^+$ is obtained by solving the elastic system, $\underset{\sim}{K}_e \, \Delta\hat{\underset{\sim}{u}} = \Delta\underset{\sim}{P}$, where $\Delta\underset{\sim}{P}$ is the instantaneous load applied at $t = 0$. With this starting procedure, the above algorithm can be used for each succeeding step.

As previously mentioned, the viscoelastic stiffness matrix, $\underset{\sim}{K}_v$, only changes its value when the size of the time step, Δt, changes. If the time step is kept constant, computation time (steps 3 and 4) may be considerably reduced by reusing the total triangularized stiffness matrix to modify each new right-hand-side vector, $\Delta\underset{\sim}{P} + \overline{\underset{\sim}{F}}_v$, and performing a simple back substitution to determine $\Delta\hat{\underset{\sim}{u}}$.

Chapter 4

VISCOPLASTICITY

GENERAL

The general theory of viscoplasticity is discussed in Appendix C.
In this section, a particular viscoplastic model called "viscoelastic-
plastic" is developed in detail. The model is a member of a family of
combo-viscoplastic models introduced in Appendix C.

The viscoelastic-plastic model is characterized by a linear
viscoelastic model within the yield surface and the combined visco-
elastic and plastic response on the yield surface. Figure 13 portrays
a one-dimensional representation of the viscoelastic-plastic model. As
suggested by the one-dimensional model, plastic deformation is not
retarded by viscous components; consequently, plastic deformation may
occur instantaneously as in classical plasticity. Accordingly, the
yield function is restricted to the same rules of classical plasticity.
The viscoelastic-plastic model is developed in detail in the next section
for a general multidimensional stress-strain state wherein previously
derived relationships for plasticity and viscoelasticity are employed.

VISCOELASTIC-PLASTIC CONSTITUTIVE DEVELOPMENT

In this section, a general constitutive relationship is developed
for the class of "viscoelastic-plastic" materials described above. The
fundamental assumption for viscoelastic-plastic materials is that the

77
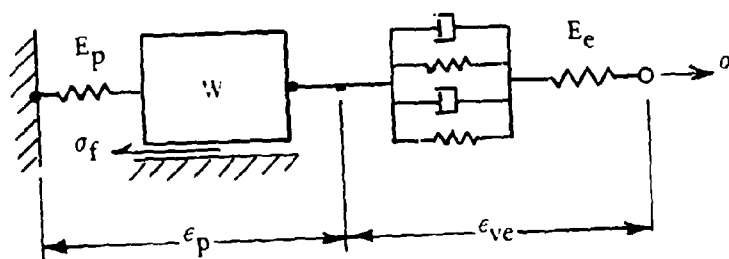
Figure 13. Viscoelastic-plastic model (kinematic).

total stress is persistently related to the viscoelastic portion of the total strain regardless of the amount of plastic straining, i.e.,

$$\underset{\sim}{\sigma} = \underset{\approx}{D^*} \ d\underset{\sim ve}{\varepsilon} \qquad (4\text{-}1)$$

where $\underset{\sim}{D^*} \ d\underset{\sim ve}{\varepsilon}$ denotes the convolution constitutive relationship previously developed in Equations 3-8 through 3-11.

In accordance with the above assumption, it is further assumed that the total strain can be decomposed into viscoelastic and plastic components, i.e.,

$$\underset{\sim}{\varepsilon} = \underset{\sim ve}{\varepsilon} + \underset{\sim p}{\varepsilon} \qquad (4\text{-}2)$$

where $\underset{\sim ve}{\varepsilon}$ is the viscoelastic strain vector, and $\underset{\sim p}{\varepsilon}$ is the plastic strain vector. Note the assumptions embodied in Equations 4-1 and 4-2 are directly analogous to the assumptions made in the elastic-plastic formulation, wherein it is assumed $\underset{\sim}{\sigma} = \underset{\approx e}{D} \ \underset{\sim e}{\varepsilon}$ and $\underset{\sim}{\varepsilon} = \underset{\sim e}{\varepsilon} + \underset{\sim p}{\varepsilon}$.

As always, the objective of this constitutive development is to determine a relationship between the current stress increment, $\Delta\sigma$, and the strain increment, $\Delta\underset{\sim}{\varepsilon}$. To this end, the development begins with the incremental equivalent of Equation 4-1 given by Equation 3-22 and is repeated here for convenience:

$$\underset{\sim}{\Delta\sigma} = \underset{\approx ve}{D} \ \underset{\sim ve}{\Delta\varepsilon} - \underset{\sim v}{\bar{\sigma}} \qquad (4\text{-}3)$$

where

$$\underset{\sim}{D}_{ve} = \underset{\sim}{D}_e - \underset{\sim}{D}_v \qquad (4\text{-}4)$$

and

$$\bar{\underset{\sim}{\sigma}}_v = \underset{\sim}{D}_K \sum_{i=1}^{N_K} K_i \, \bar{r}_i [\underset{\sim}{\varepsilon}_{ve}(t_n) - \underset{\sim}{k}_i(t_n)]$$

$$+ \underset{\sim}{D}_G \sum_{i=1}^{N_G} G_i \, \bar{q}_i [\underset{\sim}{\varepsilon}_{ve}(t_n) - \underset{\sim}{g}_i(t_n)] \qquad (4\text{-}5)$$

In Equation 4-3, the incremental quantities imply the increments from time t_n to t_{n+1}. The stress-history influence vector, $\bar{\underset{\sim}{\sigma}}_v$, is evaluated at time t_n and, therefore, can be considered as a known initial stress. All of the quantities on the right-hand side of Equations 4-4 and 4-5 were previously defined and discussed in the viscoelastic formulation. The significant point to be borne in mind is that all references to strains in Equations 4-3 and 4-5 are with respect to the viscoelastic strain and not the total strain.

To achieve the desired constitutive form, $\Delta\underset{\sim}{\varepsilon}_{ve}$ may be replaced by $\Delta\underset{\sim}{\varepsilon} - \Delta\underset{\sim}{\varepsilon}_p$ in accordance with Equation 4-3; thus, Equation 4-3 becomes:

$$\Delta\underset{\sim}{\sigma} = \underset{\sim}{D}_{ve}(\Delta\underset{\sim}{\varepsilon} - \Delta\underset{\sim}{\varepsilon}_p) - \bar{\underset{\sim}{\sigma}}_v \qquad (4\text{-}6)$$

Except for the term $\bar{\sigma}_v$, Equation 4-6 is similar to Equation 2-30 in the elastic-plastic development. Therefore, at this point, the development parallels the plastic formulation, and it is assumed the plastic flow law (Equation 2-26) remains valid, i.e.,

$$\Delta\varepsilon_p = \frac{\hat{n}^T \, \Delta\sigma}{H'} \, \hat{m} \qquad (4-7)$$

where $\hat{n}$ is the outward normal of the yield surface, $\hat{m}$ is the direction of plastic straining ($\hat{m} = \hat{n}$ implies associative law; $\hat{m} \neq \hat{n}$ implies nonassociative law), and H' is the hardening coefficient. Furthermore, it is assumed all the previously established rules for plastic deformation still hold. That is, yielding can only occur for states of stress on the yield surface with some component of the stress increment colinear with $\hat{n}$, and the methodology of tracking the universal yield surface remains unaltered.

Inserting the flow rule, Equation 4-7, into Equation 4-6 and taking the inner product with respect to the outward normal, $\hat{n}^T$, the scalar quantity $\hat{n}^T \, \Delta\sigma$ is determined as:

$$\hat{n}^T \, \Delta\sigma = \frac{\hat{n}^T (D_{ve} \, \Delta\varepsilon - \bar{\sigma}_v)}{1 + (\hat{n}^T \, D_{ve} \, \hat{m}/H')} \qquad (4-8)$$

Inserting Equation 4-8 back into Equation 4-7, the plastic strain increment is related to the total strain increment by:

$$\Delta\varepsilon_p = C_{pv}(D_{ve} \, \Delta\varepsilon - \bar{\sigma}_v) \qquad (4-9)$$

81

where

$$C_{pv} = \frac{\hat{m} \, \hat{n}^T}{H' + \hat{n}^T \, D_{ve} \, \hat{m}}$$

Lastly, returning to Equation 4-6 and replacing $\Delta \varepsilon$ by Equation 4-9, the desired viscoelastic-plastic constitutive relationship is achieved:

$$\Delta \sigma = (D_{ve} - D_{vp}) \Delta \varepsilon - \bar{\sigma}_{vp} \tag{4-10}$$

where

$$D_{vp} = D_{ve}^T \, C_{pv} \, D_{ve} \tag{4-11}$$

$$\bar{\sigma}_{vp} = (D_{ve} - D_{vp}) D_{ve}^{-1} \, \bar{\sigma}_{v} \tag{4-12}$$

In the above, D_{vp} is a viscoplastic material matrix, and $\bar{\sigma}_{vp}$ is the viscoplastic stress-history influence vector and is related to $\bar{\sigma}_{v}$ through Equation 4-12. Note $\bar{\sigma}_{vp}$ reduces to $\bar{\sigma}_{v}$ whenever $D_{vp} = 0$.

In utilizing Equation 4-10, $\bar{\sigma}_{vp}$ is treated as a known initial stress during each time interval. At the end of each time step $\bar{\sigma}_{vp}$ is updated in preparation for the next step. Summarized below are the necessary relationships to update $\bar{\sigma}_{vp}$ after $\Delta \varepsilon$ and $\Delta \sigma$ have been determined in the time interval t_n to t_{n+1}:

1. $\Delta\underset{\sim}{\varepsilon}_{ve} = \underset{\sim}{D}_{ve}^{-1}[\Delta\underset{\sim}{\sigma} + \bar{\underset{\sim}{\sigma}}_v(t_n)]$

2. $\Delta\underset{\sim}{k}_i = -r_i \Delta\underset{\sim}{\varepsilon}_{ve} - \bar{r}_i[\underset{\sim}{\varepsilon}_{ve}(t_n) - \underset{\sim}{k}_i(t_n)]$

3. $\Delta\underset{\sim}{g}_i = -q_i \Delta\underset{\sim}{\varepsilon}_{ve} - \bar{q}_i[\underset{\sim}{\varepsilon}_{ve}(t_n) - \underset{\sim}{g}_i(t_n)]$

4. $\underset{\sim}{k}_i(t_{n+1}) = \underset{\sim}{k}_i(t_n) + \Delta\underset{\sim}{k}_i$

5. $\underset{\sim}{g}_i(t_{n+1}) = \underset{\sim}{g}_i(t_n) + \Delta\underset{\sim}{g}_i$

6. $\underset{\sim}{\varepsilon}_{ve}(t_{n+1}) = \underset{\sim}{\varepsilon}_{ve}(t_n) + \Delta\underset{\sim}{\varepsilon}_{ve}$

7. $\bar{\underset{\sim}{\sigma}}_v(t_{n+1}) = \underset{\sim}{D}_K \sum_{i=1}^{N_K} K_i \bar{r}_i[\underset{\sim}{\varepsilon}_{ve}(t_{n+1}) - \underset{\sim}{k}_i(t_{n+1})]$

   $+ \underset{\sim}{D}_G \sum_{i=1}^{N_G} G_i \bar{q}_i[\underset{\sim}{\varepsilon}_{ve}(t_{n+1}) - \underset{\sim}{q}_i(t_{n+1})]$

8. $\bar{\underset{\sim}{\sigma}}_{vp}(t_{n+1}) = (\underset{\sim}{D}_{ve} - \underset{\sim}{D}_{vp})\underset{\sim}{D}_{ve}^{-1} \bar{\underset{\sim}{\sigma}}_v(t_{n+1})$

In summary, Equation 4-10 is the general viscoelastic-plastic incremental constitutive relationship useable in any boundary value formulation. The above sequence of steps provide the algorithm for updating $\bar{\underset{\sim}{\sigma}}_{vp}$ at the end of each time step. Lastly, it can be observed that Equation 4-10 reduces to the linear viscoelastic model (Equation 4-3) whenever $\underset{\sim}{D}_{vp} = \underset{\sim}{0}$ (i.e., $\underset{\sim}{C}_p = \underset{\sim}{0}$). Alternatively, if viscous components are zero (i.e., $\underset{\sim}{D}_{ve} = \underset{\sim}{D}_e$ and $\bar{\underset{\sim}{\sigma}}_v = 0$), then Equation 4-10 reduces to the elastic-plastic model.

In the next section, Equation 4-10 is incorporated into a finite element formulation, and a step-by-step solution procedure is presented.

FINITE ELEMENT VISCOELASTIC-PLASTIC FORMULATION

Beginning with the general finite element equilibrium equations (from Equation 1-6):

$$\sum \int_v B^T \Delta\sigma \, dv = \Delta P \qquad (4\text{-}13)$$

where B is the strain-to-nodal point displacement matrix (i.e., $\Delta\varepsilon = B \, \Delta\hat{u}$), ΔP is the external load increment, and $\sum$ implies the ordered summation of the elements.

Replacing $\Delta\sigma$ by the viscoelastic-plastic constitutive law, Equation 4-10, and using $\Delta\varepsilon = B \, \Delta\hat{u}$, Equation 4-13 may be written as:

$$(K_{ve} - K_{vp})\Delta\hat{u} = \Delta P + \bar{F}_{vp} \qquad (4\text{-}14)$$

where

$$K_{ve} = \sum \int_v B^T D_{ve} B \, dv \qquad (4\text{-}15)$$

$$K_{vp} = \sum \int_v B^T D_{vp} B \, dv \qquad (4\text{-}16)$$

$$\bar{F}_{vp} = \sum \int_v B^T \bar{\sigma}_{vp} \, dv \qquad (4\text{-}17)$$

84

In the above, K_{ve} is the global viscoelastic stiffness matrix and could be written as $K_{ve} = K_v + K_e$ as was done in the viscoelastic formulation. Recall that K_{ve} remains constant if the time step is constant. K_{vp} is the global plastic stiffness (reduction) matrix and is similarly defined in the plastic formulation. The vector $\bar{F}_{vp}$ will be called the viscoelastic-plastic force history vector and represents the interaction of viscous and plastic response. If $D_{vp} = 0$, $\bar{F}_{vp}$ reduces to the previously defined viscoelastic force history vector, $\bar{F}_v$.

The governing equations, as shown in Equation 4-14, are in the proper form for a direct solution by standard elimination methods. Alternatively, the plastic portion, $K_{vp} \Delta \hat{u}$, could be taken to the right-hand side and treated as an unknown force. These solution strategies will be detailed later; for now the attention is focused on computing the force history vector, $\bar{F}_{vp}$.

The calculation of $\bar{F}_{vp}$ presents the same problem as did $\bar{F}_v$ in the viscoelastic development; namely, Equation 4-17 requires the volume integration of $\bar{\sigma}_{vp}$; however, the spatial distribution of $\bar{\sigma}_{vp}$ is not known in a continuous fashion. There are two basic options available to overcome this difficulty. One method is to calculate $\bar{\sigma}_{vp}$ at a sufficient number of points to afford a proper representation in a numerical integration scheme. For example, in Gaussian quadrature, the calculation of $\bar{\sigma}_{vp}$ at the Gauss points would be appropriate. The disadvantage of this method is that each point at which $\bar{\sigma}_{vp}$ is calculated requires the storage of all the internal variables k_i and g_i.

The alternative method is to use element force history vectors (e.g., h_{K_i} and h_{G_i}) as was done in the viscoelastic formulation. However, in this case, the development is not as clean due to the interaction of viscous and plastic responses. As a result, a portion of $\bar{F}_{vp}$ is dependent on plastic strain which, in turn, must be evaluated at points within the element and numerically integrated. Consequently, as long as it is necessary to calculate plastic strains at the integration points, it is only a little more work to obtain $\bar{\sigma}_{vp}$ at Gauss points and obtain $\bar{F}_{vp}$ by the first method.

85

SOLUTION ALGORITHM

The solution procedures developed in the elastic-plastic and viscoelastic sections contain most of the concepts for solving the viscoelastic-plastic problem. Here, only the highlights of the initial strain method will be discussed.

From Equation 4-14, the proper form for the initial strain method is given as:

$$\underset{\sim}{K}_{ve} \, \Delta\hat{\underset{\sim}{u}} = \Delta\underset{\sim}{P} + \Delta\underset{\sim}{F}_{p} + \bar{\underset{\sim}{F}}_{vp} \qquad (4\text{-}18)$$

where

$$\Delta\underset{\sim}{F}_{p} = \sum \left(\int_{V} \underset{\sim}{B}^{T} \, \underset{\sim}{D}_{vp} \, \underset{\sim}{B} \, dv \right) \Delta\hat{\underset{\sim}{u}} \qquad (4\text{-}19)$$

Recall that $\underset{\sim}{K}_{ve}$ remains constant as long as the size of the time step remains constant; thus, $\underset{\sim}{K}_{ve}$ only needs to be triangularized when the time step size changes. To establish the algorithm, it is assumed all quantities are known at time t_n, and the objective is to determine the quantities at time t_{n+1}.

1. Form new load increment $\Delta\underset{\sim}{P}$, and estimate $\Delta\hat{\underset{\sim}{u}}_i = \Delta\hat{\underset{\sim}{u}}_{n-1}$

2. Calculate $\Delta\underset{\sim}{F}_p = \sum \left(\int_{V} \underset{\sim}{B}^{T} \, \underset{\sim}{D}_{vp} \, \underset{\sim}{B} \, dv \right) \Delta\hat{\underset{\sim}{u}}_i$

3. Compute $\bar{\underset{\sim}{F}}_{vp} = \sum \int_{V} \underset{\sim}{B}^{T} \, \bar{\underset{\sim}{\sigma}}_{vp} \, dv$, where $\bar{\underset{\sim}{\sigma}}_{vp}$ is given by Equation 4-12

4. Solve $\underset{\sim}{K}_{ve} \, \Delta \hat{\underset{\sim}{u}}_i = \Delta \underset{\sim}{P} + \Delta \underset{\sim}{F}_p + \bar{\underset{\sim}{F}}_{vp}$ for $\Delta \hat{\underset{\sim}{u}}_i$

5. If $\Delta \hat{\underset{\sim}{u}}_i \cong \Delta \hat{\underset{\sim}{u}}_{i-1}$, go to Step 6; otherwise, return to Step 2 for iteration.

6. Monitor each element to determine if it is in plastic region. If so, update yield surface parameters and flow law.

7. Print desired results, and return to Step 1.

The above algorithm implies $\underset{\sim}{D}_{vp}$ and $\underset{\sim}{\sigma}_{vp}$ remain constant within the time step; however, these quantities could be modified in the iteration loop to account for transitions from the viscoelastic range to the plastic range as was discussed in the section on plasticity.

This concludes the viscoelastic-plastic development. It is felt this model incorporates all of the significant aspects of viscoelasticity and plasticity into a unique model. Furthermore, the model directly reduces to plasticity or viscoelasticity by appropriate designation of the parameters.

Chapter 5

IIENTIFICATION AND APPLICATION OF VISCOELASTIC-PLASTIC MODEL

In this section, the viscoelastic-plastic model is discussed from a
conceptual viewpoint to illustrate the types of material behavior that
can be represented and the methods for determining parameters. To
supplement the discussion, the model is compared with experimental data
from sea-ice and plexiglass test specimens.

GENERAL CHARACTERISTICS

A conceptual representation of the viscoelastic-plastic model is
shown in Figure 14 where the symbols $\textcircled{P}$, $\textcircled{V}$, and $\textcircled{E}$ represent the
plastic, viscous, and elastic parts of the model. As suggested by the
figure the total strain, ε, is the sum of the parts $(\varepsilon = \varepsilon_p + \varepsilon_v + \varepsilon_e)$.
Also, the figure illustrates that the applied stress, σ, is transmitted
from $\textcircled{E}$ to $\textcircled{V}$ to $\textcircled{P}$ instantaneously at full value, because the com-
ponents are all in series. Indeed, these characteristics were used in
the previous section for developing the general constitutive model.

As a side comment, other combinations of models with different
characteristics can be developed by various arrangements of the basic
components. This is discussed in Appendix C.

To illustrate the viscoelastic-plastic model shown in Figure 14,
consider the strain response due to a constant stress, $\sigma = (1/2)\sigma_L$,
where σ_L is the linear limit. Since σ is within the yield surface, only
elastic and viscous deformation will occur. This is illustrated by the
bottom curve in Figure 15. Note the initial response is the instantaneous
elastic strain, and all additional strain accumulation is viscous.
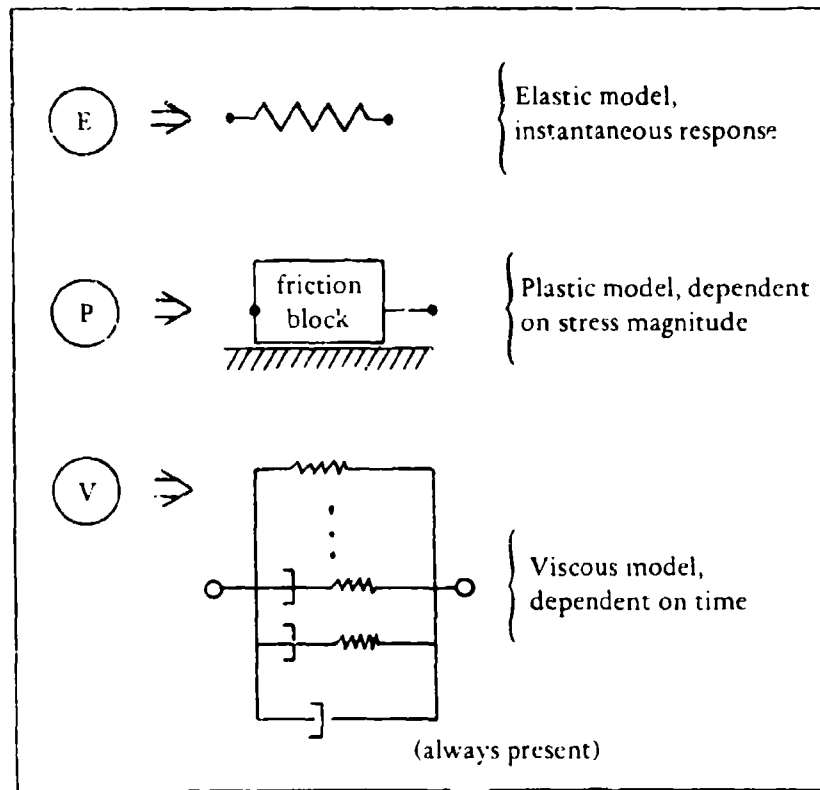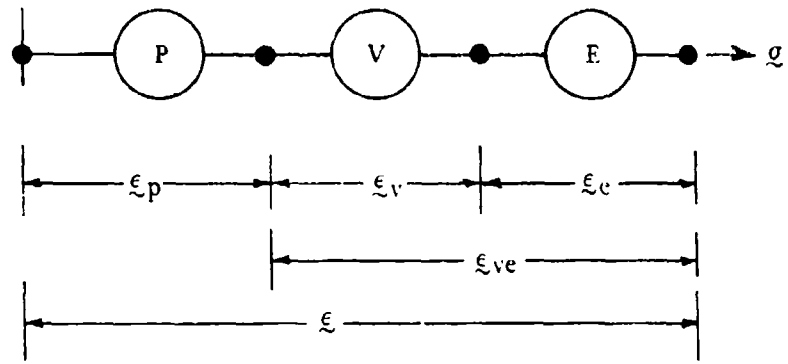
Figure 14. Conceptualization of viscoelastic-plastic model.

90
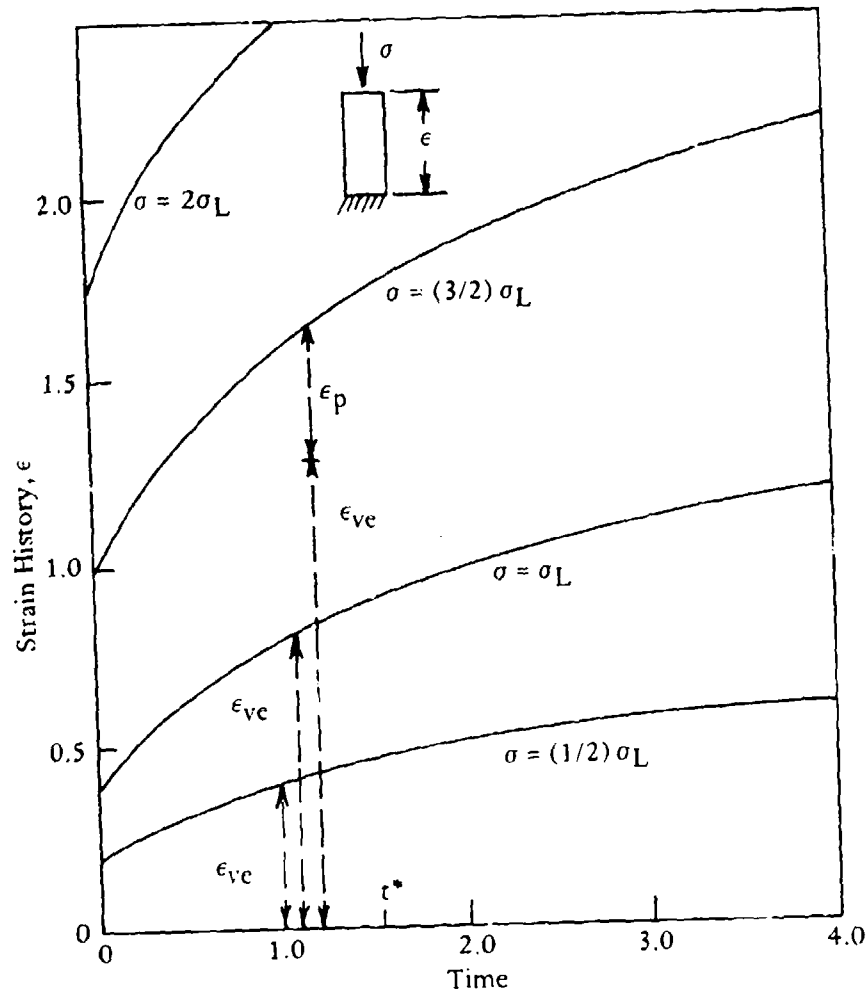
Figure 15.   Typical strain histories for various
levels of stress.

Next, consider the same test with $\sigma \cong \sigma_L$ (slightly less). Again, σ is still within the yield surface. Therefore, the strain response is double the previous strain response as shown by the next curve. Of course, this result is due to the superposition principle of linear viscoelasticity.

Now consider $\sigma = (3/2)\sigma_L$. This time the yield stress is exceeded, triggering a plastic response. Like the elastic strain, the plastic strain occurs instantaneously and, thereafter, remains constant because it only responds to stress changes. The magnitude of the plastic strain is dependent on the hardening function, shape of the yield surface, and level of stress. Figure 15 shows a representative strain history for this example. As the stress level is increased on each subsequent test, the strain magnitudes increase in a nonlinear fashion until the hardening function becomes zero, whereafter unrestrained plastic deformation occurs. Again, Figure 15 illustrates these concepts.

A significant characteristic of this model is that for states of constant stress, only the viscous strain changes with time so that the strain rate is independent of plastic deformation and is linearly related to stress level like an ordinary viscoelastic model.

The above insights are useful for determining the parameters of the model discussed next.

MODEL FITTING TECHNIQUES

The beauty of the viscoelastic-plastic model presented herein is that it is a combination of two well-known constitutive theories: viscoelasticity and plasticity. Accordingly, the material information gathered over the years for the individual theories can be used directly for the combined model.

The first step in establishing a viscoelastic-plastic model representative of a particular material is to determine the viscoelastic portion of the model (i.e., $\boxed{E}$ + $\boxed{V}$ of Figure 14). If the material is

well studied, it is likely that viscoelastic parameters can be found in the engineering literature. Otherwise, Appendix B provides a detailed guideline for converting test data into viscoelastic parameters.

In this case, the most important consideration is to use test data with state variables (i.e., load rates, temperature, moisture, etc.) as close as possible to the conditions of the problem being studied.

Since the viscoelastic model represents the linear portion of the response, it should be based on test data at low stress levels. Or, more ideally, it should be based on an unloading response history since unloading is assumed to be linear.

The plastic portion of the model may be simple or as complicated as desired. In general, a yield condition, flow rule, surface (hardening) rule, and hardening function must be determined. For many materials these are presented in the engineering literature. Also, Appendix A provides a detailed discussion on various plasticity models.

If very little is known about the material being considered, the plasticity model should be made as simple as possible; i.e., assume a simple yield condition (such as Drucker-Prager or Von Mises), assume an associative flow rule, assume an isotropic hardening surface, and calculate a hardening function directly from available test data.

To illustrate the viscoelastic-plastic model fitting procedure, consider the idealized strain history data curves that were discussed in Figure 15. The first step is to determine the viscoelastic creep function $J(t)$, satisfying the relationship $\epsilon(t) = J(t)\sigma$, $(\epsilon < \epsilon_L)$. In other words, by inspecting the data, one recognizes the lower two curves obey the linear viscoelastic superposition principle so that $J(t)$ may be determined from either one of these curves. The detailed process of determining $J(t)$ is given in Appendix B, where $J(t)$ is of the form:

$$J(t) = A + B t + \sum_{i=1}^{N} C_i (1 - e^{-t/\beta_i}) \qquad (5-1)$$

and the unknown parameters to be determined are A, B, C_1, C_2, ... C_N, β_1, β_2, ... β_N.

To identify a complete viscoelastic model, additional material data are required (e.g., shear or bulk function) as discussed in Appendix B. However, if no other data are available, some constant value of Poisson's ratio can be assumed. Methods of inverting creep functions to relaxation functions and converting uniaxial functions to bulk and shear functions are also presented in Appendix B.

After the viscoelastic parameters are determined, the plastic portion of the model is examined by constructing a plot of stress versus plastic strain. To this end, consider any particular time t* in Figure 15. By definition, the plastic strain is

$$\varepsilon_p = \varepsilon(t^*) - \varepsilon_{ve}(t^*)$$

where $\varepsilon(t^*)$ is the strain data at some stress level σ, and $\varepsilon_{ve}(t^*) = J(t^*)\sigma$. Therefore, for any time t* a plot of stress versus plastic strain may be constructed as shown in Figure 16. If the material is ideally viscoelastic-plastic, this plot will be identical for any choice of t*. However, in practice, it is prudent to consider several different values of t* to get an average overtime. In so doing, one may discover the plastic strain is highly time-dependent so that a viscoelastic-plastic model is not suitable. In this case, consult Appendix C for other combo-viscoplastic models.

Assuming the plastic strain remains reasonably constant for each stress level, the next step is to choose a plastic yield condition. Generally, the Drucker-Prager yield condition (see Appendix A) is suffi-cient to characterize material behavior from one-dimensional tests. Assuming isotropic hardening, this condition is:

$$F(\sigma, k) = \alpha \, \sigma_m + \sqrt{J_2} - k \qquad (5\text{-}2)$$

where σ_m is the average hydrostatic stress, and J_2 is the second devia-toric stress invarient. The yield surface may be visualized in principal stress space as a cone whose centerline is along the hydrostat ($\sigma_1 = \sigma_2 = \sigma_3$). The yield parameter, k, is the cone radius measured from the origin, and the parameter α measures the rate of increase of the cone radius in moving along the compression hydrostat. If $\alpha = 0$, the cone becomes a right cylinder and the Drucker-Prager condition reduces to the Von Mises yield condition.

For the problem under consideration, the data in Figure 16 contain two compression tests that exceed the elastic limit. However, because these tests have identical stress paths and intercept the same point on the yield surface, they do not provide sufficient information to deter-mine both k and α independently. If tension yield tests are conducted in addition to the compression yield tests (or, if lateral plastic strains are measured), then both k and α can be determined.

Assuming for now only compression yield data are available (which is often the case), then α must be pre-selected as some constant, say $\alpha = \alpha_o$ (most probably $\alpha_o = 0$). From Figure 16, initial plastic yielding occurs at $\sigma = \sigma_L$ so that from Equation 5-2 the initial value of k is:

$$k_o = \frac{\alpha_o}{3} \sigma_L + \frac{|\sigma_L|}{\sqrt{3}} \qquad (5\text{-}3)$$

where $\sigma_L < 0$ is the initial compressive yield stress. During plastic yielding, k increases such that it continuously satisfies the yield condition.
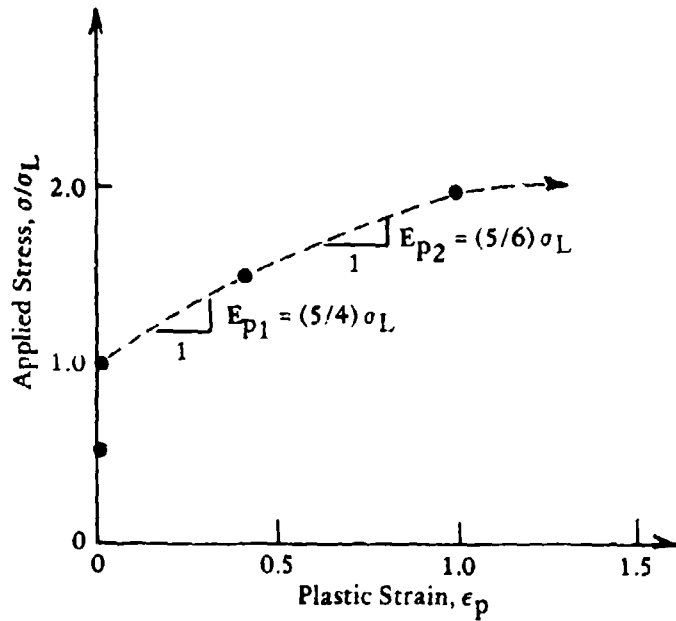
Figure 16. Typical plastic hardening curve.
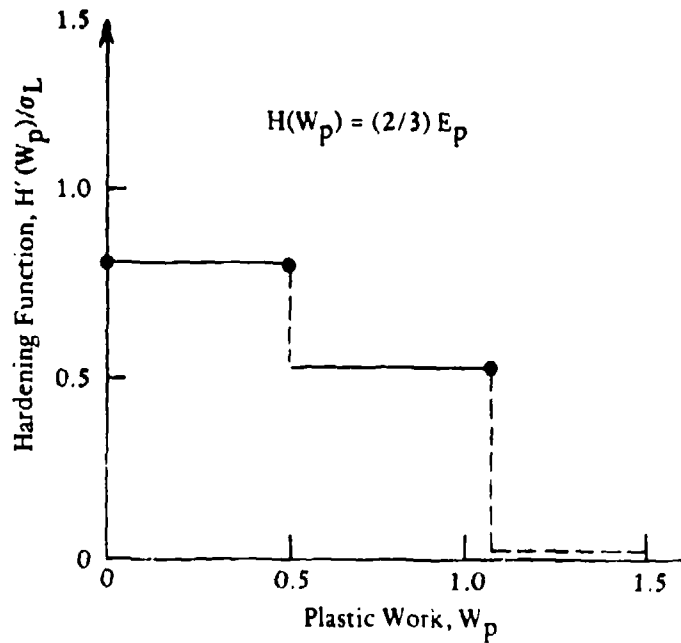
Figure 17. Hardening function.

Having established a yield condition and its parameters, one next assumes an associative flow rule and determines the hardening function. From Equation 2-24, the associative flow rule for the plastic strain increment gives the hardening function as:

$$H(W_p) = n_1^2 \frac{\Delta \sigma}{\Delta \epsilon_p} \qquad (5-4)$$

where n_1 is the component of the yield surface unit-normal collateral with the loading stress, and is given by:

$$n_1 = \frac{\sqrt{2/3}\, \alpha_0 + \sqrt{2}\, \text{Sgn}\, \sigma}{\sqrt{2\sigma_0^2 + 3}} \qquad (5-5)$$

If $\alpha_0 = 0$ (i.e., Von Mises condition), the above reduces to $n_1 = (2/\sqrt{6})$ Sgn σ.

Using Equations 5-4 with n_1 given by Equation 5-5, and $\Delta\sigma/\Delta\epsilon_p$ given by the slopes in Figure 16, the hardening function can be evaluated as a function of plastic work

$$W_p = \int_0^{\epsilon_p} \sigma\, d\epsilon_p$$

(i.e., area under σ versus ϵ_p curve). This is illustrated in Figure 17 for the case $\alpha_0 = 0$.

97

The preceding illustrates the basic strategy of identifying the parameters of the viscoelastic-plastic model. Appendixes A and B provide further insight and details. In the next section some examples are given.

COMPARISON WITH EXPERIMENTAL DATA

In this section, the versatility (and limitations) of the viscoelastic-plastic model is demonstrated by comparing it to experimental strain data from compression test specimens of Plexiglas and sea-ice.

The Plexiglas creep data were generated by Marin, Pao, and Cuff [27], and are shown by discrete data points in Figure 18 for three compressive stress levels, σ = 2,500, 3,100, and 4,000 psi. Using the model fitting procedure in the previous section (including Appendixes A and B), the viscoelastic-plastic model expression for creep strain is:

$$\varepsilon(t) = \frac{\sigma}{10^6} \left[2.57 + 0.000417t + 0.389(1 - e^{-0.3t}) \right] + \varepsilon_p$$

with ε_p = 0, when $\sigma < \sigma_L$

$$= \frac{\sigma - \sigma_L}{E_p(\varepsilon_p)}, \text{ when } \sigma > \sigma_L$$

It is assumed σ_L = 3,100 psi (initial linear limit), and $E_p(\varepsilon_p)$ = 500,000 psi is simplified to a constant. The time unit is hours.

98
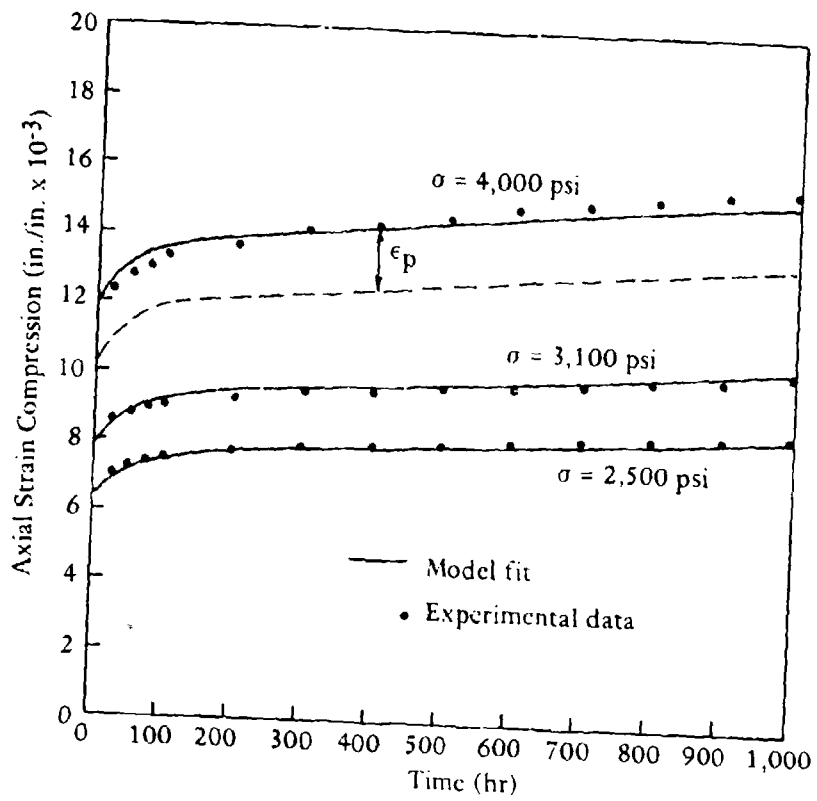
Figure 18. Comparison of viscoelastic-plastic model with experimental data for Plexiglas (Ref 27).

The above expression is plotted as a solid line together with the experimental data points for all three stress levels. For the two lower stress levels, the model is linear viscoelastic (i.e., no plastic response) and compares well with the data points. For the highest stress level (4,000 psi) a plastic strain is generated that combines with the viscoelastic strain. This gives a better fit of experimental strain than just the linear viscoelastic model as shown by the dashed line.

The above example illustrates a predominantly elastic response, a moderate amount of viscous response, and relatively little plastic response. As the stress level increases, plastic response becomes more and more significant.

The second example, sea-ice, illustrates a highly viscous material with pronounced plasticity and relatively small elastic response. The experimental data were generated by Vaudrey [28] and are shown as discrete data points in Figure 19. The data shown are for sea-ice at $-27^{\circ}C$, with ice crystals orthogonal to the direction of loading at three compressive stress levels, $\sigma = 70$, 175, and 350 psi.

A viscoelastic-plastic model fit gives the expression for axial strain as:

$$\varepsilon(t) = \frac{\sigma}{10^6} \left[2.0 + 1.43t + 21.1(1 - e^{-0.75t}) \right] + \varepsilon_p$$

with $\varepsilon_p = 0$, when $\sigma \leq \sigma_L$

$\qquad = \dfrac{\sigma - \sigma_L}{E_p(\varepsilon_p)}$, when $\sigma \geq \sigma_L$

It is assumed $\sigma_L = 250$ psi, and the hardening function, $E_p(\epsilon_p) \propto \sigma_L /$
$(1 + \epsilon_p)^2$, which approaches zero as ϵ_p becomes large.

The above model expression is plotted as solid lines in Figure 19, showing excellent agreement with the data points. In particular, the viscoelastic-plastic model is able to replicate unrestrained plastic flow that occurs at the high stress level.
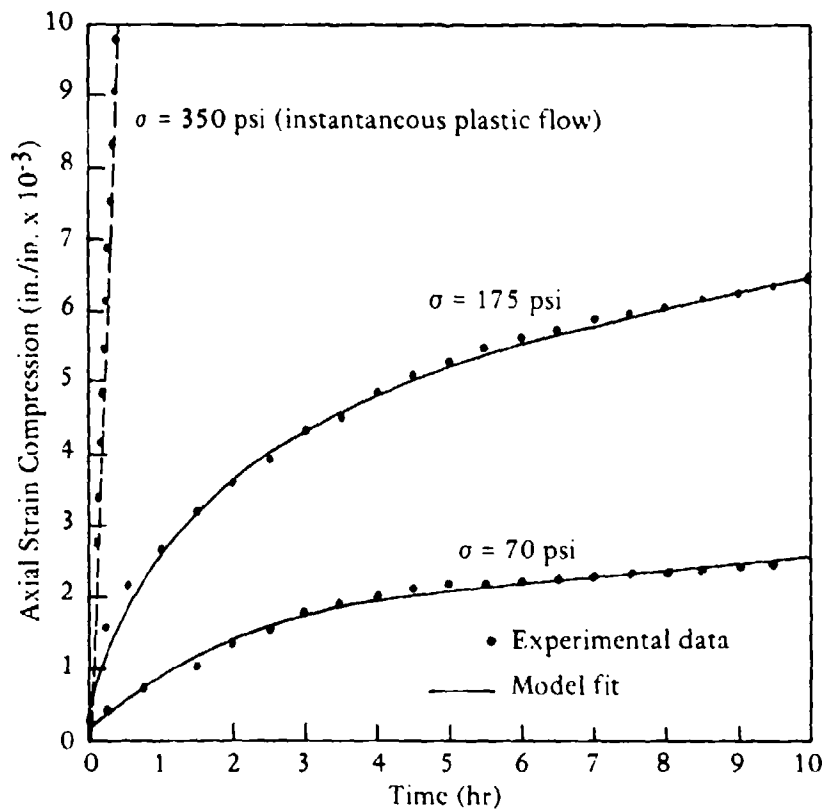
Figure 19. Comparison of viscoelastic-plastic model
with experimental data for sea-ice.

SUMMARY AND RECOMMENDATIONS

This report offers a textbook style development of viscoplasticity.
For completeness, a detailed review of viscoelasticity and plasticity is
also included. The main text focuses on the so-called "viscoelastic-
plastic model." However, this model is just one example of a general
family of combo-viscoplastic models presented in the appendixes.

Each model is initially presented with visual one-dimensional
concepts and then generalized into multidimensional stress space. The
net result is an incremental constitutive model suitable for numerical
computation. To this end, finite element algorithms are proposed for
each model.

The viscoelastic-plastic model is shown to capture the observed
creep responses of such elusive materials as plexiglass and sea-ice.
Also, it is apparent other materials, such as soil, plastic, epoxy,
concrete, etc., can be suitably approximated with this model within
certain ranges.

A primary advantage of the viscoelastic-plastic model is the ease
of parameter identification. This is because it can be divided into
separate viscoelastic and plastic identification problems. The primary
limitation is that the strain rate is independent of plastic strain for
a constant load. This limitation can be removed by employing higher
order combo-viscoplastic models.

Immediate future efforts should be directed on two fronts. First,
the algorithms developed herein should be incorporated into a finite
element program and tested on selected boundary value problems. Second,
and concurrently, higher order combo-viscoplastic models should be
investigated and compared with experimental test data. Here the objec-
tive is to identify a single "grandfather" combo-viscoplastic model that

103

contains all the desired response characteristics and is capable of degenerating to lower order models.

The net result of these efforts would be the beginnings of an analytical tool (finite element program) capable of rationally dealing with structural engineering problems encountered by the Navy.

Finally, the long-range objective should include a material identification study. That is, for each material type, subtypes would be grouped by ranges of state variables, such as temperature, moisture, impurities, etc. Then, viscoplastic parameters (i.e., parameters of the "grandfather" model) could be determined by identification procedures discussed herein. This library of data could be incorporated into the finite element program so that model parameters would be automatically retrieved (or interpolated) by specifying the material type and state variables. Alternatively, experimental data (e.g., triaxial test data) could be input into the program and the parameters determined directly.

The benefits of this plan are enormous, both technically and economically. On the technical side the plan provides a rational and uniform approach for dealing with structural materials, such as concrete, plastics, soils, sea-ice, epoxies, and a host of other time-dependent materials encountered day-to-day by Navy engineers. Economically, under current procedures, it is not uncommon for an engineer to spend more than one-half of his time groping with material models and their param-eters. The proposed plan would relieve the engineer of this burden and allow him to get on with solving the problem.

REFERENCES

1. Oak Ridge National Laboratory. ORNL-4783: Representation of creep metals, by E. Turan Onat and F. Fardshisheh. Oak Ridge, Tennessee, Aug 1972.

2. Green, A. E., and R. S. Rivlin. "The mechanics of nonlinear materials with memory, Part I," Archive for Rational Mechanics and Analysis, vol 1, 1957.

3. McLean, D. Mechanical properties of metals. Wiley, New York, N.Y., 1962.

4. Perzyna, P. "Fundamental problems in viscoplasticity," Advances in Applied Mechanics, vol 9, 1966, pp 243-377.

5. Zienkiewicz, O. C., and I. C. Cormeau. "Visco-plasticity, plasticity and creep in elastic solids, a unified numerical solution approach," International Journal for Numerical Methods in Engineering, vol 8, 1974, pp 821-845.

6. Fung, Y. C. Foundations of solid mechanics. Prentice-Hall Inc., Englewood Cliffs, N.J., 1965.

7. Bathe, K., E. Ramm and E. Wilson. "Finite element formulations for large displacement and large strain analysis," Report No. UCSESM 73-14. University of California, Berkeley, Calif., 1973.

8. Stricklin, J. A., W. E. Haisler and W. A. Von Riesemann. "Formulation, computation, and solution procedures for material and/or geometric nonlinear structural analysis by the finite element method." Sandia Corporation Report SC-CR-72-3102, Alburquerque, N.Mex., Jan 1972.

9. Hartzman, M., and J. T. Hutchinson. "Nonlinear dynamics of solids by the finite element method," Journal of Computer Structures, vol 2, 1972, pp 47-77.

10. Zienkiewicz, O. C. The finite element method in engineering science, McGraw-Hill, London, 1971.

11. Marcal, P. V. "Finite element analysis with material nonlinearities, theory and practice," Prepared for Office of Naval Research, NR-064-512, Aug 1969.

12. Grumman Aerospace Corporation. Grumman Research Department Report RE-483J: Plasticity - Theory and finite element applications, by H. Armen, Jr., H. Levine, and A. Pifko. Bethpage, N.Y., 1972.

13. Mendelson, A. Plasticity: theory and application. MacMillan Company, New York, N.Y., 1968.

14. Hill, R. Mathematical theory of plasticity. Oxford, University Press, 1950.

15. Nayak, G. C., and O. C. Zienkiewicz. "Elasto-plastic stress analysis. A generalization for various constitutive relations including strain softening," International Journal for Numerical Methods in Engineering, vol 5, 1972, pp 113-135.

REFERENCES

1. Oak Ridge National Laboratory. ORNL-4783: Representation of creep metals, by E. Turan Onat and F. Fardshisheh. Oak Ridge, Tennessee, Aug 1972.

2. Green, A. E., and R. S. Rivlin. "The mechanics of nonlinear materials with memory, Part I," Archive for Rational Mechanics and Analysis, vol 1, 1957.

3. McLean, D. Mechanical properties of metals. Wiley, New York, N.Y., 1962.

4. Perzyna, P. "Fundamental problems in viscoplasticity," Advances in Applied Mechanics, vol 9, 1966, pp 243-377.

5. Zienkiewicz, O. C., and I. C. Cormeau. "Visco-plasticity, plasticity and creep in elastic solids, a unified numerical solution approach," International Journal for Numerical Methods in Engineering, vol 8, 1974, pp 821-845.

6. Fung, Y. C. Foundations of solid mechanics. Prentice-Hall Inc., Englewood Cliffs, N.J., 1965.

7. Bathe, K., E. Ramm and E. Wilson. "Finite element formulations for large displacement and large strain analysis," Report No. UCSESM 73-14. University of California, Berkeley, Calif., 1973.

16. Hodge, P. G. "'Discussion on a new method of analyzing stress and strains in work hardening plastic solids' by W. Prager," Journal of Applied Mechanics, vol 24, 1957, pp 482-484.

17. Goel, R. P., and L. E. Malvern. "Biaxial plastic simple waves with combined kinematic and isotropic hardening," Journal of Applied Mechanics, vol 37, 1970, pp 1100-1106.

18. Prager, W. An introduction to plasticity. Addison-Wesley Publishing Co., Inc., Reading, Mass., 1959.

19. Flugge, W. Viscoelasticity. Blaisdell Publishing Company, Waltham, Mass., 1967.

20. Christensen, R. M. Theory of viscoelasticity. Academic Press Inc., New York, N.Y., 1971.

21. Naval Civil Engineering Laboratory. Technical Report R-803: Ice engineering: Viscoelastic finite element formulation, by M. G. Katona. Port Hueneme, Calif., Jan 1974.

22. Distefano, N. Nonlinear processes in engineering. Academic Press Inc., New York, N.Y., 1974.

23. Malone, D. W. "Finite elements and dynamic viscoelasticity," Journal of Engineering Mechanics Division, Proc. ASCE, Aug 1971.

24. Taylor, R. L. "An approximate method for thermoviscoelastic stress analysis," Nuclear Engineering and Design, vol 4, 1966, p 21.

25. University of California, College of Engineering. Report No. AM-67-2: A class of viscoelastic-plastic media, by A. E. Green and P. M. Naghdi. Berkeley, Calif., Mar 1967.

26. Bazant, Z. P. "Endochronic theory of inelasticity and failure of concrete," Journal of Engineering Mechanics Division, ASCE, vol 102, no. EM4, Aug 1976, pp 701-735.

27. Marin, J., Y. Pao, and G. Cuff. "Creep properties of Lucite and Plexiglass for tension, compression, bending and torsion," presented at ASME meeting, Division of Rubber and Plastics, paper no. 50-A-19, Nov 26, 1950.

28. Civil Engineering Laboratory. Technical Memorandum TM-61-76-3: Preliminary creep results from viscoelastic laboratory testing program, by K. D. Vaudrey. Port Hueneme, Calif., Mar 1976.

Appendix A

PLASTICITY MODELS AND CONCEPTS

In this appendix, plasticity concepts are elaborated for common yield conditions and flow rules with emphasis on methods of identifying plasticity parameters from experimental data.

The first and foremost requirement to establish a plasticity model is the selection of a yield condition. Using the universal form established in Equation 2-34, the general yield condition is written as:

$$F = f(\underset{\sim}{\sigma} - \bar{\sigma}_p) - \bar{k}* \qquad (A-1)$$

such that $F = 0$ implies plastic response

$\qquad\qquad F < 0$ implies nonplastic response

and $f(\underset{\sim}{\sigma} - \bar{\sigma}_p)$ = loading function

$\qquad\qquad \bar{k}*$ = yield parameter (universal weighting)

For a particular current value of the weighted plastic-tracking stress, $\bar{\underset{\sim}{\sigma}}_p$, and of the yield parameter, $\bar{k}*$, the yield surface is defined by all stress states, $\underset{\sim}{\sigma}$, such that $F = 0$. The unit normal of the yield surface in six-dimensional stress space is given by:

$$\hat{\underset{\sim}{n}} = \underset{\sim}{f}_\sigma / \sqrt{\underset{\sim}{f}_\sigma^T \underset{\sim}{f}_\sigma} \qquad\qquad (A-2)$$

where

$$\underset{\sim}{f}_\sigma = \frac{\partial f(\underset{\sim}{\sigma} - \bar{\underset{\sim}{\sigma}}_p)}{\partial \underset{\sim}{\sigma}} \qquad\qquad (A-3)$$

The unit normal, $\hat{\underset{\sim}{n}}$, is an important vector, because it controls the magnitude ($\Delta\underset{\sim}{\sigma}^T \cdot \hat{\underset{\sim}{n}}$) and direction of plastic strain. Observe from Equation A-2 that $\hat{\underset{\sim}{n}}$ is determined directly from the gradient of the loading function so that the choice of loading function dictates the general nature of plastic flow.

Loading functions are generally written as functions of the stress invariants:

$$f(\underset{\sim}{\sigma} - \bar{\underset{\sim}{\sigma}}_p) = f[\sigma_m(\underset{\sim}{\sigma} - \bar{\underset{\sim}{\sigma}}_p), J_2'(\underset{\sim}{\sigma} - \bar{\underset{\sim}{\sigma}}_p), J_3'(\underset{\sim}{\sigma} - \bar{\underset{\sim}{\sigma}}_p)] \qquad (A-4)$$

where σ_m is the spherical stress invariant and J_2' and J_3' are the second and third deviatoric stress invariants. Using the chain rule, the gradient vector is given by:

$$\underset{\sim}{f}_\sigma = \frac{\partial f}{\partial \sigma_m} \underset{\sim}{a}_1 + \frac{\partial f}{\partial J_2'} \underset{\sim}{a}_2 + \frac{\partial f}{\partial J_3'} \underset{\sim}{a}_3 \qquad\qquad (A-5)$$

The vectors a_1, a_2, and a_3 are independent of the loading function and are given by:

$$a_1 = \frac{\partial \sigma_m}{\partial \sigma} \qquad (A-6)$$

$$a_2 = \frac{\partial J_2'}{\partial \sigma} \qquad (A-7)$$

$$a_3 = \frac{\partial J'}{\partial \sigma} \qquad (A-8)$$

The foregoing has illustrated general forms for yield conditions with arbitrary loading functions. In the next section these concepts will be illustrated on a particular form.

DRUCKER-PRAGER YIELD CONDITION

A particularly useful and versatile yield condition is the so-called Drucker-Prager model. For clarity and conciseness, the model will be developed assuming isotropic hardening (i.e., $\sigma_p = 0$); however, the inclusion of universal hardening is a straightforward extension.

The Drucker-Prager yield condition is:

$$F = \left(\alpha \, \sigma_m + \sqrt{J_2'} \right) - k^* \leq 0 \qquad (A-9)$$

111

which implies the loading function is:

$$f = \alpha \, \sigma_m + \sqrt{J_2'} \qquad\qquad (A-10)$$

The invarients σ_m and J_2' are measures of hydrostatic stress and shear stress, respectively, and are defined as:

$$\sigma_m = \frac{1}{3} (\sigma_1 + \sigma_2 + \sigma_3) \qquad\qquad (A-11)$$

$$J_2' = \frac{1}{2} [\sigma_1 - \sigma_m)^2 + (\sigma_2 - \sigma_m)^2 + (\sigma_3 - \sigma_m)^2]$$

$$+ \, \tau_{12}^{\,2} + \tau_{23}^{\,2} + \tau_{31}^{\,2} \qquad\qquad (A-12)$$

where σ_1, σ_2, and σ_3 are normal stresses, and τ_{12}, τ_{23}, and τ_{31} are shear stresses.

The parameters of the yield condition are α and k*, which are selected to establish the shape of the yield surface. For example, if $\alpha = 0$, the yield surface becomes a cylinder of revolution about the hydrostat in principal stress space with radius k*, or equivalently, it may be viewed as a straight line on a $\sigma_m, \sqrt{J_2}$ graph as shown in Figure A-1a. This type of loading function is associated with the Von Mises yield criterion and is a good representation for ductile metals.

For a more general case, α is specified non zero, which provides the conical surface shown in Figure A-1b. The conical surface is associated with the standard Drucker-Prager yield criterion, which has applications in concrete, soil, rock, etc.
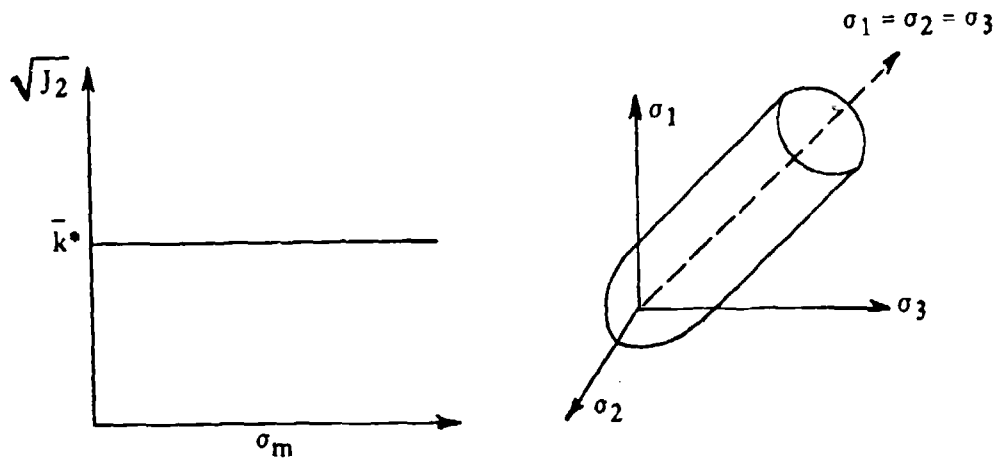
(a) Von Mises yield criterion.
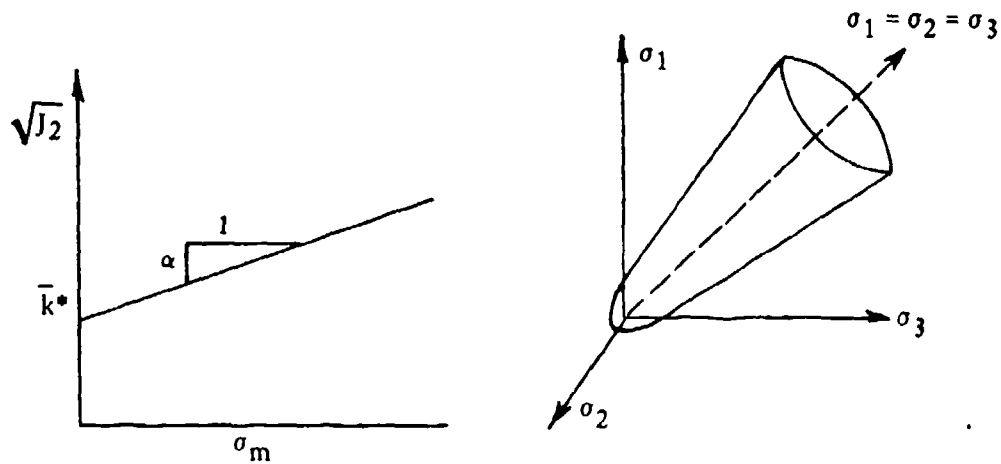
(b) Drucker-Prager yield criterion.
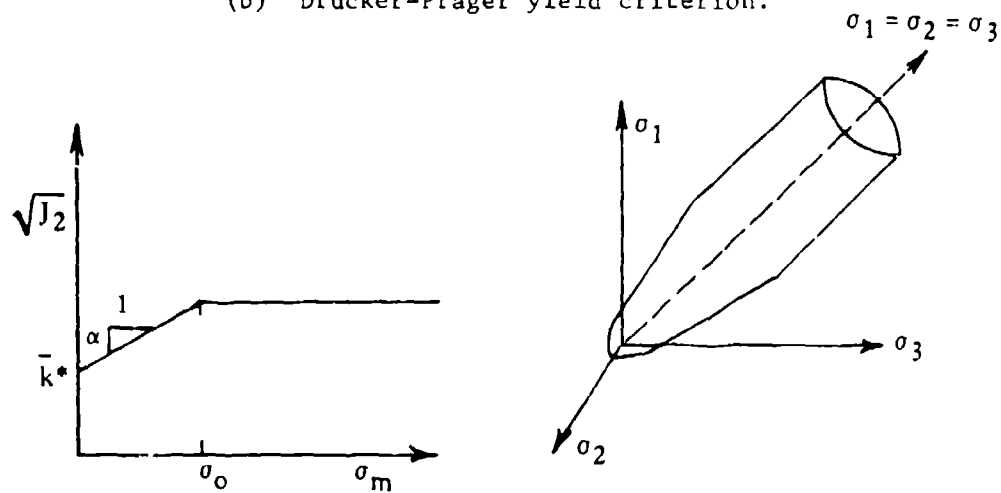
(c) Modified Drucker-Prager yield criterion.

Figure A-1. Yield criteria.

The yield condition can also be applied in piecewise continuous fashion to better approximate actual yield surfaces as indicated in Figure A-1c. To apply this model, one loading function is operable for values of $\sigma_m < \sigma_o$, and a second loading function is operable for $\sigma_m > \sigma_o$. Additional functions can be added if desired. This is termed "modified Drucker-Prager" model.

The Von Mises yield criterion only requires one parameter, k*, and therefore, only one material test to initially characterize the yield surface. The standard Drucker-Prager criterion requires determination of α and k*; thus, it requires two material tests are required. Table A-1 identifies the Vo. "se p .meter for a tensile test and the Drucker-Prager parameters for a axial strength test.

The description of and k* for Drucker-Prager are in terms of the cohesion stress, C, and internal angle of friction, θ, as determined from at least two triaxial tests. To illustrate the derivation of α and k*, consider two triaxial tests under different confining pressures and loaded axially to failure as suggested in Figure A-2. Drawing Mohr circles for both stress states at failure permits defining a straight line failure surface with constants C and θ as illustrated in Figure A-3. The failure surface prescribes what combination of shear stress and normal stress will cause failure, i.e.,

$$\tau = C + \sigma \tan \theta \qquad (A-13)$$

where τ = shear stress at failure (positive)

  σ = normal stress at failure (compression positive)

All states of stress (τ, σ) satisfying Equation A-13 are failure states, and the equation is known as a Coulomb failure criterion. The

rotated stresses, τ and σ, are related to the principal stresses, σ_1 and σ_3, through the Mohr circle geometry as:

$$\tau = \frac{(\sigma_1 - \sigma_3)}{2} \cos\theta \qquad (A-14)$$

$$\sigma = \frac{(\sigma_1 + \sigma_3)}{2} - \frac{(\sigma_1 - \sigma_3)}{2} \sin\theta \qquad (A-15)$$

Accordingly, Equation A-13 may be written as:

$$\sigma_1 - \left(\frac{1 + \sin\theta}{1 - \sin\theta} \right) \sigma_3 - \frac{2 C \cos\theta}{1 - \sin\theta} = 0 \qquad (A-16)$$

Now the objective is to put the general yield condition, $\alpha\, \sigma_m + \sqrt{J_2'} - k^* = 0$, into the form of Equation A-16 in order to equate coefficients and, thereby, determine k^* and α in terms of C and θ. For a triaxial test, we have $\sigma_m = -(\sigma_1 + 2\,\sigma_3)/3$ and $\sqrt{J_2'} = (\sigma_1 - \sigma_3)/\sqrt{3}$ (assuming compression positive and $\sigma_1 > \sigma_3$), so that the general yield condition can be written as:

$$\sigma_1 - \frac{(\sqrt{3} + 2\,\alpha)}{(\sqrt{3} - \alpha)} \sigma_3 - \frac{3\, k^*}{\sqrt{3} - \alpha} = 0 \qquad (A-17)$$

Equating the coefficients of σ_3 and the constant terms between Equations A-16 and A-17 gives the values for k^* and α in Table A-1.

Table A-1. Yield Surface Parameters

Criterion	α	k^*
Von Mises	0	$\sigma_y/\sqrt{3}$
Drucker-Prager	$\dfrac{2\sqrt{3}\sin\theta}{3-\sin\theta}$	$\dfrac{2\sqrt{3}\,C\cos\theta}{3-\sin\theta}$

where σ_y = yield stress in one-dimensional stress state

         C = shear strength at zero confining pressure

 θ = slope of triaxial strength envelope
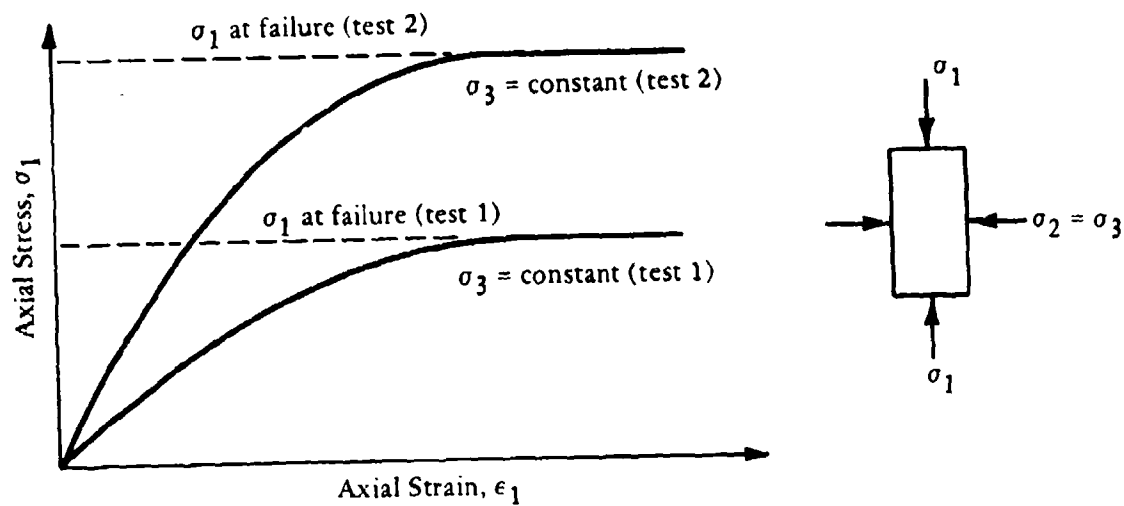
Figure A-2. Typical triaxial test data.
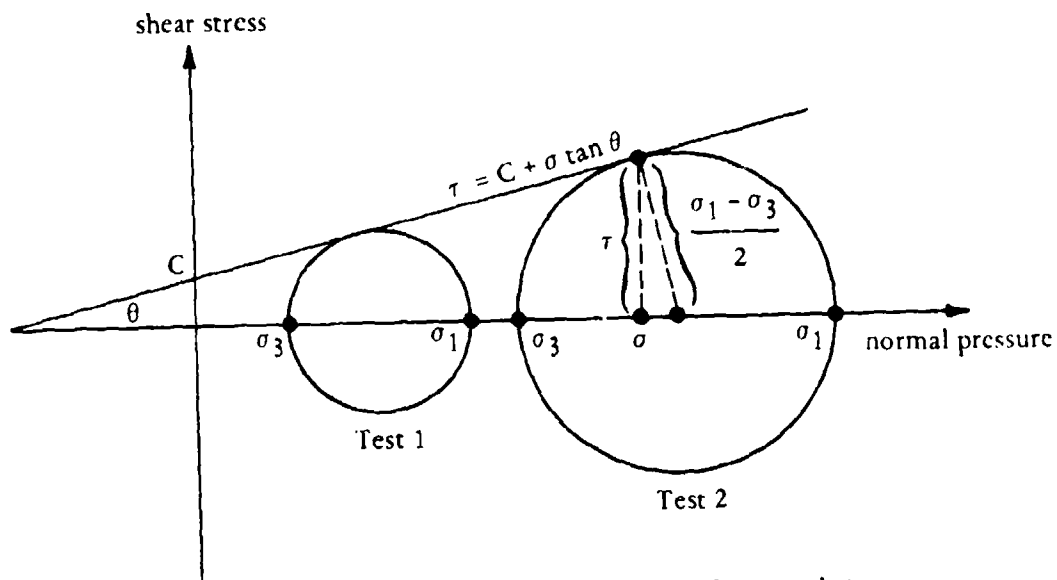
Figure A-3. Mohr circle plots of test data.

It should be appreciated that the determination of α and k* can be achieved in a direct manner without the need of computing C and θ. That is, Equation A-17 can be used directly by inserting the failure stresses, σ_1 and σ_3, for the two test specimens, thereby providing two equations for the two unknowns k* and α.

DRUCKER-PRAGER ASSOCIATIVE FLOW RULE AND HARDENING FUNCTION

In general, an associative rule (e.g., Equation 2-26) can be written as:

$$\Delta \underset{\sim p}{\varepsilon} = \frac{1}{H'} \underset{\sim}{N} \Delta \underset{\sim}{\sigma} \tag{A-18}$$

where $\quad \underset{\sim}{N} = \underset{\sim}{\hat{n}} \, \underset{\sim}{\hat{n}}^T$

In the above, $\Delta \underset{\sim p}{\varepsilon}$ is the plastic strain increment, $\Delta \underset{\sim}{\sigma}$ is the total stress increment, H' is the hardening function, and $\underset{\sim}{N}$ is dependent on the unit normal of the yield surface, $\underset{\sim}{\hat{n}}$.

Consider the Drucker-Prager loading function (Equation A-10) for states of stress characteristic of common tests (such as, triaxial or confined compression); i.e.,

σ_1: independent stress

$\sigma_2 = \sigma_3$: independent stress

$\tau_{12} = \tau_{13} = \tau_{23} = 0$

113

The yield surface unit normal for this stress state is:

$$\hat{\underset{\sim}{n}} = A \begin{Bmatrix} \beta \\ 1 \\ 1 \\ 0 \\ 0 \\ 0 \end{Bmatrix} \tag{A-20}$$

where

$$\beta = \frac{2\alpha + 2\sqrt{3}\ \text{sgn}}{2\alpha - \sqrt{3}\ \text{sgn}}$$

$$A = \frac{2\alpha - \sqrt{3}\ \text{sgn}}{\sqrt{6(2\alpha^2 + 3)}}$$

$$\text{sgn} = \text{sign of } (\sigma_1 - \sigma_3)$$

Assuming the material is initially isotropic, the two independent stresses (say σ_1 and σ_3) produce a corresponding strain state as follows:

ε_1: independent strain

$\varepsilon_2 = \varepsilon_3$: independent strain

$\gamma_{12} = \gamma_{23} = \gamma_{13} = 0$

With the above symmetry, the plastic flow rule (Equation A-18) can be reduced to the following:

$$\begin{Bmatrix} \Delta\varepsilon_1 \\ \Delta\varepsilon_3 \end{Bmatrix}_{plastic} = \frac{A^2}{H'} \begin{bmatrix} \beta^2 & 2\beta \\ \beta & 2 \end{bmatrix} \begin{Bmatrix} \Delta\sigma_1 \\ \Delta\sigma_3 \end{Bmatrix}_{total} \tag{A-21}$$

119

The correspo⌐ding elastic strains for this stress state are:

$$
\left\{ \begin{array}{c} \Delta\varepsilon_1 \\ \Delta\varepsilon_3 \end{array} \right\}_{elastic} = \frac{1}{E} \begin{bmatrix} 1 & -2\,\nu \\ -\nu & (1-\nu) \end{bmatrix} \left\{ \begin{array}{c} \Delta\sigma_1 \\ \Delta\sigma_3 \end{array} \right\}_{total}
\qquad \text{(A-22)}
$$

Therefore, the total stress-strain relationship is given by the sum of elastic and plastic strain as:

$$
\left\{ \begin{array}{c} \Delta\varepsilon_1 \\ \Delta\varepsilon_2 \end{array} \right\} = \begin{bmatrix} \left(\dfrac{A^2\beta^2}{H'} + \dfrac{1}{E}\right) & \left(\dfrac{2\,A^2\,\beta}{H'} - \dfrac{2\,\nu}{E}\right) \\[2ex] \left(\dfrac{A^2\,\beta}{H'} - \dfrac{\nu}{E}\right) & \left(\dfrac{2\,A^2}{H'} + \dfrac{1-\nu}{E}\right) \end{bmatrix} \left\{ \begin{array}{c} \Delta\sigma_1 \\ \Delta\sigma_2 \end{array} \right\}
\qquad \text{(A-23)}
$$

Equation A-23 is applicable for any test data conforming to the symmetry conditions: $\Delta\varepsilon_2 = \Delta\varepsilon_3$, $\Delta\sigma_2 = \Delta\sigma_3$, and all shear stress and strains are zero.

For a triaxial test, $\Delta\sigma_1$ and $\Delta\sigma_3$ are specified, and $\Delta\varepsilon_1$ is the measured axial strain increment (elastic and plastic). Assuming the elastic properties E and ν are determined by standard procedures, the hardening function $H'(\varepsilon_p)$ can be determined from Equation A-23 as:

$$
H'(\varepsilon_p) = \frac{A^2\,\beta(\beta\,\Delta\sigma_1 + 2\,\Delta\sigma_2)}{\Delta\varepsilon_1 - \dfrac{\Delta\sigma_1}{E} + \dfrac{2\,\nu\,\Delta\sigma_2}{E}}
\qquad \text{(A-24)}
$$

As another example, a one-dimensional strain test specifies $\Delta\sigma_1$ and measures $\Delta\varepsilon_1$ with the constraint $\Delta\varepsilon_3 = 0$. For this case, the hardening function is given by:

$$H'(\varepsilon_p) = \frac{A^2[2 + \beta^2(1 - \nu) + 4\,\beta\,\nu] - \dfrac{\Delta\varepsilon_1}{\Delta\sigma_1}(2\,A^2\,E)}{\dfrac{1}{E}(2\,\nu^2 + \nu - 1) + \dfrac{\Delta\varepsilon_1}{\Delta\sigma_1}(1 - \nu)} \qquad \text{(A-25)}$$

It is interesting to note that for the one-dimensional strain case, a perfectly plastic material, $H'(\varepsilon_p) = 0$, does not result in unrestrained plastic flow. This is because the lateral stress, σ_3, adjusts to keep the stress state on the yield surface.

DRUCKER'S POSTULATE AND FLOW RULES

Drucker's postulate may be stated as: "Given a stress state in equilibrium on the yield surface and an external load cycle slowly applied and removed, then the external agency does positive work during loading, and the net work over the cycle is non-negative."

A material conforming to this postulate is termed stable. Also, a mathematical flow law ensuring this condition is admissible (i.e., will not create energy). In equation form, Drucker's postulate is:

$$d\underset{\sim}{\sigma}^T(d\underset{\sim}{\varepsilon}_p + d\underset{\sim}{\varepsilon}_e) > 0 \qquad \text{(loading)}$$

$$d\underset{\sim}{\sigma}^T(d\underset{\sim}{\varepsilon}_p + d\underset{\sim}{\varepsilon}_e) - d\underset{\sim}{\sigma}^T(d\underset{\sim}{\varepsilon}_p) \geq 0 \qquad \text{(full cycle)}$$

The first relationship signifies both elastic and plastic work increments are positive during loading. The second relationship implies unloading work is all elastic so that for a full cycle we must have:

$$d\underset{\sim}{\sigma}^T \, d\underset{\sim}{\varepsilon}_p \, \geq \, 0 \qquad\qquad (A-26)$$

Now replacing $d\varepsilon_p$ with the general flow rule (Equation 2-26) the above equation becomes:

$$\frac{(d\sigma^T \cdot \hat{\underset{\sim}{n}})(d\sigma^T \cdot \hat{\underset{\sim}{m}})}{H'} \, \geq \, 0 \qquad\qquad (A-27)$$

where $\hat{\underset{\sim}{m}}$ is the assumed direction of plastic straining. If $\hat{\underset{\sim}{m}} = \hat{\underset{\sim}{n}}$, the flow rule is said to be associative; otherwise, it is nonassociative.

By virtue of the yield criterion, the scalar product $d\underset{\sim}{\sigma}^T \cdot \hat{\underset{\sim}{n}}$ is always non-negative during plastic deformation. Therefore, Equation A-27 is always satisfied for an associative flow rule, since H' is also non-negative for stable materials.

In order for a nonassociative flow rule to satisfy the stability criterion, we must have $d\underset{\sim}{\sigma}^T \cdot \hat{\underset{\sim}{m}} > 0$ for any $d\underset{\sim}{\sigma}$ that causes plastic flow. Further implications of nonassociative rules are beyond the scope of this appendix and require additional research.

Appendix B

IDENTIFICATION OF VISCOELASTIC RELAXATION AND CREEP FUNCTIONS

The intent of this appendix is to provide guidelines for converting viscoelastic data into creep and/or relaxation functions of an exponential series form. Specifically, the following three basic problems will be addressed:

1. Obtaining a creep function from creep data, or obtaining a relaxation function from relaxation data.

2. Inverting a creep function to a relaxation function and vice versa.

3. Transforming relaxation functions from one type to another, such as transforming a Young's Modulus function into bulk and/or shear functions.

I. CREEP AND RELAXATION FUNCTIONS FROM VISCOELASTIC DATA

The objective is to curve-fit (by least-square error) an exponential series with available viscoelastic data to achieve either a creep or relaxtion function. The exponential series has the general form:

$$Y(t, \underset{\sim}{\phi}) = A + Bt + \sum_{k=1}^{N} C_k (1 - e^{-X_k t}) \qquad \text{(B-1)}$$

where A, B, C_1, C_2, ... C_N, X_1, X_2, ... X_N are unknown parameters to be determined. In this form, the term A is the initial elastic response, B is the rate of linear response, C_k is the long-time viscous response, and X_k is the inverse of retardation or relaxation time. For convenience, these parameters are denoted by $\underset{\sim}{\phi}$, i.e.:

$$\underset{\sim}{\phi} = \left\{ \phi_1, \phi_2, \dots \phi_M \right\} = \left\{ A, B, C_1, C_2, \dots C_N, X_1, X_2, \dots X_N \right\} \quad (B-2)$$

where $M = 2(N + 1)$

The form of Equation B-1 is applicable for either a creep or relaxation function with the necessary provisions of $Y(t,\underset{\sim}{\phi}) > 0$ and $X_k > 0$ to insure decay of each exponential term. In the case of a relaxation function, $Y(t,\underset{\sim}{\phi})$ must be a monotonically decreasing function so that the linear parameter $B \equiv 0$. However, a creep function monotonically increases; thus, the parameter B need not be specified zero. Figure B-1 illustrates example forms of Equation B-1 for creep and relaxation functions.

The known viscoelastic data represent either creep data or relaxation data. Here, creep data are defined as a recorded strain history corresponding to a material specimen subjected to a constant unit of stress, such as axial stress, shear stress, or hydrostatic stress. Conversely, relaxation data are defined as a recorded stress history corresponding to a material specimen subjected to a constant unit of strain deformation (e.g., axial, shear, volumetric, etc.)

In either case, it is assumed the data are reduced to a set of discrete values (Y_i, t_i), $i = 1, 2, \dots n$, where Y_i is the creep/relaxation data point at time t_i.

These discrete data may be written as a piecewise linear function of time as follows:

$$\overline{Y}(t) \;=\; W_i \;+\; \dot{Y}_i\, t, \qquad \text{for } t_i < t < t_{i+1} \qquad (B\text{-}3)$$

where
$$W_i \;=\; (Y_i - \dot{Y}_i\, t_i)$$

$$\dot{Y}_i \;=\; (Y_{i+1} - Y_i)/(t_{i+1} - t_i)$$

In the above, $\overline{Y}(t)$ is a piecewise function connecting successive data points, as illustrated in Figure B-2 for the case of creep data. Higher order interpolation functions could be used if desired.

To fit the function $Y(t,\underset{\sim}{\phi})$ (Equation B-1) to the viscoelastic data $\overline{Y}(t)$ (Equation B-3), the least-square-error method with Newton-Raphson solution procedure is used as follows.

First define error:

$$\text{error}(t,\underset{\sim}{\phi}) \;=\; Y(t,\underset{\sim}{\phi}) \;-\; \overline{Y}(t) \qquad (B\text{-}4)$$

Squaring the error and summing it by integrating over the time of interest, $0 \le t \le t_n$, gives the net square error:

$$\varepsilon(\underset{\sim}{\phi}) \;=\; \int_0^{t_n} [Y(t,\underset{\sim}{\phi}) - \overline{Y}(t)]^2 \, dt \qquad (B\text{-}5)$$
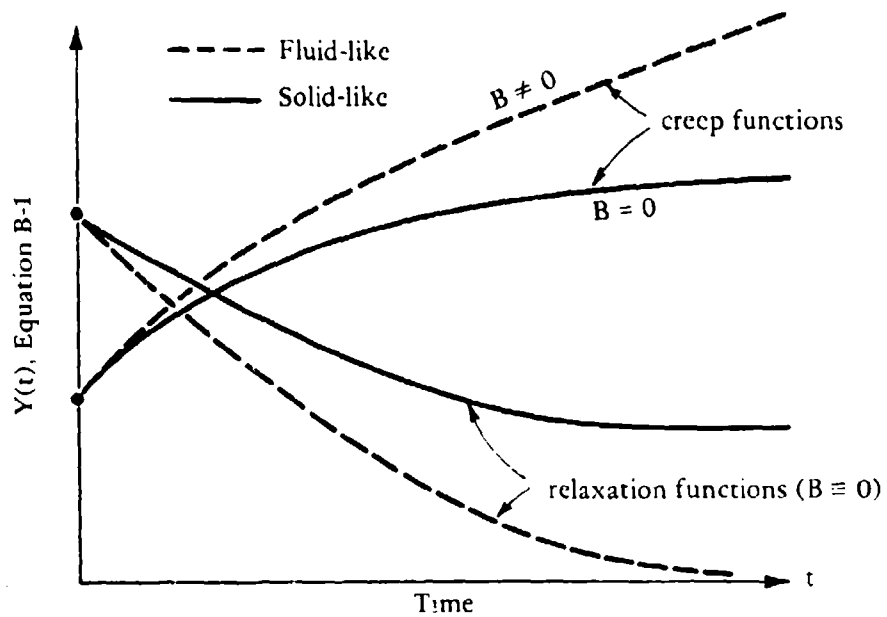
Figure B-1.   General forms of Equation B-1.
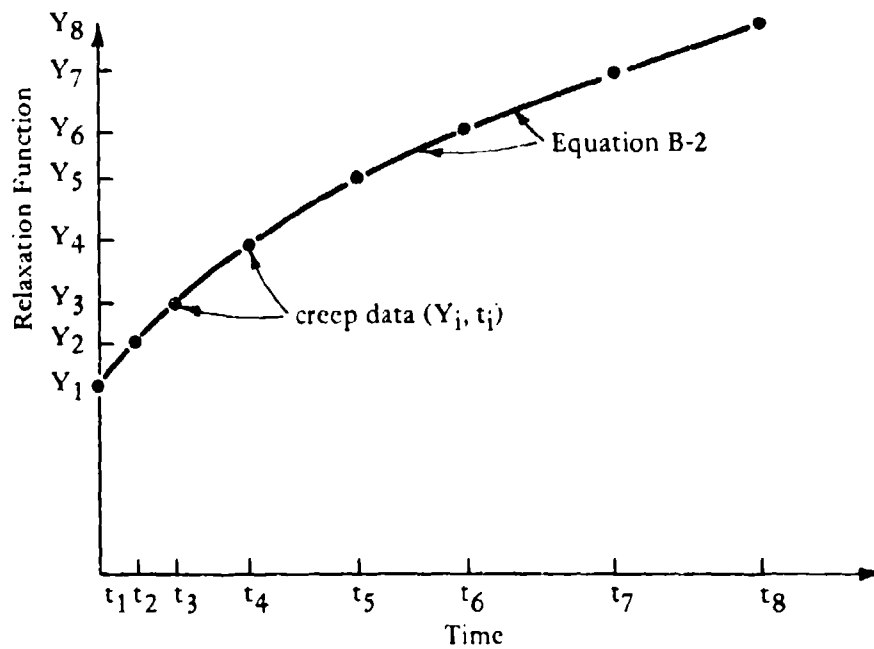
Figure B-2.   Creep data example.

Minimizing this net error with respect to each unknown parameter, $\phi_m = (A, B, C, \ldots C_N, X_1, X_2, \ldots X_N)$ gives M equations:

$$\frac{\partial \varepsilon(\phi)}{\partial \phi_m} = 2 \int_0^{t_n} [Y(t,\underset{\sim}{\phi}) - \overline{Y}(t)] \frac{\partial Y(t,\phi)}{\partial \phi_m} dt = 0 \qquad (B\text{-}6)$$

where $m = 1, 2, \ldots M$. For brevity, the above equations are denoted by an M-dimensional vector equation as:

$$\underset{\sim}{f}(\underset{\sim}{\phi}^O) = \underset{\sim}{0} \qquad (B\text{-}7)$$

where $\underset{\sim}{\phi}^O = \left\{ A^O, B^O, \underset{\sim k}{C}^O, \underset{\sim k}{X}^O \right\}$ represents the solution vector satisfying Equation B-7. Since the equations are nonlinear with respect to the parameters $\underset{\sim k}{X}$, an iterative solution technique is required. In the following, a Newton-Raphson iterative solution procedure is presented.

The Newton-Raphson procedure is based on a Taylor series expansion of Equation B-7, where $\underset{\sim}{\phi}^O$ is written as:

$$\underset{\sim}{\phi}^O = \underset{\sim}{\phi}^S + \underset{\sim}{\Delta \phi} \qquad (B\text{-}8)$$

such that $\underset{\sim}{\phi}^S$ is any estimate of $\underset{\sim}{\phi}^O$, and $\underset{\sim}{\Delta \phi}$ corrects the estimate to satisfy Equation B-8. The objective is to successively obtain a better estimate of $\underset{\sim}{\phi}^S$ so that $\underset{\sim}{\Delta \phi} \to 0$. To this end, the Taylor series expansion of Equation B-7 can be written as:

$$\underset{\sim}{f}(\underset{\sim}{\phi}^s + \underset{\sim}{\Delta\phi}) = \underset{\sim}{0} = \underset{\sim}{f}(\underset{\sim}{\phi}^s) + \underset{\sim}{F}(\underset{\sim}{\phi}^s) \cdot \underset{\sim}{\Delta\phi} + \text{higher order terms} \quad \text{(B-9)}$$

where $\quad \underset{\sim}{F}(\underset{\sim}{\phi}^s) = \partial(\underset{\sim}{f})/\partial\underset{\sim}{\phi}$

$\underset{\sim}{F}(\underset{\sim}{\phi}^s)$ is an MxM-dimensional Jacobian matrix evaluated at $\underset{\sim}{\phi}^s$, and the higher order terms are second order and above products of $\underset{\sim}{\Delta\phi}$ (i.e., squares, cubes, etc.).

If $\underset{\sim}{\Delta\phi}$ is small so that higher order terms are negligible, then $\underset{\sim}{\Delta\phi}$ may be approximately determined as:

$$\underset{\sim}{\Delta\phi} \cong -\underset{\sim}{F}^{-1}(\underset{\sim}{\phi}^s) \cdot \underset{\sim}{f}(\underset{\sim}{\phi}^s) \quad \text{(B-10)}$$

With this approximation for $\underset{\sim}{\Delta\phi}$ a better estimate for $\underset{\sim}{\phi}^s$ is:

$$\underset{\sim}{\phi}^{s+1} = \underset{\sim}{\phi}^s + \underset{\sim}{\Delta\phi} \quad \text{(B-11)}$$

Returning to Equation B-10, the process is repeated utilizing $\underset{\sim}{\phi}^{s+1}$ in place of $\underset{\sim}{\phi}^s$. After a sufficient number of iterations, we have $\underset{\sim}{\Delta\phi} \to 0$ and $\underset{\sim}{\phi}^{s+1} \to \underset{\sim}{\phi}^o$, providing the desired solution.

The major effort in the above algorithm is establishing the vector $\underset{\sim}{f}(\underset{\sim}{\phi}^s)$ and the Jacobian $\underset{\sim}{F}(\underset{\sim}{\phi}^s)$ for each iteration. These somewhat laborious developments are given next.

For specificity, the M equations represented by $\underset{\sim}{f}(\underset{\sim}{\phi}) = \underset{\sim}{0}$ and defined by Equation B-6 are distinguished by the parameter groups A, B, C_j, and X_j as follows:

$$f_A = \frac{\partial \epsilon(\underset{\sim}{\phi})}{\partial A} = \int_0^{t_n} [Y(t,\underset{\sim}{\phi}) - \overline{Y}(t)] \, dt \qquad (B-12)$$

$$f_B = \frac{\partial \epsilon(\underset{\sim}{\phi})}{\partial B} = \int_0^{t_n} [Y(t,\underset{\sim}{\phi}) - \overline{Y}(t)] \, t \, dt \qquad (B-13)$$

$$f_{C_j} = \frac{\partial \epsilon(\underset{\sim}{\phi})}{\partial C_j} = \int_0^{t_n} [Y(t,\underset{\sim}{\phi}) - \overline{Y}(t)](1 - e^{-X_j t}) \, dt$$

$$j = 1, 2, \ldots N \qquad (B-14)$$

$$f_{X_j} = \frac{\partial \epsilon(\underset{\sim}{\phi})}{\partial X_j} = \int_0^{t_n} [Y(t,\underset{\sim}{\phi}) - \overline{Y}(t)] \, C_j \, t \, e^{-X_j t} \, dt$$

$$j = 1, 2, \ldots N \qquad (B-15)$$

where the common factor 2 has been divided out of all M equations.
Performing the indicated time integration for Equations B-12 through
B-15 gives the results presented in Table B-2, where the functions P, Q,
R, and S are defined in Table B-1.

Next, expressing the components of the Jacobian matrix $\underset{\sim}{F}$ in a
similar notation, we have:

$$F_{AA} = \frac{\partial f_A}{\partial A} = \int_0^{t_n} dt \qquad (B-16)$$

129

Table B-1. Function Definitions and Values for Some Exponential Integrations

Function	Definition	Integrated Value
$P(t_b, t_a, X) =$	$\displaystyle\int_{t_a}^{t_b} e^{-Xt}\, dt =$	$\displaystyle\frac{e^{-Xt_b} - e^{-Xt_a}}{-X}$
$Q(t_b, t_a, X) =$	$\displaystyle\int_{t_a}^{t_b} t\, e^{-Xt}\, dt =$	$\displaystyle\frac{t_b\, e^{-Xt_b} - t_a\, e^{-Xt_a}}{-X} - \frac{P(t_b, t_a, X)}{-X}$
$R(t_b, t_a, X) =$	$\displaystyle\int_{t_a}^{t_b} t^2\, e^{-Xt}\, dt =$	$\displaystyle\frac{t_b^2\, e^{-Xt_b} - t_a^2\, e^{-Xt_a}}{-X} - \frac{2\, Q(t_b, t_a, X)}{-X}$
$S(t_b, t_a, X) =$	$\displaystyle\int_{t_a}^{t_b} t^3\, e^{-Xt}\, dt =$	$\displaystyle\frac{t_b^3\, e^{-Xt_b} - t_a^3\, e^{-Xt_a}}{-X} - \frac{3\, R(t_b, t_a, X)}{-X}$

Table B-2. Integrated Expressions for Error Functions $\underline{f}(\phi)$ and Special Term q_{X_j}

Error Functions	$f_A =$	$A\, t_n + B\, \dfrac{t_n^2}{2} + \displaystyle\sum_{k=1}^{N} C_k[t_n - P(t_n,0,X_k)] - \left\{ \displaystyle\sum_{i=1}^{n-1} W_i(t_{i+1} - t_i) + \dot{Y}_i\, \dfrac{(t_{i+1}^2 - t_i^2)}{2} \right\}$
	$f_B =$	$A\, \dfrac{t_n^2}{2} + B\, \dfrac{t_n^3}{3} + \displaystyle\sum_{k=1}^{N} C_k\left[\dfrac{t_n^2}{2} - Q(t_n,0,X_k) \right] - \left\{ \displaystyle\sum_{i=1}^{n-1} W_i\, \dfrac{(t_{i+1}^2 - t_i^2)}{2} + \dot{Y}_i\, \dfrac{(t_{i+1}^3 - t_i^3)}{3} \right\}$
	$f_{C_j} =$	$A[t_n - P(t_n,0,X_j)] + B\left[\dfrac{t_n^2}{2} - Q(t_n,0,X_j) \right] + \displaystyle\sum_{k=1}^{N} C_k[t_n - P(t_n,0,X_j) - P(t_n,0,X_k)$ $+ P(t_n,0,X_j+X_k)] - \left\{ \displaystyle\sum_{i=1}^{n-1} W_i[t_{i+1} - t_i - P(t_{i+1},t_i,X_j)] \right.$ $\left. + \dot{Y}_i\left[\dfrac{t_{i+1}^2 - t_i^2}{2} - Q(t_{i+1},t_i,X_j) \right] \right\}$
	$f_{X_j} =$	$A\, C_j\, Q(t_n,0,X_j) + B\, C_j\, R(t_n,0,X_j) + C_j \displaystyle\sum_{k=1}^{N} C_k[Q(t_n,0,X_j) - Q(t_n,0,X_j+X_k)]$ $- \left\{ C_j \displaystyle\sum_{i=1}^{n-1} W_i\, Q(t_{i+1},t_i,X_j) + \dot{Y}_i\, R(t_{i+1},t_i,X_j) \right\}$
Special Function	$g_{X_j} =$ *	$- A\, C_j\, R(t_n,0,X_j) + B\, C_j\, S(t_n,0,X_j) + C_j \displaystyle\sum_{k=1}^{N} C_k[R(t_n,0,X_j) - R(t_n,0,X_j+X_k)]$ $- \left\{ C_j \displaystyle\sum_{i=1}^{n-1} W_i\, R(t_{i+1},t_i,X_j) + \dot{Y}\, S(t_{i+1},t_i,X_j) \right\}$

*Special function g_{X_j} is used in $F_{X_j X_j}$ in Jacobian Matrix:

$$g_{X_j} = C_j \int_0^{t_n} [Y(t,\phi) - \overline{Y}(t)]\, t^2\, e^{-X_j t}$$

$$F_{AB} = \frac{\partial f_A}{\partial B} = \int_0^{t_n} t \, dt \qquad (B-17)$$

$$F_{AC_\ell} = \frac{\partial f_A}{\partial C_\ell} = \int_0^{t_n} (1 - e^{-X_\ell t}) \, dt \qquad (B-18)$$

$$F_{AX_\ell} = \frac{\partial f_A}{\partial X_\ell} = \int_0^{t_n} C_\ell \, t \, e^{-X_\ell t} \, dt \qquad (B-19)$$

$$F_{BB} = \frac{\partial f_B}{\partial B} = \int_0^{t_n} t^2 \, dt \qquad (B-20)$$

$$F_{BC_\ell} = \frac{\partial f_B}{\partial C_\ell} = \int_0^{t_n} t(1 - e^{-X_\ell t}) \, dt \qquad (B-21)$$

$$F_{BX_\ell} = \frac{\partial f_B}{\partial X_\ell} = \int_0^{t_n} C_\ell \, t^2 \, e^{-X_\ell t} \, dt \qquad (B-22)$$

$$F_{C_j C_\ell} = \frac{\partial f_{C_j}}{\partial C_\ell} = \int_0^{t_n} (1 - e^{-X_\ell t})(1 - e^{-X_j t}) \, dt \qquad (B-23)$$

$$F_{C_j X_\ell} = \frac{\partial f_{C_j}}{\partial X_\ell} = \int_0^{t_n} C_\ell \, t \, e^{-X_\ell t} (1 - e^{-X_j t}) \, dt$$

$$+ \int_0^{t_n} [Y(t, \phi) - \bar{Y}(t)] t \, e^{-X_j} \left\langle \frac{\partial X_j}{\partial X_\ell} \right\rangle dt \quad (B\text{-}24)$$

$$F_{X_i X_\ell} = \frac{\partial f_{X_j}}{\partial X_\varrho} = \int_0^{t_n} C_j \, C_\ell \, t^2 \, e^{-(X_j + X_\ell) t} \, dt$$

$$(B\text{-}25)$$

$$+ \int_0^{t_n} [Y(t, \phi) - \bar{Y}(t)] (-t^2 \, C_j \, e^{-X_j t}) \left\langle \frac{\partial X_i}{\partial X_\ell} \right\rangle dt$$

The integrated expressions for Equations B-16 through B-25 are given in Table B-3. Note $\underset{\sim}{F}$ is always symmetric by virtue of mixed partial derivatives, i.e., $F\phi_j \phi_\ell = \partial^2 \varepsilon / \partial \phi_\ell \, \partial \phi_j$.

To summarize, the following steps comprise the curve-fitting algorithm:

1. Make initial estimate of parameters:

$$\phi^s = \left\{ A^s, \ B^s, \ C_1^{\ s}, \ C_2^{\ s} \ \dots \ C_N^{\ s}, \ X_1^{\ s}, \ X_2^{\ s} \ \dots \ X_N^{\ s} \right\}$$

2. Compute error functions $\underset{\sim}{f}(\phi^s)$ and Jacobian matrix $\underset{\sim}{F}(\phi^s)$ (Tables B-2 and B-3).

3. Solve for estimate correction $\Delta\phi$, i.e.,

$$\underset{\sim}{F}(\phi^s) \cdot \underset{\sim}{\Delta\phi} = -\underset{\sim}{f}(\phi^s)$$

133

Table B-3. Integrated Expressions for Jacobian Matrix

Columns of Jacobian Matrix

$\phi_\ell \rightarrow$	A	B	$\cdots C_\ell \cdots$	$\cdots X_\ell \cdots$
$F_{A\phi} =$	t_n	$t_n^2/2$	$t_n - P(t_n,0,X_\ell)$	$C_\ell \, Q(t_n,0,X_\ell)$
$F_{B\phi} =$	sym	$t_n^3/3$	$t_n^2/2 - Q(t_n,0,X_\ell)$	$C_\ell \, R(t_n,0,X_\ell)$
$\cdots F_{C_j\phi} \cdots$	$\leftarrow$ sym $\rightarrow$		$t_n - P(t_n,0,X_j) - P(t_n,0,X_\ell) + P(t_n,0,X_j+X_\ell)$	$C_\ell \, Q(t_n,0,X_\ell) - C_\ell \, Q(t_n,0,X_\ell+X_j) + \left\langle f_{X_j}/C_j \right\rangle$
$\cdots F_{X_j\phi} \cdots$		$\leftarrow$ sym $\rightarrow$	$\leftarrow$ sym $\rightarrow$	$C_j C_\ell \, R(t_n,0,X_\ell+X_j) - \left\langle g_{X_j} \right\rangle$

Rows of Jacobian Matrix

$\langle\ \rangle$ Singularity bracket only has value when $j = \ell$

4. Update estimate, $\phi^{s+1} = \phi^s + \Delta\phi$; if $|\Delta\phi|$ is near zero, solution is complete. Otherwise, return to step 2 using ϕ^{s+1} to replace ϕ^s.

For the implementation of this algorithm it is prudent to provide the capability of specifying any combination of the parameters at pre-determined values. This is useful if the algorithm cannot converge on a solution when all parameters are unspecified. In particular, the con-stant term A should be specified as the initial elastic response. This is the reason the exponential terms were written as $C(1 - e^{-Xt})$, instead of simply Ce^{-Xt} as presented in the main text. Also, if all X_k are specified, then a linear solution is achieved (no iterations).

II. INVERTING CREEP AND RELAXATION FUNCTIONS

Once a creep or relaxation is determined, its inverse can be determined by the procedure outlined in this section. It is assumed the creep or relaxation functions are characterized by exponential series as follows:

$$J(t) = J_a + J_b t + \sum_{j=1}^{M} J_j e^{-\beta_j t} \qquad (B-26)$$

$$Y(t) = Y_a + \sum_{i=1}^{N} Y_i e^{-\alpha_i t} \qquad (B-27)$$

In the above, $J(t)$ represents a general creep function, and $Y(t)$ represents a general relaxation function. These forms intentionally exclude materials that do not exhibit an initial elastic response.

The objective can now be stated as: given the parameters of the creep function $(J_a, J_b, J_1, \ldots J_M, \beta_1, \ldots \beta_M)$, what are the corresponding parameters of relaxation function $(Y_a, Y_1, \ldots Y_N, \alpha_1, \ldots \alpha_N)$? Or conversely, given the relaxation parameters, what are creep parameters?

As illustrated in Figure B-1, the behavior of a material is different depending on whether the material is solid-like or fluid-like. Accordingly, the creep and relaxation functions may be subdivided into two types as follows:

1. Solid-like creep/relaxation function forms ($M = N$, $J_b = 0$):

$$J(t) = J_a + \sum_{j=1}^{N} J_j \, e^{-\beta_j t} \qquad\qquad (B-28)$$

$$Y(t) = Y_a + \sum_{i=1}^{N} Y_i \, e^{-\alpha_i t} \qquad\qquad (B-29)$$

2. Fluid-like creep/relaxation function forms ($M = N - 1$):

$$J(t) = J_a + J_b \, t + \sum_{j=1}^{N-1} J_j \, e^{-\beta_j t} \qquad\qquad (B-30)$$

$$Y(t) = \sum_{i=1}^{N} Y_i \, e^{-\alpha_i t} \qquad\qquad (B-31)$$

where the following restrictions on the parameters are implied:

$$J_a, \; J_b, \; Y_a, \; Y_i, \; \alpha_i, \; \beta_j \; > \; 0$$

$$J_i \; < \; 0$$

$$J_a \; + \; \sum_{j=1}^{M} J_i \; > \; 0$$

Note the solid-like creep and relaxation functions have identical forms: each contain a constant term and decaying exponential series. However, the fluid-like creep function contains the linear term $J_b t$ which permits continued creep (or flow) for all time. The corresponding fluid-like relaxation function contains no constant term or linear term, but rather an additional exponential term. This permits the stress to relax to zero under a fixed strain.

To determine the respective inverse functions for either the fluid-like or solid-like forms, the fundamental convolution identity between creep and relaxation functions is exploited:

$$\int_0^t J^\star \; dY \; = \; 1$$

or, in expanded form:

$$J(t) \, Y(0) \; + \; \int_0^t J(t - \tau) \, \frac{\partial Y}{\partial \tau} \, d\tau \; = \; 1 \qquad\qquad (B\text{-}32)$$

For the solid-like case each function contains 2N+1 parameters. Upon inserting Equations B-28 and B-29 into the above identity and integrating, the results may be grouped into time functions of $e^{-\alpha_i t}$, $e^{-\beta_i t}$, and a constant. The groups of terms associated with each exponential time function must be zero, and the constant terms must equal 1 in order to satisfy Equation B-32 for all time. This gives 2N+1 relationships between the constants as follows:

$$J_a \, Y_a \; = \; 1 \qquad\qquad (B\text{-}33)$$

$$J_a \prod_{k=1}^{N} (\beta_k - \alpha_i) \; - \; \alpha_i \sum_{j=1}^{N} J_j \prod_{\substack{k=1 \\ k \neq j}}^{N} (\beta_k - \alpha_i) \; = \; 0$$

$$i = 1, 2, \ldots N \qquad (B\text{-}34)$$

$$\left(Y_a + \sum_{i=1}^{N} Y_i \right) \prod_{k=1}^{N} (\beta_j - \alpha_k) \; + \; \sum_{i=1}^{N} \alpha_i \, Y_i \prod_{\substack{k=1 \\ k \neq i}}^{N} (\beta_j - \alpha_k) \; = \; 0$$

$$j = 1, 2, \ldots N \qquad (B\text{-}35)$$

If the creep function parameters are known, the relaxation parameters α_1, α_2, ... α_N are determined by solving for the roots of the N-degree polynomial of α in Equation B-34. Next, the relaxation coefficients Y_1,

$Y_2, \ldots Y_N$ are determined by the linear solution of Equation B-35, with $Y_a = 1/J_a$. On the other hand, if relaxation parameters are known, the creep parameters $\beta_1, \beta_2, \ldots \beta_N$ are determined from the roots of Equation B-35 first, then the creep coefficients are determined from Equation B-34, with $J_a = 1/Y_a$. Table B-4 provides solutions for N = 1 and 2.

In a similar manner, parameter relationships for fluid-like materials can be developed by inserting Equations B-30 and B-31 into the convolution identity. For convenience, the following expression is used.

$$\int_0^t Y^* \, dJ = 1$$

For this case, there are 2N parameters per function along with 2N relationships between the creep and relaxation functions given as:

$$J_b \sum_{i=1}^{N} Y_i / \alpha_i = 1 \qquad (B-36)$$

$$\alpha_i \prod_{k=1}^{N-1} (\alpha_i - \beta_k) \left(J_a + \sum_{j=1}^{N-1} J_j \right) - J_b \prod_{k=1}^{N-1} (\alpha_i - \beta_k)$$

$$+ \alpha_i \sum_{j=1}^{N-1} \beta_j J_j \prod_{\substack{k=1 \\ k \neq j}}^{N-1} (\alpha_i - \beta_k) = 0$$

$$i = 1, 2, \ldots N \qquad (B-37)$$

Table B-4. Creep to Relaxation Function Inversions for Solid-Like Materials

Given Creep Function: $\quad J(t) = J_a + \sum_{j=1}^{N} J_j e^{-\beta_j t}$

$\qquad\qquad\qquad\qquad\qquad N$ = number of exponential terms

Relaxation Function is: $\quad Y(t) = Y_a + \sum_{i=1}^{N} Y_i e^{-\alpha_i t}$

N	Y_a	α_1	Y_1	α_2	Y_2
1	$\dfrac{1}{J_a}$	$\beta_1\left(\dfrac{J_a}{J_a + J_1}\right)$	$\dfrac{1}{J_a}\left(\dfrac{\alpha_1}{\beta_1} - 1\right)$	0	0
2	$\dfrac{1}{J_a}$	$\dfrac{1}{2}(\beta_1 r_1 + \beta_2 r_2 + R)$	$\dfrac{1}{J_a D}\left(\dfrac{\beta_1}{\beta_1 - \alpha_2} - \dfrac{\beta_2}{\beta_2 - \alpha_2}\right)$	$\dfrac{1}{2}(\beta_1 r_1 + \beta_2 r_2 - R)$	$\dfrac{1}{J_a D}\left(\dfrac{\beta_2}{\beta_2 - \alpha_1} - \dfrac{\beta_1}{\beta_1 - \alpha_2}\right)$

where: $\quad r_1 = (J_a + J_2)/(J_a + J_1 + J_2)$

$\qquad\qquad r_2 = (J_a + J_1)/(J_a + J_1 + J_2)$

$\qquad\qquad R_a = J_a/(J_a + J_1 + J_2)$

$$R = \sqrt{(\beta_1 r_1)^2 + 2\beta_1\beta_2(r_1 r_2 - r_a) + (\beta_2 r_2)^2}$$

$$D = \beta_1\beta_2\left[\frac{1}{(\beta_1 - \alpha_1)(\beta_2 - \alpha_2)} - \frac{1}{(\beta_1 - \alpha_2)(\beta_2 - \alpha_1)}\right]$$

$$\sum_{\substack{i=1}}^{N} Y_i \prod_{\substack{k=1 \\ k \neq i}}^{N} (\alpha_i - \beta_j) = 0 \qquad j = 1, 2, \ldots N-1 \qquad (B-38)$$

If creep parameters are known, the relaxation parameters α_1, α_2, $\cdots$ α_N are determined from solving the roots of the polynomial given by Equation B-37. Thereafter, Y_1, Y_2, $\cdots$ Y_N are determined by the linear solution of the N-1 equations of Equation set B-38 together with Equation B-36. On the other hand, if relaxation parameters are given, the N-1 roots of Equation B-38 give β_1, β_2, $\cdots$ β_{N-1}, and the creep coefficients J_a, J_b, J_1, J_2, $\cdots$ J_{N-1} are determined by the N equations in Equation set B-37 together with Equation B-36. Table B-5 shows solutions for N = 1 and 2.

III. RELAXATION FUNCTION INTERRELATIONSHIPS

Thus far, relaxation and creep functions have been denoted in a general manner by the functions Y(t) and J(t), respectively. However, in practice, Y(t) represents a particular kind of relaxation function, such as shear modulus, bulk modulus, Young's modulus, or confined modulus, etc. Similarly, J(t) represents the corresponding inverse function.

If experimental data are available for one particular type of function, it may be necessary to convert the data to another type of function. For example, suppose a Young's modulus relaxation function E(t) has been determined from a test coupon along with an observed time function for Poisson's ratio $\nu(t)$. If it is desired to determine the equivalent bulk and shear relaxation functions, then the material data must be transformed.

Table B-5. Creep to Relaxation Function Inversions for Fluid-Like Materials

Given Creep Function: $J(t) = J_a + J_b t + \sum_{j=1}^{N-1} J_j e^{-\beta_j t}$

Relaxation Function is: $Y(t) = \sum_{i=1}^{N} Y_i e^{-\alpha_i t}$

N	α_1	Y_1	α_2	Y_2
1	$\dfrac{J_b}{J_a}$	$\dfrac{1}{J_a}$	0	0
2	$\dfrac{1}{2}(\beta_1 r_a + r_b + R)$	$\dfrac{1}{J_a + J_1}\left(\dfrac{\alpha_1 - \beta}{\alpha_1 - \alpha_2}\right)$	$\dfrac{1}{2}(\beta_1 r_a + r_b - R)$	$\dfrac{1}{J_a + J_1}\left(\dfrac{\beta - \alpha_2}{\alpha_1 - \alpha_2}\right)$

where: $r_a = J_a/(J_a + J_1)$

$r_b = J_b/(J_a + J_1)$

$R = \sqrt{(\beta_1 r_a)^2 + 2\,\beta_1 r_b (r_a - 2) + r_b^2}$

142

To transform from one function type to another, the same relation-
ships that apply in elasticity between scalar moduli also apply in
viscoelasticity between functional moduli. To prove this assertion,
recall the general viscoelastic constitutive relationship for isotropic
materials has the form:

$$
\begin{Bmatrix} \sigma_{xx} \\ \sigma_{yy} \\ \sigma_{zz} \\ \tau_{xy} \\ \tau_{yz} \\ \tau_{xz} \end{Bmatrix} =
\begin{bmatrix}
D_a & D_b & D_b & 0 & 0 & 0 \\
 & D_a & D_b & 0 & 0 & 0 \\
 & & D_a & 0 & 0 & 0 \\
 & & & D_c & 0 & 0 \\
 & \text{Sym} & & & D_c & 0 \\
 & & & & & D_c
\end{bmatrix} * d
\begin{Bmatrix} \varepsilon_{xx} \\ \varepsilon_{yy} \\ \varepsilon_{zz} \\ \varepsilon_{xy} \\ \varepsilon_{yz} \\ \varepsilon_{xz} \end{Bmatrix}
\qquad \text{(B-39)}
$$

where D_a, D_b, and D_c are functions of time, and the symbol * is the
convolution operator. It is evident that Equation B-39 has the same
form as an elastic constitutive matrix, and, like an elastic matrix, the
terms D_a, D_b, and D_c are composed of, at most, two independent material
properties, which in this case are functions of time. Possible time
function pairs are: Young's modulus and Poisson's ratio, bulk modulus
and shear modulus, and confined modulus and lateral stress coefficient.
Clearly, it makes no difference what pair or combination of material
time functions is used as long as they combine to produce the same time
functions for $D_a(t)$, $D_b(t)$, and $D_c(t)$. Therefore, the various visco-
elastic moduli (functions) have the same interrelationships as the
corresponding elastic moduli.

Table B-6 provides some useful interrelationships to aid in trans-
forming from one type of function to another.

143

Table B-6. Interrelationships Among Elastic and
Viscoelastic Material Functions

Material Function*	Young's Modulus and Poisson's Ratio, E, ν	Bulk Modulus and Shear Modulus, K, G	Confined Modulus and Lateral Coefficient, M_s, X_o
Young's Modulus, $E =$	E	$\dfrac{9\,G\,K}{3K + G}$	$M_s \dfrac{(1 + 2K_o)(1 - K_o)}{1 + K_o}$
Poisson's Ratio, $\nu =$	ν	$\dfrac{3K - 2G}{2(3K + G)}$	$\dfrac{K_o}{1 + K_o}$
Bulk Modulus, $K =$	$\dfrac{E}{3(1 - 2\nu)}$	K	$\dfrac{M_s}{3}(1 + 2K_o)$
Shear Modulus, $G =$	$\dfrac{E}{2(1 + \nu)}$	G	$\dfrac{M_s}{2}(1 - K_o)$
Confined Modulus, $M_s =$	$\dfrac{E(1 - \nu)}{(1 + \nu)(1 - 2\nu)}$	$K + \dfrac{4}{3}G$	M_s
Lateral Coefficient, $K_o =$	$\dfrac{\nu}{1 - \nu}$	$\dfrac{3K - 2G}{3K + 4G}$	K_o

*All parameters may be functions of time.

144

To illustrate the procedure for transforming viscoelastic functions, consider the example of determining bulk and shear relaxation functions given test data from a simple creep test. That is, a test coupon of the material is axially loaded with a constant stress, and axial and radial strain are recorded. Then the following steps are required:

1. Normalize experimental data. Divide axial strain by applied stress to get creep data (this corresponds to inverse of Young's modulus relaxation function). Also, divide radial strain data by axial strain data to get Poisson's ratio function, $\bar{\nu}(t)$.

2. Determine creep function. Using the creep data, employ the methods of Part I of this Appendix to determine the best-fitting creep function.

3. Determine Young's modulus relaxation function. Invert the above creep function to get the corresponding Young's modulus relaxation function, $E(t)$. Use the techniques in Part II of this Appendix for inverting.

4. Transform to bulk modulus relaxation function. From Table B-6, the bulk modulus is given as $K(t) = 1/3\, E(t)/[1 - \bar{\nu}(t)]$. If the experimental data show $\bar{\nu}(t)$ is constant (or near constant), then $K(t)$ has the same form as $E(t)$ and only differs by the scalar divisor, $3(1 - \bar{\nu})$. If, on the other hand, $\bar{\nu}(t)$ is not constant, $K(t)$ can be determined by the best-fit procedure in Part I of this Appendix where the data points are $\bar{K}(t_i) = 1/3\, E(t)_i/[1 - \bar{\nu}(t_i)]$.

5. Transform to shear modulus relaxation function. Again using Table B-6, the shear modulus is given as $G(t) = 1/2\, E(t)/[1 + \bar{\nu}(t)]$. As discussed in step 4, if $\bar{\nu}(t)$ is constant, $G(t)$ is known directly from $E(t)$. Otherwise, $\bar{G}(t)$ must be determined by the best-fit procedure using the data points: $\bar{G}(t_i) = 1/2\, E(t_i)/[1 + \bar{\nu}(t_i)]$.

The above steps illustrate one set of transformations for a particular type of experimental data. Other types of transformations with other types of experimental data can be treated in a similar manner.

Appendix C

A PERSPECTIVE OF VISCOPLASTIC MODELS

Throughout this Appendix, the term "viscoplastic" is used as a general term to embrace all constitutive models that contain elements of elasticity, viscosity, and plasticity. In the main text the discussion focused on a particular viscoplastic model called "viscoelastic-plastic."

The objective of this Appendix is to present a broad view of viscoplastic models and demonstrate the characteristics of different models. Concepts and imagery are emphasized as opposed to detailed equations and solution algorithms.

To begin with, we recognize that viscoplasticity is a phenomological approach for characterizing the behavior of materials. That is, mathematical models are sought which can replicate the observed performance of materials. Yet, the mathematical models must conform to certain thermodynamic restrictions.

Three mathematical models or constitutive theories that satisfy thermodynamic restrictions and are well accepted are: elasticity, viscoelasticity, and plasticity. These separate theories can (1) be directly combined to provide viscoplastic models (combo-viscoplasticity) or (2) the separate theories can be altered or extended to provide viscoplastic models (neo-viscoplasticity). This is an important distinction and is the first major division in the hierarchy of viscoplastic models as shown in Figure C-1. In the right branch of this figure, P, V, and E represent classical models for characterizing plastic, viscous, and elastic response. Various combinations and arrangements of these basic components define a particular combo-viscoplastic model,

Viscoplastic
Models

Neo-viscoplasticity

models introduce
extended theories
(VI'·ʸ)

Combo-viscoplasticity

models composed of
classical theories
(E) , (V) , (P)
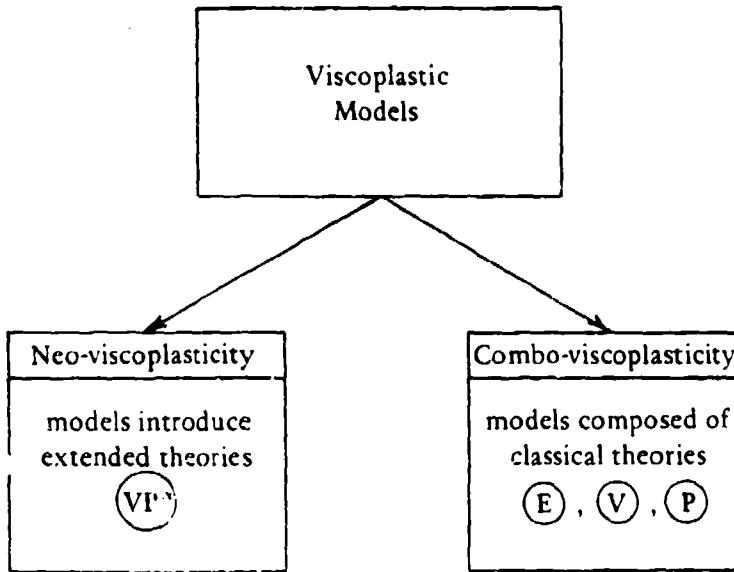
Figure C-1. Two classes of viscoplastic models.

Symbol	Visual Model (one-dimensional)	General Description
(E)	σ_e ϵ_e	• Elastic response • Linear with σ_e • Time independent
(V)	(optional) σ_v (always present) ϵ_v	• Viscous response • Linear with σ_v • Time dependent (no initial response)
(P)	σ_p friction block ϵ_p	• Plastic response • Nonlinear with σ_p, depending on hardening function. • Time independent

Figure C-2. Components of combo-viscoplastic model.

148

such as the viscoelastic-plastic model presented in the main text. Other combo-viscoplastic models will be illustrated in subsequent paragraphs.

The properties of the classical models, (P), (V), and (E), are illustrated in Figure C-2. The identification of each component may be as simple or complicated as needed. For example, (E) may be isotropic (two parameters) or anistropic (three to twenty-one parameters). Also, the component (V) may be isotropic or anistropic, and each relaxation function may have as many parameters as required. Lastly, (P) may represent any classical plasticity model, ranging from a simple non-hardening Von Mises yield criterion (one parameter) to complicated "capped" yield functions with universal hardening (e.g., twenty-seven parameters).

The important distinction for combo-viscoplasticity is that each component, (E), (V), and (P), remains within its classical limitations. That is, the viscous component, (V), deforms with time under constant load and responds in proportion to the load magnitude acting on (V). The plastic component, (P), deforms as a function of the current load magnitude acting on (P). There is no explicit reference to time in the (P) model except implicity through the load.

Contrast the above to neo-viscoplasticity (left branch of Figure C-1), where the component (VP) may represent a modified plasticity formulation with a flow rule explicitly dependent on time (see for example, Green and Naghdi [25], Zienkiewicz and Cormeau [5], and Perzyna [4]. Alternatively, (VP) may represent a modified viscoelastic formulation, which accounts for plastic-type responses by the assumption of intrinsic time. Effectively, this means real time in portions of the viscoelastic model is replaced with intrinsic time, which is actually a measure of strain. This method is called the "endochronic theory" (see Bazant [26].

The relative merits of the various neo-viscoplastic models will not be argued here. However, it's the author's contention that combo-viscoplastic models are preferable to the neo-viscoplastic models for

the following reasons: (1) combo models provide a rational approach for synthesizing a constitutive model, (2) combo models are formed from well-accepted constitutive theories that satisfy thermodynamic restrictions, (3) parameter identification for combo models is relatively easy, (4) pre-existing elastic, plastic, and viscoelastic material information can be used directly, and (5) virtually any type of observed material behavior can be replicated by some combo-viscoplastic model.

There is no limit to the number of component elements that can be used to synthesize a combo-viscoplastic model. However, five-element models are probably a practical upper limit. As an example, consider the five-element model shown at the top of Figure C-3, along with the example four- and three-element models. Here, the models are restricted to those containing at least $\textcircled{P}$, $\textcircled{V}$, and $\textcircled{E}$ and have an initial elastic response. (Note: the models shown are all named using hyphen (-) to denote a series connection between two elements and a slash (/) to denote a parallel coupling. However, for expressing $\textcircled{V}$-$\textcircled{E}$ the hyphen is omitted, i.e., viscoelastic = visco-elastic, and for $\textcircled{P}$-$\textcircled{E}$ we write elastoplastic = elastic-plastic.)

To appreciate the different behavior of these models, compare the nature of the viscoelastic-plastic model (c) with the elastic-visco/ plastic model (d) as they respond (deform) for a suddenly applied stress. If the stress is less than the elastic limit ($\sigma < \sigma_L$), model (c) behaves viscoelastically and model (d) elastically, as shown in Figure C-4. If the applied stress is greater than the elastic limit ($\sigma > \sigma_L$) and the hardening function $\neq 0$, then model (c) responds with an instantaneous elastic plus plastic strain followed by a viscoelastic creep. On the other hand, model (d) responds with an instantaneous elastic response (regardless of stress level) and progresses with plastic strain at rate dependent on $\textcircled{V}$.

As another example, consider the four-element model (b). This model is capable of representing primary, secondary, and tertiary creep ranges, as shown in Figure C-5. Materials, such as soils, plastics, and sea-ice, exhibit this type of behavior.
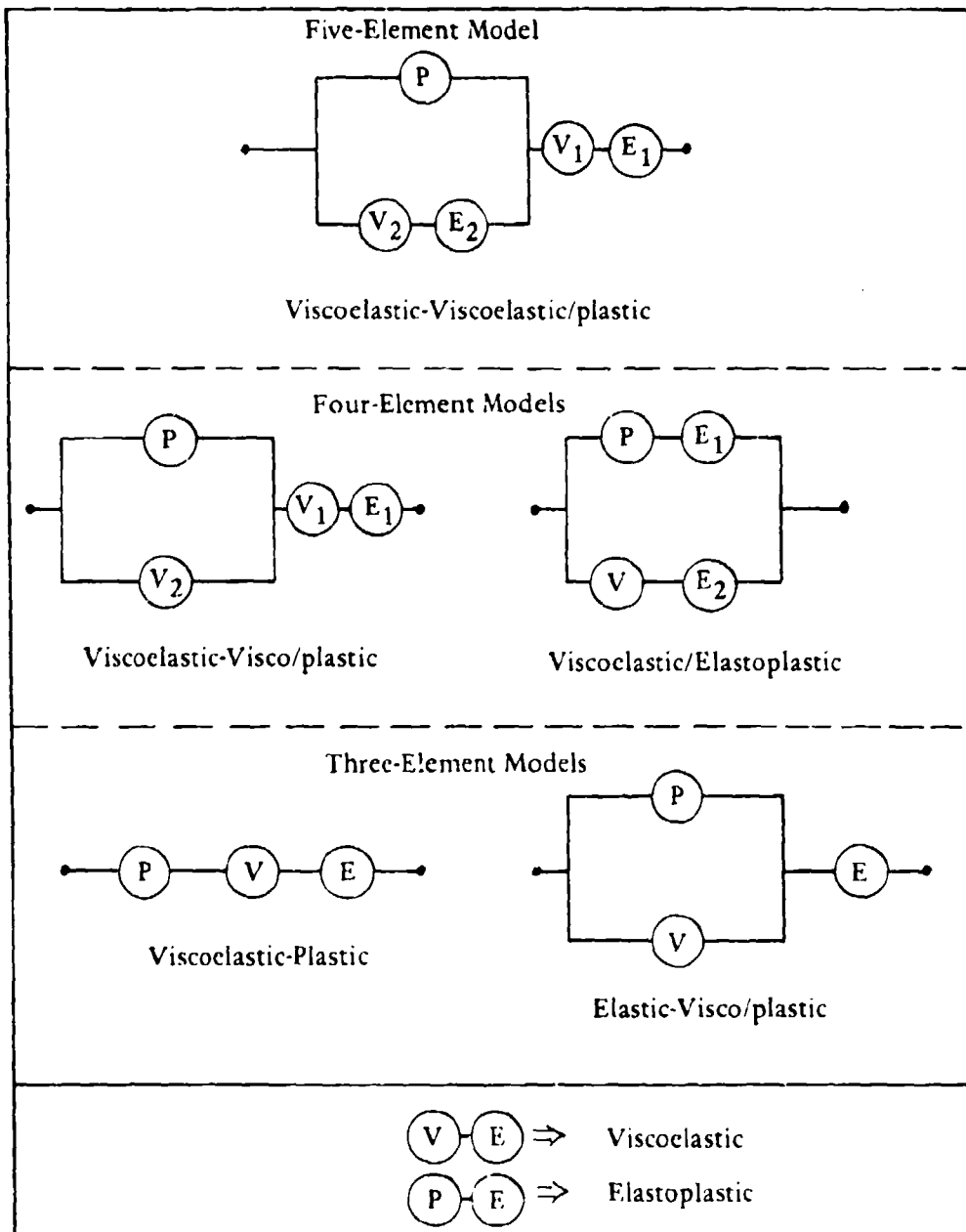
Figure C-3. A five-element combo-viscoplastic element and its family.
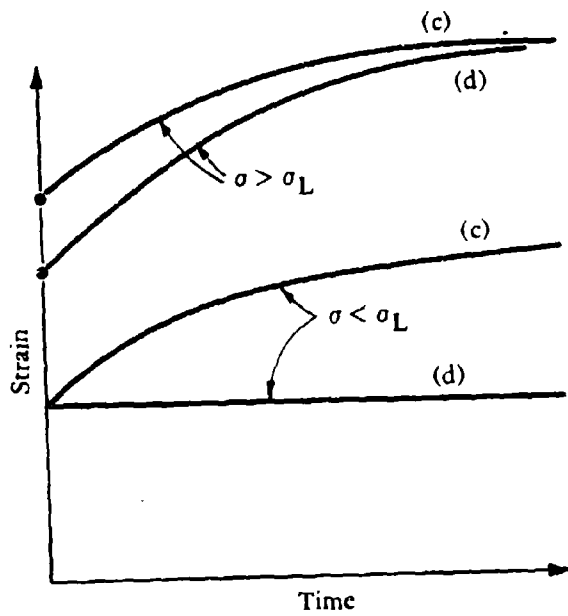
Figure C-4. Typical behavior of models (c) and (d).
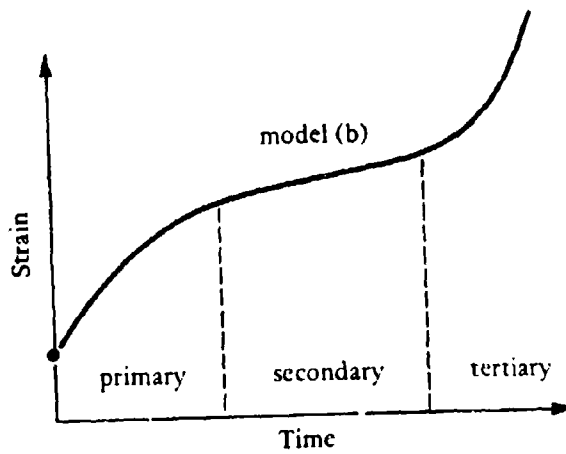
Figure C-5. Typical behavior of model (b).

SYNTHESIZING COMBO-VISCOPLASTIC MODELS

To synthesize a viscoplastic model (i.e., stress-strain relation-
ship) from a particular configuration of $\textcircled{E}$, $\textcircled{V}$, and $\textcircled{P}$ requires
following a few simple rules. To wit, elements in series have the same
stress and deform separately, whereas elements in parallel have the same
strain and split the net stress between them. In the main text, these
rules were used to synthesize the series model, viscoelastic-plastic.
Here the synthesis procedure is demonstrated for the parallel assembly,
viscoelastic/elastoplastic, shown in Figure C-6.

Using the notation in the figure, we have:

$$\underset{\sim}{\sigma} = \underset{\sim}{\sigma}_{ep} + \underset{\sim}{\sigma}_{ve} \qquad\qquad (C-1)$$

$$\underset{\sim}{\varepsilon} = \underset{\sim}{\varepsilon}_{ep} + \underset{\sim}{\varepsilon}_{ve} \qquad\qquad (C-2)$$

where $\underset{\sim}{\sigma}_{ep}$ and $\underset{\sim}{\varepsilon}_{ep}$ are the stress and strain vectors in the elastoplastic
subassembly, and $\underset{\sim}{\sigma}_{ve}$ and $\underset{\sim}{\varepsilon}_{ve}$ are the stress and strain vectors in the
viscoelastic subassembly. Both series' subassemblies were developed
fully in the main text. Thus, from Equation 2-33, the elastoplastic
stress-strain relationship is:

$$\Delta\underset{\sim}{\sigma}_{ep} = (\underset{\sim}{D}_2 - \underset{\sim}{D}_p)\Delta\underset{\sim}{\varepsilon}_{ep} \qquad\qquad (C-3)$$

where $\underset{\sim}{D}_2$ is the elastic matrix representing $\textcircled{E_2}$, and $\underset{\sim}{D}_p$ is the plas-
ticity matrix, which is a function of $\underset{\sim}{\sigma}_{ep}$ (i.e., not total stress σ).
Similarly, from Equation 3-22, the viscoelastic stress-strain relation-
ship is:

$$\Delta\sigma_{\sim ve} = (D_{\sim 1} + D_{\sim v})\Delta\varepsilon_{\sim ve} + \bar{\sigma}_{\sim v} \qquad \text{(C-4)}$$

where $D_{\sim 1}$ is the elastic matrix representing $\boxed{E_1}$, $D_{\sim v}$ is the viscoelastic matrix dependent on time step, and $\bar{\sigma}_{\sim v}$ is the stress history matrix.

Adding Equations C-3 and C-4 and using the relationship in Equations C-1 and C-2, the final stress-strain relationship is:

$$\Delta\sigma_{\sim} = (D_{\sim e} + D_{\sim v} - <D_{\sim p}>)\Delta\varepsilon_{\sim} - \bar{\sigma}_{\sim v} \qquad \text{(C-5)}$$

In the above, $D_{\sim e} = D_{\sim 1} + D_{\sim 2}$ is the total elastic matrix. If $D_{\sim 1} = 0_{\sim}$, the model degenerates to an elastoplastic model, or if $D_{\sim 2} = 0_{\sim}$, the model is viscoelastic. Any other linear combination of $D_{\sim 1}$ and $D_{\sim 2}$ provides a viscoplastic model.

Other combo-viscoelastic models can be developed by following the procedures outlined above.
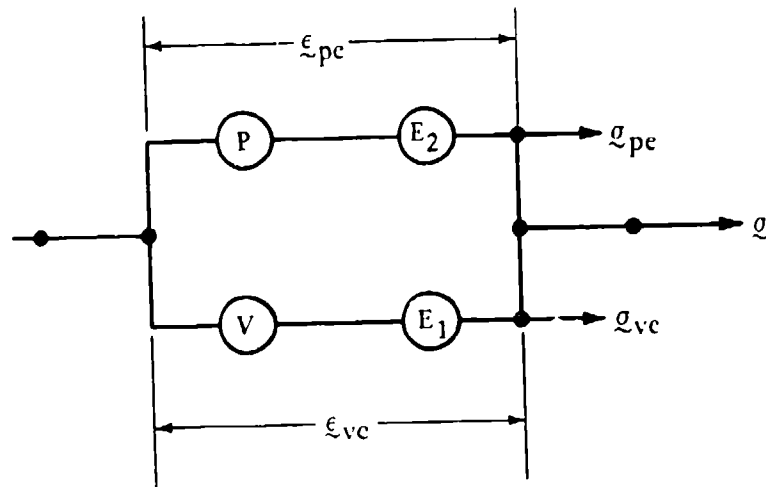
Figure C-6. Viscoelastic/elastoplastic model.

DISTRIBUTION LIST

AF HQ Prees Washington DC (R P Reid)
AFB AFCEC/XR,Tyndall FL; CESCH, Wright-Patterson; MAC/DET (Col. P. Thompson) Scott, IL; SAMSO/MNNF,
    Norton AFB CA; Stinfo Library, Offutt NE
ARCTICSUBLAB Code 54T, San Diego, CA
ARMY BMDSC-RE (H. McClellan) Huntsville AL; DAEN-MCE-D (R L Wight) Washington DC; DAEN-MCE-D
    Washington DC; ERADCOM Tech Supp Dir. (DELSD-L) Ft. Monmouth, NJ; Tech. Ref. Div., Fort Huachuca, AZ
ARMY - CERL Library, Champaign IL
ARMY COASTAL ENGR RSCH CEN Fort Belvoir VA; R. Jachowski, Fort Belvoir VA
ARMY CORPS OF ENGINEERS MRD-Eng. Div., Omaha NE; Seattle Dist. Library, Seattle WA
ARMY ENG DIV ED-CS (S.Bolin) Huntsville, AL; HNDED-CS, Huntsville AL; Hnded-Sr, Huntsville, AL
ARMY ENG WATERWAYS EXP STA Library, Vicksburg MS
ARMY ENGR DIST. Library, Portland OR
ARMY ENVIRON. HYGIENE AGCY B620, Edgewood Arsenal MD; Water Qual Div (Doner), Aberdeen Prov
    Ground, MD
ARMY MATERIALS & MECHANICS RESEARCH CENTER Dr. Lenoe, Watertown MA
ARMY MISSILE R&D CMD Redstone Arsenal AL Sci. Info. Cen (Documents)
ARMY MOBIL EQUIP R&D COM Mr. Cevasco, Fort Belvoir MD
ARMY-PLASTEC Picatinny Arsenal (A M Anzalone, SMUPA-FR-M-D) Dover NJ
ASST SECRETARY OF THE NAVY Spec. Assist Energy (P. Waterman), Washington DC
BUREAU OF RECLAMATION Code 1512 (C. Selander) Denver CO
CINCLANT Civil Engr. Supp. Plans. Ofr Norfolk, VA
CINCPAC Fac Engrng Div (J44) Makalapa, HI
CNM NMAT 08T246 (Dieterle) Wash. DC
CNO Code NOP-964, Washington DC; OP987J (J. Boosman), Pentagon
COMOCEANSYSPAC SCE, Pearl Harbor HI
DEFENSE CIVIL PREPAREDNESS AGENCY J.O. Buchanan, Washington DC
DEFENSE DOCUMENTATION CTR Alexandria, VA
DEFENSE INTELLIGENCE AGENCY Dir., Washington DC
DNA STTL, Washington DC
DOD Explosives Safety Board (Library), Washington DC
DOE Dr. Cohen
DTNSRDC Code 1706, Bethesda MD; Code 172 (M. Krenzke), Bethesda MD
DTNSRDC Code 4121 (R. Rivers), Annapolis, MD
FLTCOMBATTRACENLANT PWO, Virginia Bch VA
HEDSUPPACT PWO, Taipei, Taiwan
MARINE CORPS BASE Camp Pendleton CA 92055; Code 43-260, Camp Lejeune NC; M & R Division, Camp Lejeune
    NC; PWO, Camp S. D. Butler, Kawasaki Japan
MARINE CORPS DIST 9, Code 043, Overland Park KS
MARINE CORPS HQS Code LFF-2, Washington DC
MCAS Facil. Engr. Div. Cherry Point NC; Code PWE, Kaneohe Bay HI; Code S4, Quantico VA; J. Taylor, Iwakuni
    Japan; PWD, Dir. Maint. Control Div., Iwakuni Japan; PWO Kaneohe Bay HI
MCDEC P&S Div Quantico VA
MCLSBPAC B520, Barstow CA
MCRD PWO, San Diego Ca
NAD Engr. Dir. Hawthorne, NV
NAF PWO Sigonella Sicily; PWO, Atsugi Japan
NAS CO, Guantanamo Bay Cuba; Code 114, Alameda CA; Code 183 (Fac. Plan BR MGR); Code 187, Jacksonville FL;
    Code 18700, Brunswick ME; Code 6234 (G. Trask), Point Mugu CA; Code 70, Atlanta, Marietta GA; Dir Util Div.,
    Bermuda; ENS Buchholz, Pensacola, FL; Lead. Chief. Petty Ofir PW Self Help Div, Beeville TX; PW of
    Maguire), Corpus Christi TX; PWD Maint. Div., New Orleans, Belle Chasse LA; PWD, Willow Grove PA; PWO
    (M. Elliot), Los Alamitos CA; PWO Belle Chasse, LA, PWO Chase Field Beeville, TX, PWO Key West FL; PWO
    Whiting Fld, Milton FL; PWO, Dallas TX; PWO, Glenview IL, PWO, Kingsville TX, PWO, Miramar, San Diego
    CA; SCE Lant Fleet Norfolk, VA; SCE Norfolk, VA, SCE, Barbers Point HI
NATL RESEARCH COUNCIL Naval Studies Board, Washington DC
NATPARACHUTETESTRAN PW Engr, El Centro CA
NAVACT PWO, London UK
NAVAEROSPREGMEDCEN SCE, Pensacola FL
NAVAL FACILITY PWO, Barbados, PWO, Brawdy Wales UK; PWO, Cape Hatteras, Buxton NC

NAVCOASTSYSLAB CO, Panama City FL; Code 423 (D. Good), Panama City FL; Code 715 (J. Quirk) Panama City, FL; Library Panama City, FL

NAVCOMMAREAMSTRSTA PWO, Norfolk VA; PWO, Wahiawa HI; SCE Unit I Naples Italy

NAVCOMMSTA Code 401 Nea Makri, Greece; PWO, Adak AK; PWO, Exmouth, Australia

NAVCONSTRACEN CO (CDR C.L. Neugent), Port Hueneme, CA

NAVEDTRAPRODEVCEN Tech. Library

NAVEDUTRACEN Engr Dept (Code 42) Newport, RI

NAVEODFAC Code 605, Indian Head MD

NAVFACENGCOM Code 043 Alexandria, VA; Code 044 Alexandria, VA; Code 0451 Alexandria, VA; Code 0453 (D. Potter) Alexandria, VA; Code 0454B Alexandria, Va; Code 04B5 Alexandria, VA; Code 101 Alexandria, VA; Code 10133 (J. Leimanis) Alexandria, VA; Code 1023 (T. Stevens) Alexandria, VA; Code 104 Alexandria, VA; Code 2014 (Mr. Taam), Pearl Harbor HI; Morrison Yap, Caroline Is.; P W Brewer Alexandria, VA; PC-22 (E. Spencer) Alexandria, VA; PL-2 Ponce P.R. Alexandria, VA

NAVFACENGCOM - CHES DIV. Code 101 Wash, DC; Code 402 (R. Morony) Wash, DC; Code 405 Wash, DC; Code FPO-1 (C Bodey) Wash, DC; Code FPO-1 (Ottsen) Wash, DC; Code FPO-1SP (Dr. Lewis) Wash, DC; Code FPO-1SP13 (T F Sullivan) Wash, DC; Code FPO-IP12 (Mr. Scola), Washington DC; Scheessele, Code 402, Wash, DC

NAVFACENGCOM - LANT DIV.; Eur. BR Deputy Dir, Naples Italy; RDT&ELO 09P2, Norfolk VA

NAVFACENGCOM - NORTH DIV. (Boretsky) Philadelphia, PA; Code 09P (LCDR A.J. Stewart); Code 1028, RDT&ELO, Philadelphia PA; Design Div. (R. Masino), Philadelphia PA; ROICC, Contracts, Crane IN

NAVFACENGCOM - PAC DIV. Code 402, RDT&E, Pearl Harbor HI; Commander, Pearl Harbor, HI

NAVFACENGCOM - SOUTH DIV. Code 90, RDT&ELO, Charleston SC; Dir., New Orleans LA

NAVFACENGCOM - WEST DIV. Code 04B; 09P/20; RDT&ELO Code 2011 San Bruno, CA

NAVFACENGCOM CONTRACT AROICC, Point Mugu CA; AROICC, Quantico, VA; Eng Div dir, Southwest Pac, Manila, PI; OICC, Southwest Pac, Manila, PI; OICC/ROICC, Balboa Canal Zone; ROICC (Ervin) Puget Sound Naval Shipyard, Bremerton, WA; ROICC AF Guam; ROICC LANT DIV., Norfolk VA; ROICC Off Point Mugu, CA; ROICC, Diego Garcia Island; ROICC, Keflavik, Iceland; ROICC, Pacific, San Bruno CA

NAVHOSP LT R. Elsbernd, Puerto Rico

NAVMAG SCE, Guam

NAVMIRO OIC, Philadelphia PA

NAVOCEANSYSCEN Code 409 (D. G. Moore), San Diego CA; Code 5311(T) (E. Hamilton) San Diego CA; Code 6565 (Tech. Lib.), San Diego CA; Research Lib., San Diego CA

NAVORDSTA PWO, Louisville KY

NAVPETOFF Code 30, Alexandria VA

NAVPGSCOL Code 61WL (O. Wilson) Monterey CA

NAVPHIBASE CO, ACB 2 Norfolk, VA; Code S3T, Norfolk VA; Harbor Clearance Unit Two, Little Creek, VA; OIC, UCT ONE Norfolk, Va

NAVREGMEDCEN Code 3041, Memphis, Millington TN; SCE (D. Kaye); SCE (LCDR B. E. Thurston), San Diego CA; SCE, Camp Pendleton CA

NAVSCOLCECOFF C35 Port Hueneme, CA; C44A (R. Chittenden), Port Hueneme CA; CO, Code C44A Port Hueneme, CA

NAVSEASYSCOM Code OOC (LT R. MacDougal), Washington DC

NAVSEC Code 6034 (Library), Washington DC

NAVSECGRUACT PWO, Torri Sta, Okinawa

NAVSHIPREPFAC Library, Guam; SCE Subic Bay

NAVSHIPYD; Code 202.4, Long Beach CA; Code 202.5 (Library) Puget Sound, Bremerton WA; Code 400, Puget Sound; Code 404 (LT J. Riccio), Norfolk, Portsmouth VA; Code 410, Mare Is., Vallejo CA; Code 440 Portsmouth NH; Code 440, Norfolk; Code 440, Puget Sound, Bremerton WA; Code 440.4, Charleston SC; L.D. Vivian; Library, Portsmouth NH; PWO, Mare Is.; Tech Library, Vallejo, CA

NAVSTA CO Naval Station, Mayport FL; CO Roosevelt Roads P.R. Puerto Rico; Engr. Dir., Rota Spain; Maint. Div. Dir-Code 531, Rodman Canal Zone; PWD (LTJG.P.M. Motolenich), Puerto Rico; PWO Midway Island; PWO, Keflavik Iceland; PWO, Mayport FL; ROICC, Rota Spain; SCE, Guam; SCE, Subic Bay, R.P.; Utilities Engr Off. (LTJG A.S. Ritchie), Rota Spain

NAVSUBASE LTJG D.W. Peck, Groton, CT

NAVSUPPACT CO, Seattle WA, Code 413, Seattle WA; Engr. Div. (F. Mollica), Naples Italy; LTJG McGarrah, Vallejo CA

NAVSURFWPNCEN PWO, White Oak, Silver Spring, MD

NAVTECHTRACEN SCE, Pensacola FL

NAVWPNCEN Code 2636 (W. Bonner), China Lake CA; PWO (Code 26), China Lake CA; ROICC (Code 702), China Lake CA

NAVWPNSTA EARLE FNS G.A. Lowry, Fallbrook CA; Maint. Control Dir., Yorktown VA; PW Office (Code 09C1) Yorktown, VA; Security Offr, Colts Neck NJ

NAVWPNSUPPCEN Code 09 (Boennighausen) Crane IN
NCBU 405 OIC. San Diego, CA
NCBC CEL (CAPT N. W. Petersen), Port Hueneme, CA; CEL AOIC Port Hueneme CA; Code 10 Davisville, RI;
    Code 155, Port Hueneme CA; Code 156, Port Hueneme. CA; PW Engrg. Gulfport MS; PWO (Code 80) Port
    Hueneme, CA
NCBU 411 OIC, Norfolk VA
NCR 20. Commander
NMCB 133 (ENS T.W. Nielsen); 5, Operations Dept.; 74, CO; Forty, CO; THREE, Operations Off.
NORDA Code 440 (Ocean Rsch Off) Bay St. Louis MS
NRL Code 8400 (J. Walsh), Washington DC; Code 8441 (R.A. Skop), Washington DC; Rosenthal. Code 8440. Wash.
    DC
NSC Code 54.1 (Wynne), Norfolk VA
NSD SCE, Subic Bay, R.P.
NTC Code 54 (ENS P. G. Jackel), Orlando FL; Commander Orlando. FL
NUSC Code 131 New London, CT; Code EA123 (R.S. Munn), New London CT; Code TA131 (G. De la Cruz), New
    London CT
ONR Code 700F Arlington VA; Dr. A. Laufer, Pasadena CA
PHIBCB 1 P&E, Coronado, CA
PMTC Code 4253-3, Point Mugu, CA; Pat. Counsel, Point Mugu CA
PWC ENS J.E. Surash. Pearl Harbor HI; ACE Office (LTJG St. Germain) Norfolk VA; CO Norfolk. VA; CO, Great
    Lakes IL; Code 116 (LTJG. A. Eckhart) Great Lakes. IL; Code 120, Oakland CA; Code 120C (Library) San Diego,
    CA; Code 128, Guam; Code 200, Great Lakes IL; Code 200, Oakland CA; Code 220 Oakland. CA; Code 220.1,
    Norfolk VA; Code 30C (Boettcher) San Diego, CA; Code 680, San Diego CA; Library, Subic Bay, R.P.; OIC
    CBU-405, San Diego CA; XO Oakland, CA
SPCC Code 122B, Mechanicsburg. PA; PWO (Code 120) Mechanicsburg PA
U.S. MERCHANT MARINE ACADEMY Kings Point, NY (Reprint Custodian)
US GEOLOGICAL SURVEY Off. Marine Geology, Piteleki, Reston VA
USAF SCHOOL OF AEROSPACE MEDICINE Hyperbaric Medicine Div, Brooks AFB, TX
USCG (G-ECV) Washington Dc; (G-ECV/61) (Burkhart) Washington. DC, G-EOE-4/61 (T. Dowd), Washington DC
USCG ACADEMY LT N. Stramandi, New London CT
USCG R&D CENTER D. Motherway, Groton CT; Tech. Dir. Groton, CT
USNA Ch. Mech. Engr. Dept Annapolis MD; Ocean Sys. Eng Dept (Dr. Monney) Annapolis, MD; PWD Engr. Div.
    (C. Bradford) Annapolis MD; PWO Annapolis MD
AMERICAN CONCRETE INSTITUTE Detroit MI (Library)
CALIF. DEPT OF NAVIGATION & OCEAN DEV. Sacramento, CA (G. Armstrong)
CALIFORNIA STATE UNIVERSITY LONG BEACH, CA (CHELAPATI); LONG BEACH, CA (YEN)
COLORADO STATE UNIV., FOOTHILL CAMPUS Fort Collins (Nelson)
CORNELL UNIVERSITY Ithaca NY (Serials Dept. Engr Lib.)
DAMES & MOORE LIBRARY LOS ANGELES, CA
DUKE UNIV MEDICAL CENTER B. Muga. Durham NC; DURHAM, NC (VESIC)
FLORIDA ATLANTIC UNIVERSITY BOCA RATON, FL. (MC ALLISTER); Boca Raton FL (Ocean Engr Dept., C.
    Lin)
FLORIDA ATLANTIC UNIVERSITY Boca Raton FL (W. Tessin)
FLORIDA TECHNOLOGICAL UNIVERSITY ORLANDO, FL (HARTMAN)
GEORGIA INSTITUTE OF TECHNOLOGY Atlanta GA (School of Civil Engr., Kahn); Atlanta GA (B. Mazanti)
IOWA STATE UNIVERSITY Ames IA (CE Dept. Handy)
VIRGINIA INST. OF MARINE SCI. Gloucester Point VA (Library)
LEHIGH UNIVERSITY BETHLEHEM, PA (MARINE GEOTECHNICAL LAB., RICHARDS); Bethlehem PA
    (Fritz Engr. Lab No. 13, Beedle); Bethlehem PA (Linderman Lib. No.30, Flecksteiner)
LIBRARY OF CONGRESS WASHINGTON, DC (SCIENCES & TECH DIV)
MICHIGAN TECHNOLOGICAL UNIVERSITY Houghton, MI (Haas)
MIT Cambridge MA; Cambridge MA (Rm 10-500, Tech. Reports. Engr. Lib.); Cambridge MA (Whitman)
NEW MEXICO SOLAR ENERGY INST. Dr Zwibel Las Cruces NM
NORTHWESTERN UNIV Z.P. Bazant Evanston IL
NY CITY COMMUNITY COLLEGE BROOKLYN, NY (LIBRARY)
UNIV. NOTRE DAME Katona, Notre Dame, IN
OREGON STATE UNIVERSITY (CE Dept Grace) Corvallis, OR; CORVALLIS, OR (CE DEPT. BELL);
    CORVALLIS, OR (CE DEPT. HICKS); Corvalis OR (School of Oceanography)
PENNSYLVANIA STATE UNIVERSITY UNIVERSITY PARK, PA (GOTOLSKI)
PURDUE UNIVERSITY Lafayette IN (Leonards); Lafayette, IN (Altschaeffl); Lafayette, IN (CE Engr. Lib)
SAN DIEGO STATE UNIV. I. Noorany San Diego, CA; Dr. Krishnamoorthy, San Diego CA

SEATTLE U Prof Schwaegler Seattle WA
SOUTHWEST RSCH INST King, San Antonio, TX; R. DeHart, San Antonio TX
STANFORD UNIVERSITY Engr Lib, Stanford CA; Stanford CA (Gene)
STATE UNIV. OF NEW YORK Buffalo, NY
TEXAS A&M UNIVERSITY COLLEGE STATION, TX (CE DEPT); College Station TX (CE Dept, Herbich)
UNIVERSITY OF CALIFORNIA BERKELEY, CA (CE DEPT, GERWICK); BERKELEY, CA (CE DEPT,
    MITCHELL); Berkeley CA (B. Bresler); Berkeley CA (Dept of Naval Arch.); Berkeley CA (R. Williamson);
    DAVIS, CA (CE DEPT, TAYLOR); LIVERMORE, CA (LAWRENCE LIVERMORE LAB, TOKARZ); La Jolla
    CA (Acq. Dept, Lib. C-075A); Los Angeles CA (Engr I, K. Lee); M. Duncan, Berkeley CA; SAN DIEGO, CA, LA
    JOLLA, CA (SEROCKI)
UNIVERSITY OF DELAWARE Newark, DE (Dept of Civil Engineering, Chesson)
UNIVERSITY OF HAWAII Dr Chiu Honolulu, HI; HONOLULU, HI (SCIENCE AND TECH. DIV.); Honolulu HI
    (Dr. Szilard)
UNIVERSITY OF ILLINOIS Metz Ref Rm, Urbana IL; URBANA, IL (DAVISSON); URBANA, IL (LIBRARY);
    URBANA, IL (NEWARK); Urbana IL (CE Dept, W. Gamble)
UNIVERSITY OF MASSACHUSETTS (Heronemus), Amherst MA CE Dept
UNIVERSITY OF MICHIGAN Ann Arbor MI (Richart)
UNIVERSITY OF NEBRASKA-LINCOLN Lincoln, NE (Ross Ice Shelf Proj.)
UNIVERSITY OF NEW MEXICO J Nielson-Engr Matls & Civil Sys Div, Albuquerque NM
UNIVERSITY OF TEXAS Inst. Marine Sci (Library), Port Arkansas TX
UNIVERSITY OF TEXAS AT AUSTIN AUSTIN, TX (THOMPSON); Austin TX (R. Olson); Austin, TX (Breen)
UNIVERSITY OF WASHINGTON Dept of Civil Engr (Dr. Mattock), Seattle WA; SEATTLE, WA (MERCHANT);
    SEATTLE, WA (OCEAN ENG RSCH LAB, GRAY); Seattle WA (E. Linger); Seattle, WA Transportation,
    Construction & Geom. Div
URS RESEARCH CO. LIBRARY SAN MATEO, CA
ALFRED A. YEE & ASSOC. Honolulu HI
AMETEK Offshore Res. & Engr Div
APPLIED TECH COUNCIL R. Scholl, Palo Alto CA
ARVID GRANT OLYMPIA, WA
ATLANTIC RICHFIELD CO. DALLAS, TX (SMITH)
AUSTRALIA Dept. PW (A. Hicks), Melbourne
BECHTEL CORP. SAN FRANCISCO, CA (PHELPS)
BELGIUM HAECON, N.V., Gent
BROWN & ROOT Houston TX (D. Ward)
CANADA Mem Univ Newfoundland (Chari), St Johns; Surveyor, Nenninger & Chenevert Inc., Montreal; Warnock
    Hersey Prof. Srv Ltd. La Sale, Quebec
CF BRAUN CO Du Bouchet, Murray Hill, NJ
CHEVRON OIL FIELD RESEARCH CO. LA HABRA, CA (BROOKS)
CONCRETE TECHNOLOGY CORP. TACOMA, WA (ANDERSON)
CONRAD ASSOC. Van Nuys CA (A. Luisoni)
DRAVO CORP Pittsburgh PA (Giannino); Pittsburgh PA (Wright)
NORWAY DET NORSKE VERITAS (Library), Oslo
EVALUATION ASSOC. INC KING OF PRUSSIA, PA (FEDELE)
FORD, BACON & DAVIS, INC. New York (Library)
FRANCE Dr. Dutertre, Boulogne; L. Pliskin, Paris; P. Jensen, Boulogne
GEOTECHNICAL ENGINEERS INC. Winchester, MA (Paulding)
GLIDDEN CO. STRONGSVILLE, OH (RSCH LIB)
GRUMMAN AEROSPACE CORP. Bethpage NY (Tech. Info. Ctr)
HALEY & ALDRICH, INC. Cambridge MA (Aldrich, Jr.)
HONEYWELL, INC. Minneapolis MN (Residential Engr Lib.)
HUGHES AIRCRAFT Culver City CA (Tech. Doc. Ctr)
ITALY M Caroni, Milan; Sergio Tattoni Milano; Torino (F. Levi)
MAKAI OCEAN ENGRNG INC. Kailua, HI
JAMES CO. R. Girdley, Orlando FL
LAMONT-DOHERTY GEOLOGICAL OBSERV. Palisades NY (McCoy); Palisades NY (Selwyn)
LOCKHEED MISSILES & SPACE CO. INC. Mgr Naval Arch & Mar Eng Sunnyvale, CA; Sunnyvale CA
    (Rynewicz); Sunnyvale, CA (Phillips)
LOCKHEED OCEAN LABORATORY San Diego CA (F. Simpson)
MARATHON OIL CO Houston TX (C. Seay)
MC CLELLAND ENGINEERS INC Houston TX (B. McClelland)
MCDONNEL AIRCRAFT CO. Dept 501 (R H. Fayman), St Louis MO

MEDALL & ASSOC. INC. J.T. GAFFEY II SANTA ANA, CA
MEXICO R. Cardenas
MOBIL PIPE LINE CO. DALLAS, TX MGR OF ENGR (NOACK)
MUESER, RUTLEDGE, WENTWORTH AND JOHNSTON NEW YORK (RICHARDS)
NEW ZEALAND New Zealand Concrete Research Assoc. (Librarian), Porirua
NEWPORT NEWS SHIPBLDG & DRYDOCK CO. Newport News VA (Tech. Lib.)
NORWAY DET NORSKE VERITAS (Roren) Oslo; I. Foss, Oslo; J. Creed, Ski; Norwegian Tech Univ (Brandtzaeg),
    Trondheim
OFFSHORE DEVELOPMENT ENG. INC. BERKELEY, CA
PACIFIC MARINE TECHNOLOGY LONG BEACH, CA (WAGNER)
PORTLAND CEMENT ASSOC. SKOKIE, IL (CORELY); Skokie IL (Rsch & Dev Lab, Lib.)
PRESCON CORP TOWSON, MD (KELLER)
RAND CORP. Santa Monica CA (A. Laupa)
RAYMOND INTERNATIONAL, INC. E Colle Soil Tech Dept, Pennsauken, NJ
RIVERSIDE CEMENT CO Riverside CA (W. Smith)
SANDIA LABORATORIES Library Div., Livermore CA
SCHUPACK ASSOC SO. NORWALK, CT (SCHUPACK)
SEATECH CORP. MIAMI, FL (PERONI)
SHELL DEVELOPMENT CO. Houston TX (E. Doyle)
SHELL OIL CO. HOUSTON, TX (MARSHALL)
SOUTH AMERICA N. Nouel, Valencia, Venezuela
SWEDEN GeoTech Inst; VBB (Library), Stockholm
TIDEWATER CONSTR. CO Norfolk VA (Fowler)
TRW SYSTEMS CLEVELAND, OH (ENG. LIB.); REDONDO BEACH, CA (DAI)
UNITED KINGDOM Cement & Concrete Assoc Wexham Springs, Slough Bucks; Cement & Concrete Assoc. (Lit.
    Ex), Bucks; D. Lee, London; D. New, G. Maunsell & Partners, London; Library, Bristol; Shaw & Hatton (F.
    Hansen), London; Taylor, Woodrow Constr (014P), Southall, Middlesex; Univ. of Bristol (R. Morgan), Bristol
WATT BRIAN ASSOC INC. Houston, TX
WESTINGHOUSE ELECTRIC CORP. Annapolis MD (Oceanic Div Lib, Bryan); Library, Pittsburgh PA
WISS, JANNEY, ELSTNER, & ASSOC Northbrook, IL (J. Hanson)
WOODWARD-CLYDE CONSULTANTS (A. Harrigan) San Francisco; PLYMOUTH MEETING PA (CROSS, III)
AL SMOOTS Los Angeles, CA
BARA, JOHN P. Lakewood, CO
BROWN, ROBERT University, AL
BULLOCK La Canada
F. HEUZE Boulder CO
CAPT MURPHY Sunnyvale, CA
GREG PAGE EUGENE, OR
R.F. BESIER Old Saybrook CT
T.W. MERMEL Washington DC